Optimization of hydrogen formation using *Parageobacillus thermoglucosidasius* DSM 6285

Zur Erlangung des akademischen Grades einer
DOKTORIN DER NATURWISSENSCHAFTEN (DR. RER. NAT.)

von der KIT-Fakultät für Chemieingenieurwesen und Verfahrenstechnik des
Karlsruher Instituts für Technologie (KIT)
genehmigte

DISSERTATION

von
M. Sc. Magda Stephania Ardila Mahecha
aus Bogotá, Kolumbien

Tag der mündlichen Prüfung: 30.09.2025
Erstgutachter: Prof. Dr. rer. nat. Christoph Syldatk
Zweitgutachter: Prof. Dr. rer. nat. Nicolaus Dahmen
KIT-Associate Fellow: Dr. rer. nat. Anke Neumann

Acknowledgment

My gratitude expands to Prof. Dr. Christoph Syldatk, who welcomed me into his group and gave me fruitful advice during the seminars. I also want to express my appreciation to Prof. Dirk Holtmann, for his expertise and mentorship throughout my PhD.

I am grateful that during this journey, my supervisor Dr. Anke Neumann was there all the time, her support, constant encouragement, and insightful advice were essential for my success. I want to extend my gratitude to Dr. Habibu Aliyu and Dr. Pieter de Maayer, who always offered their perspectives and supported me, greatly enriching this work.

All my colleagues at TeBi and EBT working groups were always surrounding me with company and discussions that enriched my research and made lab work fun. Special thanks to Alberto, Aline, Andrè, Anna-Lena, Arabi, Christin, Daniel, Emely, Emily, Flávio, Jakub, Kevin, Lea, Lisa, Lukas, Nebyat, Michael, Nicklas, Selina, and Sonja. I would like to extend my appreciation to the technical and administrative staff, especially to Beate, Daniela, Marvin, Michaela, Pascal, and Susanne. To my students Luca, Mona, Sabrina, and Tommy, whom I was lucky to supervise.

To my friends here and in Colombia; I am deeply grateful for your love and care. Merve, Rita, Sasha, and Sue, you have been in the highs and lows. I am so happy the universe decided to cross our paths. Leen, who at the distance has never failed to send me words of hope and inspiration. My dear friends, Anshika, Bhavya, Lape, Mariana, Mery, Michaela, Monali, Nan and Pauli, thank you for always being there.

Finally, I am so grateful to my family, my parents, Magda and German, and my brother Camilo. Always supporting my dreams and being on endless calls to feel the distance a bit less. I would never have imagined starting this journey without your love. My partner Loui, for the many memories and constant support in our joint doctoral ride. To my abuelita Mariela, you will always be in my mind and heart.

Preamble

This thesis is based on peer-reviewed research articles. All of them were drafted during this work and describe the relevant results of optimizing the hydrogen production process with *Parageobacillus thermoglucosidasius* DSM 6285. From the evaluation of different feeding strategies in bioreactor scale to the challenges of working on high-pressure fermentations, that allowed to understand the limitations of both, the process and the microorganism. Changes in figure format and citation style have been adjusted to adapt the text for the dissertation.

Chapter 1 describes the theoretical background, placing emphasis on the current industrial and biological technologies for hydrogen production, microorganisms encountered in nature that can produce H_2 with special mention of the genus *Parageobacillus*. The different reactor configurations for gas fermentation are also described.

Chapter 2 presents the results of a batch and two semi-continuous fermentation in 2.5 L stirred tank reactors with *P. thermoglucosidasius* DSM 6285. Two feeding intervals were described for the semi-continuous mode to evaluate the effect on H_2 production. A carbon monoxide dehydrogenase (CODH) enzyme assay was performed to compare the feeding strategies with the batch fermentation. This chapter is based on the publication:

Batch and semi-continuous fermentation with *Parageobacillus thermoglucosidasius* DSM 6285 for H_2 production. Magda S. Ardila, Habibu Aliyu, Pieter de Maayer, Anke Neumann. Biotechnology for Biofuels and Bioproducts, 2025.

Chapter 3 outlines the importance of oxygen perturbation on *P. thermoglucosidasius* hydrogenogenesis, together with the effects of synthesis gas (syngas) on the water-gas shift (WGS) reaction-driven H_2 production. This chapter is based on the publication:

The effects of synthesis gas feedstocks and oxygen perturbation on hydrogen production by *Parageobacillus thermoglucosidasius*. Michael Mol, Magda S. Ardila, Bronwyn Ashleigh Mol, Habibu Aliyu, Anke Neumann, and Pieter de Maayer.
Microbial Cell Factories, 2024.

Chapter 4 further evaluated the effect of increasing CO and H_2 partial pressures in lab-defined syngas on a bioreactor scale. Opening the possibility of scale-up of the process, as the challenges for gas fermentation are still under research. Additionally, acetate was evaluated as an additional carbon source and its effects on H_2 production in *P. thermoglucosidasius*. This chapter is based on the submitted manuscript:

Evaluation of lab-defined syngas and acetate as substrates for H_2 production with *Parageobacillus thermoglucosidasius* DSM 6285. Magda S. Ardila, Habibu Aliyu, Pieter de Maayer, Anke Neumann.
Manuscript submitted for publication.

Chapter 5 demonstrates the capability of *P. thermoglucosidasius* DSM 6285 to withstand N_2, and H_2 partial pressures up to 3.0 bar. However, the increase of CO partial pressure to 3.0 bar had an inhibitory effect, delaying H_2 production. The electron balance at the end of the fermentation process presented a 95% selectivity towards H_2 production. This chapter is based on the publication:

Effect of different partial pressures on H_2 production with *Parageobacillus thermoglucosidasius* DSM 6285. Magda S. Ardila, Habibu Aliyu, Pieter de Maayer, Anke Neumann.
Fermentation, 2024.

List of publications

Peer-reviewed original publications

2024

Effect of different partial pressures on H_2 production with *Parageobacillus thermoglucosidasius* DSM 6285. Magda S. Ardila, Habibu Aliyu, Pieter de Maayer, Anke Neumann.
Fermentation (2024), 10, 592. https://doi.org/10.3390/fermentation10110592

The effects of synthesis gas feedstocks and oxygen perturbation on hydrogen production by *Parageobacillus thermoglucosidasius*. Michael Mol, Magda S. Ardila, Bronwyn Ashleigh Mol, Habibu Aliyu, Anke Neumann, and Pieter de Maayer.
Microbial Cell Factories (2024), 23:125. https://doi.org/10.1186/s12934-024-02391-4

2025

Batch and semi-continuous fermentation with *Parageobacillus thermoglucosidasius* DSM 6285 for H_2 production. Magda S. Ardila, Habibu Aliyu, Pieter de Maayer, Anke Neumann.
Biotechnology for Biofuels and Bioproducts (2025), 18:3. https://doi.org/10.1186/s13068-024-02597-z

Evaluation of lab-defined syngas and acetate as substrates for H_2 production with *Parageobacillus thermoglucosidasius* DSM 6285. Magda S. Ardila, Habibu Aliyu, Pieter de Maayer, Anke Neumann.
Manuscript submitted for publication.

Poster presentations in conferences

2022

Semi-continuous fermentation with *Parageobacillus thermoglucosidasius* DSM 6285 for H_2 production.

DECHEMA, Mainz, Germany.

2023

Use of gas mixtures as a substrate for H_2 production with *Parageobacillus thermoglucosidasius* DSM 6285
DECHEMA, Weimar, Germany.

Effect of different partial pressures on H_2 production with *Parageobacillus thermoglucosidasius* DSM 6285
19th International Conference on Renewable Resources and Biorefineries, Riga, Latvia.

Oral presentations in conferences

2022

Influence of biomass on hydrogen production with *Parageobacillus thermoglucosidasius* DSM 6285.
VAAM – Jahrestagung, Online.

2023

Hydrogen production with *Parageobacillus thermoglucosidasius* DSM 6285: Impact of hydraulic retention time in a continuous fermentation.
VAAM – Jahrestagung, Göttingen, Germany.

2024

Use of gas mixtures as a substrate for H_2 production with *Parageobacillus thermoglucosidasius* DSM 6285
Carbon recycling Network Conference, Manchester, UK.

Abstract

Hydrogen has gained attention as a clean and versatile energy carrier, offering a high energetic yield and a promising alternative to fossil fuels. In light of increasing global efforts to reduce carbon emissions, sustainable methods for hydrogen production are gaining significant attention. Traditional hydrogen production relies on thermal processes such as steam reforming, CO_2 reforming, and catalytic partial oxidation. However, biological hydrogen production presents a viable and environmentally better alternative. Among biological systems, hydrogenogenic carboxydotrophic microorganisms have demonstrated the ability to produce hydrogen (H_2) using carbon monoxide (CO) as a substrate. One such organism, the thermophilic Gram-positive bacterium *Parageobacillus thermoglucosidasius* DSM 6285, is capable of performing the water gas shift (WGS) reaction. In this process, CO reacts with water under anaerobic conditions to yield H_2 and CO_2.

This study aimed to optimize hydrogen production using *P. thermoglucosidasius* through various fermentation approaches while evaluating the effects of different gas compositions and partial pressures on the process. Batch and semi-continuous fermentation strategies were compared to assess the impact of feeding intervals and the addition of glucose as a supplementary carbon source. It was found that carbon monoxide dehydrogenase (CODH) activity remained relatively constant with daily feedings. A 24-hour feeding interval led to stable H_2 production, while a 48-hour interval introduced substantial variation in output. These results indicate that more frequent substrate supplementation supports consistent hydrogenogenesis.

Further investigations explored the use of synthesis gas (syngas), a CO-rich mixture, as a substrate. Employing syngas led to improved H_2 yields but negatively impacted biomass accumulation, suggesting a trade-off between product formation and cell growth. Additionally, the introduction of oxygen into the system reduced hydrogen output but enhanced biomass production and accelerated the consumption of acetate. This highlights the importance of balancing oxidative and reductive conditions to optimize both growth and product yield.

The scalability of this biological process was tested at the bioreactor level using lab-defined syngas and acetate. Varying the partial pressures of CO and H_2 did not inhibit hydrogen

production, confirming the robustness of the organism under controlled conditions. Acetate was evaluated as a replacement for glucose in a two-phase fermentation, and the process maintained high selectivity for hydrogen production. However, increasing CO partial pressure to 3.0 bar completely halted hydrogen formation and led to diminished biomass recovery, indicating a threshold for CO tolerance. In contrast, increasing nitrogen and hydrogen partial pressures had no significant inhibitory effects. An electron balance conducted at the end of the fermentation showed that 95% of electrons were directed toward H_2 formation, while the remainder contributed to the production of organic acids.

Although challenges remain in scaling up this biological hydrogen production system, the findings demonstrate that *P. thermoglucosidasius* has considerable potential as a microbial platform for sustainable energy generation. The effects of gas composition, feeding frequency, and partial pressures are critical variables that influence hydrogen yields and process stability. Further research is needed to refine these parameters and address the limitations observed under high CO concentrations. This study lays essential groundwork for future advancements in optimizing microbial hydrogen production systems for industrial applications, contributing to the broader goal of achieving carbon-neutral energy solutions.

Zusammenfassung

Wasserstoff hat sich aufgrund seines hohen energetischen Potenzials und seiner Rolle als sauberer, kohlenstoffneutraler Energieträger als vielversprechende Alternative zu fossilen Brennstoffen etabliert. Angesichts der zunehmenden globalen Bemühungen zur Reduktion von CO_2-Emissionen rücken nachhaltige Methoden zur Wasserstoffproduktion zunehmend in den Fokus. Während die herkömmliche Wasserstoffgewinnung meist auf thermischen Verfahren wie der Dampfreformierung, der CO_2-Reformierung oder der partiellen Oxidation basiert, stellt die biologische Wasserstoffproduktion eine umweltfreundliche Alternative dar. Wasserstoffogene carboxydotrophe Mikroorganismen können Wasserstoff (H_2) unter Verwendung von Kohlenmonoxid (CO) als Substrat produzieren. Ein solcher Organismus ist das thermophile, grampositive Bakterium *Parageobacillus thermoglucosidasius* DSM 6285, das in der Lage ist, die sogenannte Wasser-Gas-Shift-Reaktion (WGS) durchzuführen. Dabei reagiert CO unter anaeroben Bedingungen mit Wasser zu H_2 und CO_2.

Diese Studie zielte darauf ab, die Wasserstoffproduktion durch *P. thermoglucosidasius* mittels verschiedener Fermentationsansätze zu optimieren und den Einfluss unterschiedlicher Gasmischungen sowie partieller Drücke auf den Prozess zu untersuchen. Im Vergleich zwischen Batch- und semi-kontinuierlicher Fermentation wurde die Auswirkung unterschiedlicher Substratzufuhr-Intervalle sowie die Zugabe von Glukose als zusätzlicher Kohlenstoffquelle analysiert. Die Aktivität der Kohlenmonoxid-Dehydrogenase (CODH) blieb bei täglicher Substratzugabe relativ konstant. Ein 24-Stunden-Zyklus führte zu stabiler H_2-Produktion, während ein 48-Stunden-Intervall starke Schwankungen verursachte. Dies zeigt, dass eine häufigere Substratzugabe eine gleichmäßigere Wasserstoffproduktion unterstützt.

Im weiteren Verlauf wurde Synthesegas (Syngas), ein CO-reiches Gasgemisch, als alternatives Substrat eingesetzt. Dabei konnte eine gesteigerte Wasserstoffausbeute festgestellt werden, allerdings ging dies mit einer reduzierten Biomassebildung einher – ein Hinweis auf einen Zielkonflikt zwischen Zellwachstum und Produktbildung. Die Zugabe von Sauerstoff führte zwar zu einer verminderten H_2-Ausbeute, förderte jedoch das Zellwachstum und beschleunigte den Verbrauch von Acetat. Dies unterstreicht die Bedeutung eines ausgewogenen Redoxmilieus zur Optimierung von Wachstum und Produktbildung.

Die Skalierbarkeit des Prozesses wurde im Bioreaktor unter Verwendung von labordefiniertem Syngas und Acetat getestet. Unterschiedliche partielle Drücke von CO und H_2 hemmten die Wasserstoffproduktion nicht, was die Robustheit des Prozesses unter kontrollierten Bedingungen bestätigt. In einem Zwei-Phasen-Fermentationsverfahren wurde Acetat anstelle von Glukose verwendet, wobei weiterhin eine hohe Selektivität für H_2 beibehalten wurde. Wurde der partielle CO-Druck jedoch auf 3,0 bar erhöht, kam es zum vollständigen Stopp der Wasserstoffproduktion und zu einer geringen Biomasserückgewinnung. Im Gegensatz dazu zeigten erhöhte Drücke von Stickstoff und Wasserstoff keine hemmende Wirkung. Eine Elektronenbilanz am Ende der Fermentation ergab, dass 95 % der Elektronen in die H_2-Produktion flossen, der Rest wurde zur Bildung organischer Säuren genutzt.

Trotz bestehender Herausforderungen bietet die Skalierung dieses biologischen Wasserstoffproduktionsprozesses mit *P. thermoglucosidasius* vielversprechende Perspektiven. Die Untersuchung verschiedener Gasmischungen und partieller Drücke liefert wertvolle Erkenntnisse zur Optimierung der Ausbeuten und Prozessstabilität. Diese Arbeit bildet die Grundlage für zukünftige Studien zur Maximierung der Wasserstoffproduktion in biologischen Systemen und leistet einen Beitrag zur Entwicklung kohlenstoffneutraler Energiequellen.

Table of contents

1. Theoretical Background and Research Proposal

1.1. Hydrogen production

Replacing fossil energy and the reduction of greenhouse gas emissions rely on the usage of alternative energy. Among the numerous options, biological, geothermal, hydroelectric, solar, tidal and wind represent sustainable energy alternatives, capable of meeting current and future global energy demand [1].

Hydrogen emerges as a clean, efficient, and versatile energy carrier that produces only water as a result of its production [2,3]. Hydrogen has the highest gravimetric energy density; and the lowest volumetric density compared to other fuels, this is most important during transportation and storage for carrying the same amount of energy, it may require a bigger tank, but it will have a lower shipping load [4]. Renewable energy-based configurations include solar photovoltaic power, geothermal power generation, and biomass gasification [5].

1.1.1. Industrial hydrogen production

Thermal processes including steam reforming, CO_2 reforming, and catalytic partial oxidation are commonly used for hydrogen and synthesis gas production, with the first one being an established technology that produces the highest H_2 yield with the highest purity and thermal efficiency, however with high CO_2 emissions this technology is on due to be replaced [6]. The role of fossil fuels as main supply for H_2 production is correlated with costs as they depend on fuel prices, which remain lower compared to biological methods [7]. While steam reforming is an endothermic process, partial oxidation is exothermic, being less energy consuming [6]. Partial oxidation involves the conversion of steam, oxygen and hydrocarbons to H_2 and steam reforming relies on hydrocarbons and steam [7].

The second group of methods comprises hydrocarbon pyrolysis, where only the hydrocarbon goes through thermal decomposition, giving out elemental carbon and H_2 as a result, when carrying out between 50 and 200 °C, and requiring a two-step reaction when occurring at a temperature higher than 350 °C [7].

It is also important to mention electrolytic processes, that includes electrolysis, photo-reduction and thermolysis, producing H_2 and O_2 from water with the use of an acid or an alkali electrolyte, however its high electricity consumption and relatively lower yield compared to steam reforming is a drawback of one of the most renewable methods for hydrogen production [6].

1.1.2. Biological hydrogen production

Biological processes for hydrogen production include direct and indirect bio-photolysis, microbial electrolysis cells, and photo and dark fermentations. Bacteria and algae may produce hydrogen enzyme systems through processes such as photolysis, making use of water and sunlight or through dark fermentation, using biomass or organic acids using hydrogenases or nitrogenases enzymatic systems [7,8] (Figure 1). Dark fermentation has evolved as a simple light-independent strategy, potentially using substrates from renewable sources [9]. It uses anaerobic bacteria or fungi under anoxic and dark conditions to perform carbohydrate fermentations with substrates including glucose, starch, and cellulose [7]. There are still some challenges for the dark fermentation process, such as the biocatalyst nature and metabolism, interactions between microbes when working with open cultures, feedback inhibition, and reactor configuration [10].

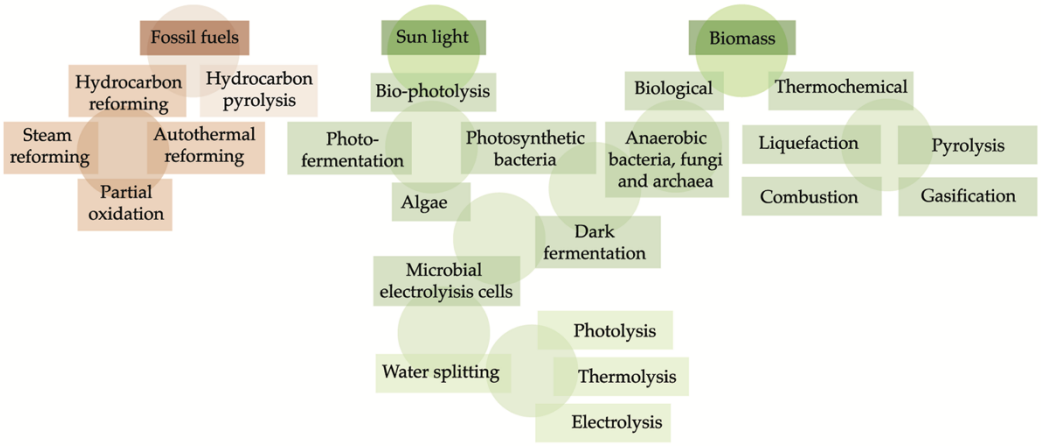

Figure 1. Hydrogen production sources and methods overview [7,8,11].

The improvement of the platform requires an evaluation of the substrates, microorganisms and bioreactor system used, and the optimal conditions will be achieved. The type of substrate whether natural complex substrates like cellulose, waste biomass or simple sugars like glucose, can determine different H_2 production yields, together with reactor types and process parameters in a fermentation process [12]. Not only that but changes in the microbial community composition, when working with open cultures can lead to instability in H_2 producing reactors, even the reactor design has been shown to affect the diversity of the community [13]. Many other characteristics need to be identified and acknowledged in the platform, as seen in Figure 2, most of them will be discussed along the review.

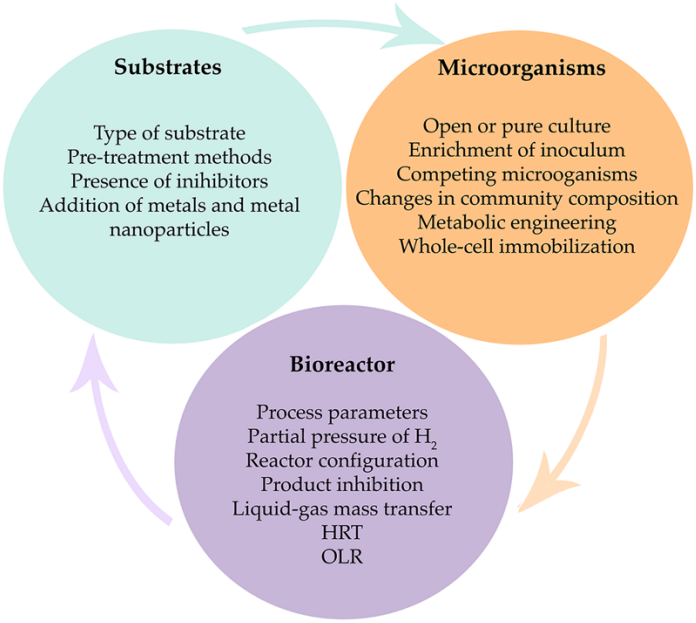

Figure 2. Parameters for improvement of anaerobic biohydrogen platform [9,12].

Facultative hydrogen-producing bacteria, such as *Enterobacter, Enterococcus, Citrobacter,* and *Klebsiella*, are essential due to their ability to remove oxygen in the reactor, especially when working with mixed cultures [9]. High-temperature fermentation has the distinct advantage of being compatible with downstream processes. Thermophiles also have lower contamination risks, high hydrogen production rates (HPR), higher productivity and yields, and better degradation of complex substrates [14–16]. Notable biohydrogen-producing thermophiles *include Thermotoga neapolitana, Thermotoga elfii, Caldicellulosiruptor saccharolyticus,* and *Thermococcus kodakaraensis* KOD1 [17]. Emerging bacterial and archaeal genomes harboring CODH suggest CO oxidation capacity, either as an energy conservation strategy or as a primary carbon source. Microorganisms encoding multiple CODH operons is still under investigation, and potentially constitute different CO-utilization pathways [18–20].

1.2. Substrate diversity and hydrogen-producing metabolic pathways

Steam reforming of natural gas serves as the largest source of hydrogen, with drawbacks, including CO_2 emissions and high energy consumption [6]. Conversely, biological processes such as biophotolysis, photo-fermentation, and dark fermentation represent sustainable and environment-friendly hydrogen sources [6,16,21,22]. Fermentative hydrogen production or dark fermentation yields hydrogen under anaerobic conditions using organic substrates [23]. Both strict anaerobes and facultative anaerobic bacteria can conduct hydrogenogenic dark fermentation. Nevertheless, the ability of the latter group to recover from oxygen contamination is an advantage during fermentation [23].

A microorganism could degrade complex substrates such as starch, and the resulting hydrolysate can be used by a second bacteria able to produce hydrogen; this was described with *Caldimonas taiwanensis* On1, which was able to hydrolyze starch completely, which was later used by five *Clostridium* isolates*, C. butyricum* CGS2, *C. butyricum* CGS5, *C. pasteurianum* CH1, *C. pasteurianum* CH5, and *C. pasteurianum* CH7 [24]. Also, the strain *Enterobacter aerogenes* can produce biohydrogen using starch hydrolysate as substrate [25]. The ability to degrade cellulose and hemicellulose polymers through the production of enzymes such as xylanases, xylosidases, arabinofuranosidases, and glucuronidases is highly desired. The identification and characterization of loci coding for the degradation of cellulose and hemicellulose are therefore pursued in microorganisms that can also produce hydrogen, the presence of a centralized hemicellulose utilization locus was described for *Geobacillus* strains, but the high variation between strains gives the conclusion that the different enzymes found over the strains reflect their natural environment needs [26].

Two pathways are involved in H_2 production, either through the pyruvate formate lyase (PFL) pathway or by the pyruvate ferredoxin oxidoreductase (PFOR) pathway, as seen in Figure 3. Glucose is converted to pyruvate, and later to acetyl-CoA, and afterwards to reduced ferredoxin through the PFOR pathway or pyruvate can be converted to formate when undergoing the PFL pathway [2,27]. Then pyruvate is converted into acetyl-CoA and CO_2 through the pyruvate-ferredoxin oxidoreductase, which also reduces ferredoxin; the reduced form of ferredoxin reduce protons to H_2 [28,29].

The final hydrogen yield depends on the main metabolite pathway, while acetate yields 4 mol H_2 mol glucose^{-1}, butyrate, and ethanol only gives 2 mol H_2 per mol glucose^{-1} [2,29]. The highest ATP production comes from acetate and butyrate production through the Acetyl-CoA branch; when an alternative electron sink is required, butyrate is favored over acetate to avoid increasing the hydrogen partial pressure and the drop of pH. These pathways decrease hydrogen yield but can be used for liquid biofuel production [30]. Many by-products, such as ethanol, acetate, propionate, or butyrate, can also be produced; H_2 is not the only fermentation product (Figure 3).

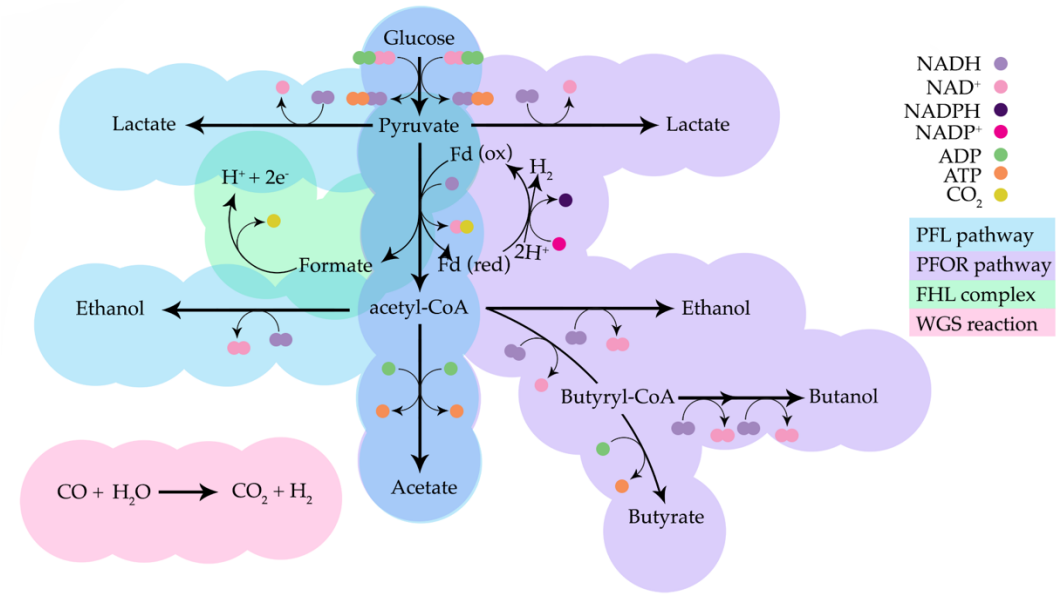

Figure 3. Glucose-derived fermentation pathways for hydrogen production. Adapted from [2,31].

The PFOR pathway is mainly used by obligate anaerobes, including *Clostridium*, who can also produce hydrogen by additional hydrogenases, such as the NADH-dependent (NADH- [FeFe]) and bifurcating NADH-Fdred-dependent hydrogenase (NADH-Fdred- [FeFe]) [32]. In the other hand, the PFL pathway is most common in facultative anaerobes, here formate is converted into H_2 and CO_2 through a formate hydrogen lyase (FHL) complex, that contains a nickel-iron [NiFe] hydrogenase [33]. The microorganisms that use the PFL pathway cannot therefore, use NADH for H_2 production [34].

Biological H_2 production has a broad spectrum of substrates that can go from organic waste to carboxylates and waste gases; some microorganisms can use CO as an energy source to produce H_2. This depends on the water-gas shift (WGS) reaction, catalyzed by two metalloenzymes, a nickel-containing carbon monoxide de-hydrogenase (NiFe-CODH) and an energy-conserving NiFe-hydrogenase [11,20,35–37].

Anaerobic bacterial communities have been reported for the conversion from CO to H_2; as compared to pure strains, mixed communities are more productive due to their robust biomass structure and efficient CO conversion to biohydrogen [11,38]. Exclusive use of CO was achieved with an initial concentration of 3.8 mmol L^{-1}, and maximum H_2 production of 29.9 mmol L^{-1} was obtained for an initial CO concentration of 5.12 mmol L^{-1}, using an open culture and evaluating H_2 product inhibition on biomass growth and H_2 production, it was found that there was product inhibition at high concentrations of H_2 [11,38]. However, when working with mixed communities, the insufficient knowledge about the community composition and the mechanisms of cooperation or competitive relationships should be addressed [39]. For mixed communities, carboxydotrophic microorganisms may be able to remove CO and produce CO_2

and H_2, reducing the toxicity of CO and feeding other pathways such as methanogenesis and sulfate reduction when desired [18,40]. The inhibition of methanogenesis pathways is therefore desired due to the conversion of hydrogen to methane; this can be achieved by controlling the pH, the loading rate, oxidation rate, and oxidation and reduction potential (ORP) [41].

1.3. Microorganisms involved in biohydrogen production

Hydrogen-producing microbes under anoxic conditions can be divided into spore-forming obligate anaerobes, non-spore-forming obligate anaerobes, and facultative anaerobes, while microorganisms widely studied, such as Clostridium constitute the first group, others such as Ethanoligenens, Acetanaerobacterium, and Megasphera are part of the second group. The facultative anaerobes enclose different genus including Citrobacter, Klebsiella, Enterobacter, Bacillus, and Pseudomonas [10].

Dark fermentation is one of the most promising approaches due to its simplicity, ease of scale-up, high rates of biohydrogen production, and practicality of using a wide range of substrates, including organic wastes [11,22,42]. Microorganisms can produce hydrogen through the mediation of hydrogenases; these can be found in both aerobic and anaerobic microbes and support H_2-based respiration, fermentation, and carbon fixation processes [2].

Conversely, energy conservation in the Ni-CODH/ECH complex relies on the sequential reactions from CO oxidation to proton motive force generation; hydrogenogenic CO oxidizers will couple CO oxidation with proton reduction to produce hydrogen using this enzymatic complex [36,37]. Even though CO is toxic for some microbes, others show a high tolerance; in this group, photosynthetic bacteria such as Rubrivivax gelatinosus and Rhodospirillum rubrum, as well as the non-phototrophic facultative anaerobes Citrobacter amalonaticus Y19, Carboxydothermus hydrogenoformans, Carboxydocella thermautotrophica, Thermosinus carboxydivorans, Cal-danaerobacter subterraneus, and Parageobacillus thermoglucosidasius, among other bacteria, have been reported [11,20,35–37]. A detailed description of some microorganisms involved in anoxic biological H_2 production can be found in Table 1.

Despite the extensive application of Clostridium spp. for biohydrogen production, optimizing fermentation conditions, including temperature, pH, and incubation time, remain a priority toward platform scale-up [29]. Other microorganisms, including Enterobacter, are also affected by substrate concentration, temperature, or even pre-treatment when a complex substrate is used [16].

Table 1. Microorganisms involved in anoxic biological hydrogen production.

Microorganism	Metabolic pathways for the production of hydrogen	Substrates used	Hydrogen yield	References

Bacillus cereus	Glycolytic pathway	Glucose	156.4 mL H_2 g volatile solids^{-1}	[43]
Clostridium	Glycolytic pathway Acetate type fermentation Butyrate type fermentation	Glucose Organic waste	1.5 to 3 mol H_2 mol hexose^{-1}	[2,9]
Enterobacter	Glycolytic pathway	Glucose Organic waste	2 mol H_2 mol hexose^{-1}	[11]
Enterobacter aerogenes CDC 819–56	Glycolytic pathway	Wastewater stream	7.42 mmol H_2 mol glucose^{-1}	[44]
Escherichia coli	Glycolytic pathway	Glucose	2 mol H_2 mol glucose^{-1}	[45]
Ethanoligenens harbinense YUAN-3	Glycolytic pathway	Glucose	2.62 mol H_2 mol glucose^{-1}	[46]
Janthinobacterium agaricidamnosum	Glycolytic pathway	Glucose	0.86 mol H_2 mol glucose^{-1}	[47]
Klebsiella pneumoniae	Glycolytic pathway	Wastewater stream	1.67 mol H_2 mol glucose^{-1}	[48]
Megasphaera	Linked to lactic acid production	Glucose Wastewater stream	11 mL H_2 g COD fed^{-1}	[9,49]
Neocallimastix camerooni G341	Glycolytic pathway	Enset fiber	0.51 mmol H2 per 8.58 mmol enset fiber	[50]
Polaromonas jejuensis	Glycolytic pathway	Glucose	1.57 mol H_2 mol glucose^{-1}	[47]
Rhodospirillum rubrum	WGS reaction	CO Malate Formate Acetate	16 mmol g^{-1} acetate cell^{-1} h^{-1}	[35]
Carboxydothermus hydrogenoformans	WGS reaction	CO	83.3 mmol g^{-1} h^{-1}	[35]
Moorella stamsii	WGS reaction	CO	NR	[51]
Parageobacillus thermoglucosidasius	WGS reaction	CO Glucose	0.8 mmol H_2 mmol CO^{-1}	[52]
Caldanaerobactersubterraneus ssp.	WGS reaction	CO	NR	[53]
Thermoanaerobacter thermohydrosulfuricus	WGS reaction	CO	0.2 mol H_2 mol glucose^{-1}	[54]

Desulfotomaculum carboxydivorans sp.	WGS reaction	CO	NR	[55]
Dictyoglomuscarboxydivorans	WGS reaction	CO	NR	[56]

NR: Not reported

1.3.1. *Parageobacillus thermoglucosidasius*

The diversity of the genus *Parageobacillus* include facultative anaerobic and anaerobic, thermophilic bacilli with a wide range of metabolic products [57]. One study suggested that the strain *P. thermoglucosidasius* Y4.1MC1 could perform the Wood-Ljungdahl pathway [58]. Their versatility has expanded to gas susbstrates as well, increasing the potential of this microorganisms for biotechnological and industrial use, the genome description revealed that they harbor a fifteen gene genomic region, including the genes that code for CODH and Ni-Fe group 4a hydrogenase, specifically *cooCSF* and *phcABCDEFGHIJKL* [59].

Parageobacillus thermoglucosidasius can produce hydrogen, performing WGS, as explained above [60,61]. The tolerance to the toxicity caused by CO of *P. thermoglucosidasius* is of great advantage, together with the ability to direct the metabolism to organic acids and other products, potentially generating energy through the WGS reaction [62].

1.4. Different reactor configurations

Different parameters are important when choosing a specific reactor configuration, affecting the mass transfer, the dynamics in the phases encountered during fermentation, as well as the microbial community. Continuous Stirred-Tank Reactors (CSTR) are mainly used, followed by Upflow Anaerobic Sludge Blanket Reactors (UASB), Expanded Granular Sludge Bed Reactors (EGSB), Fixed Bed Reactors (FBR), Sequencing Batch Reactors (SBR) [9]. Another configuration is the hollow fiber membrane (HFM) bioreactor, used to overcome the gas-liquid mass transfer limitation [11,63].

The most commonly used reactor is the CSTR; both impellers and baffles provide good mixing of the liquid media inside the reactor and improve gas-liquid mass transfer, as well as a high stirring rate, which creates small-sized bubbles that have a more extensive surface area for the gas availability. This type of reactor also allows a continuous mode of operation [30].

Hydrogen partial pressure can influence hydrogen production as a lower partial pressure in the headspace facilitates the mass transfer of hydrogen from the liquid to the gas phase; many strategies can be used to remove dissolved hydrogen from the media, such as sparging with N_2 and CO_2, using an H_2-permeable membrane to withdraw dissolved hydrogen, and decreasing the operating pressure in the reactor [12,64,65]. Lowering hydrogen partial pressure by reducing the total pressure in the headspace of a batch reactor was performed with *Clostridium*

butyricum TM-9A, the different hydrogen partial pressure experiments were performed increasing the liquid to gas phase ratio from 1:1 to 1:3, 1:6, 1:9 and 1:12, as a result, the molar hydrogen yield increased from 2.67 to 3.1 mol H_2 mol glucose $^{-1}$ with the optimum hydrogen partial pressure of 10.1 kPa, which can be explained due to the effect that high partial pressure causes the production of reduced products such as ethanol and lactate [27,66]. The effect on pressure is dependent on the microorganism, both *Clostridium acetobutylicum* and *Clostridium beijerinckii* showed a negative effect on the volumetric HPR when the hydrogen partial pressure increased, this was explained due to the electron flow from the reduced ferredoxin to molecular hydrogen via the hydrogenase, as it becomes thermodynamically less feasible [67,68]. The presence of metals has been ob-served to lower hydrogen partial pressure in methanogen species, the availability of nickel can influence the consumption of CO and H_2 in these microorganisms [69].

A reduced pressure process was employed to improve dark hydrogen fermentation in a CSTR and evaluate different HRTs, overall, an increase in hydrogen yield and hydrogen production efficiency was observed under a reduced pressure of 380 mmHg and a low HRT of 6 h [70]. It has also been observed that the optimum pH for biohydrogen production depends on the HRT when evaluating mixed sugars that resemble complex substrates [71]. Other studies have evaluated the hydrogenase activity and the correlation to hydrogen partial pressure, where increasing hydrogen partial pressure causes an increase in hydrogenase activity [72]. There is a direct influence between the built-in H_2 partial pressure in the reactor and the metabolic shift to the production of acids, such as acetate, butyrate, propionate, and ethanol, which affects the conversion efficiencies of the reactions [10]. Additionally, the effect of increased toxicity of CO to the cells should be evaluated when increasing the pressure, as CO solubility increases [20,64].

While CSTR has a mixed flow, which allows homogenous mixing through the reactor and increases the mass transfer, other reactors have a plug-flow pattern that allows a longitudinal separation of the media and is usually used when toxic compounds are present. The liquid flow pattern of most reactors can be found in between both patterns, which challenges the mixing [30]. The use of a dynamic membrane bioreactor for continuous hydrogen production was reported before [73], and the effect of shear velocity was evaluated on the influence of the formation, detachment, structure, and stability of biofilm, where too high shear velocity had a negative effect on biohydrogen production and biomass retention in the reactor.

Although an increase in the agitation speed has been reported to increase the gas-liquid mass transfer, it is not economically feasible as it increases the power costs, however, the impeller configuration has been evaluated, with the Rushton-type being the favorite due to higher mass transfer compared to other impellers [74]. A decrease in pH due to dissolved CO_2 and high shear stress can also be problematic when high agitation speed is used [75].

Granular biomass systems such as the upflow anaerobic sludge blanket (UASB) reactors are characterized by high retentions of biomass; their use for hydrogen production was described for a mixed mixture where the hydrogen productivity increased up to 62 mL H2 L^{-1} h^{-1} when the reactor was operated with an upflow gas recirculation [76].
Low gas-liquid mass transfer in CO conversion to biohydrogen is one of the current challenges faced for the improvement of the platform, some reactors such as the hollow fiber membrane (HFM) have been shown to have the highest kLa for CO, and has also been shown suitable for syngas fermentation [11,77]. One limitation is that membrane permeability tends to decrease over time due to membrane fouling and aging, which was observed in a study evaluating CO conversion to biohydrogen with *Carboxydothermus hydrogenoformans* using an HFM reactor, where H_2 yield of 92 mmol $mmol^{-1}$ was constant over many operational assessed parameters [78].

Different parameters have been evaluated to improve gas-liquid mass transfer, the ratio of gas recirculation over CO feed rates influenced CO conversion efficiency in a gas-lift reactor operated with *Carboxydothermus hydrogenoformans*, where the best performance was limited over a ratio of 40, and the gas-liquid mass transfer was limited below the same proportion, using a recirculation rate of 71 L day^{-1} [79].

The use of continuous fermentations can provide stable hydrogen production for an extended period in comparison to a batch process, it also reduces the inhibition by toxic metabolites accumulated in the media, parameters such as the time when the medium is replaced, the volume of the media and the feeding rate should be evaluated [80].

Enhancing the biohydrogen platform has included some new strategies, such as the use of iron nanoparticles for the enhancement of CO solubility and improvement of biohydrogen yield. The difference between adding nanoparticles resulted in nearly 44% enhancement in the aqueous solubility of CO compared to the experiment control, in addition, improve the gas-liquid mass transfer, there is also an enhancement in the metabolic pathway involved in H_2 production [81,82].

The presence of homoacetogenic microorganisms can cause the consumption of H_2 to produce acetic acid, one experiment performed with an open culture tried to verify the presence of homoacetogens. For this reason, a real-time PCR was performed, but it was found that the abundance of the Fe hydrogenase gene was higher in the reactor, therefore the influence of homoacetogenesis remains to be elucidated [13].

Recently, the relationship between hydraulic retention time (HRT) and pH was described for a mixed culture using a synthetic lignocellulose hydrolysate to produce hydrogen from cellobiose, xylose, and arabinose, HRT from 24 to 3 h and pH 5, 5.5, 6 and 6.5 were evaluated, showing that the highest HPR was between HRT of 24 and 12 h, using pH 6.5 [71]. In another study, five different HRT, including 6, 9, 12, 16, and 24h, were evaluated on a dark fermentation

using fruit-vegetable waste during 47 days of operation, with a mixed culture, finding an optimum HRT of 9 h for a HPR of 11.8 NL/L/d [83].

Pilot-scale studies of hydrogen production with dark fermentation processes have not been so frequent; the use of co-substrates was evaluated in a batch process that was performed with *Enterobacter cloacae* IIT-BT 08 in 2 L bioreactor with studies at 50 L (bench scale) and 100 L (pilot scale), to produce biohydrogen with an overall enhancement of hydrogen yield at increasing the scale of the fermentation. However, some obstacles were described as the clogging in a recirculation pump and high downtime of the process, among others [8].

There has been an attempt to model different parameters such as the effect of substrate concentrations, inhibitor concentrations, temperature, pH, and dilution rates on hydrogen production. However, many models could not incorporate hydrogen partial pressure or regulation mechanisms or many parameters in parallel [84]. Recently, it was also pursued to make a quantitative analysis of literature data on hydrogen production through dark fermentation, using a statistical multi-linear regression model, finding the best performance with acidic pH, short residence time, and high substrate concentration. Still, more focus on optimization is needed to achieve higher biohydrogen yields [85].

The effect of different gas flow rates on hydrogen production through dark fermentation was evaluated in a 1 L reactor, and it was shown that between 10 to 50 mL min^{-1} of a mixture of CO_2:N_2 (75:25), an increase in hydrogen production was observed. The result was an asymptotic profile from 50 to 200 mL min^{-1} [86].

Table 2. Advantages and disadvantages of different reactor configurations

Reactor	Inoculum source	Advantages	Disadvantages	References
Continuous Stirred-Tank Reactors (CSTRs)	Anaerobic sludge, compost	- Easy design and operation - Mixing can improve gas-liquid mass transfer	- HRT limits biomass concentration when working at low RT. - Instability in H_2 production	[9,73,74]
Upflow Anaerobic Sludge Blanket (UASB) Reactors	Anaerobic sludge, compost, methanogenic granules, mixed culture, wastewater	- Granules formation brings protection to the microorganisms - High biomass retention	- Instability in the reactor can change microbial communities	[9,10]

Expanded Granular Sludge Bed (EGSB) Reactors	Granular sludge, wastewater, winery effluent	- Less mass transfer limitations in comparison to UASB - Liquid recirculation can increase the contact between the substrate and the microorganism	- Instability linked to operational conditions	[9,30]
Fixed Bed Reactors	Anaerobic sludge, wastewater	- High biomass attachment	- Liquid-gas mass transfer limitations due to overgrowth	[9]
Sequencing Batch Reactors (SBRs)	Anaerobic sludge, wastewater	- Diverse control strategies, wide instrumentation applicability, flexible operation	- Highly dependent on HRT, hydrogen production decreased with a reduction in HRT	[10,87]

1.5. Research Proposal

There is an urgent need to develop carbon-neutral technologies for energy production in order to reduce dependence on fossil fuels. Current industrial hydrogen (H_2) production is largely non-renewable and incurs high environmental and economic costs. Therefore, the development of a biohydrogen production platform represents a promising alternative. One particularly attractive option is the use of carbon monoxide (CO) from industrial waste gases as a substrate for renewable hydrogen generation, contributing to a more sustainable bioeconomy.

Parageobacillus thermoglucosidasius can produce H_2 via the water-gas shift (WGS) reaction, where CO and water are converted into H_2 and CO_2. Previous studies have demonstrated complete CO conversion in sealed bottle experiments; however, these systems were constrained by their closed environment [52]. Scaling up to bioreactor batch fermentations resulted in decreased H_2 production once glucose was depleted, despite the continued supply of CO. This observation highlighted the need for a semi-continuous system that could maintain stable H_2 production. Additionally, acetate will be tested as an alternative carbon source to glucose, offering a more realistic reflection of industrial waste streams. These studies will explore how acetate affects hydrogen production, microbial metabolism, and overall system efficiency.

Another important environmental constraint when utilizing industrial gas streams is the presence of oxygen. Although *P. thermoglucosidasius* DSM 6285 has demonstrated the ability to consume oxygen in bottles experiments and two-phase fermentation setups, the effect of oxygen on its hydrogenogenic activity has not been fully characterized. It is essential to understand how the presence of oxygen at different stages of fermentation influences hydrogen yield, microbial viability, and the organism's ability to recover from oxidative stress. A set of experiments could assess oxygen depletion kinetics and shifts in metabolic activity under these conditions.

In parallel, the feasibility of using synthesis gas (syngas) as a substrate for hydrogen production is being investigated. While previous work has shown that this microorganism can utilize various CO ratios [62], industrial syngas often contains impurities and additional gases such as methane. This research will evaluate whether *P. thermoglucosidasius* can maintain effective

hydrogen production in these more complex gas mixtures. Performance will be assessed by monitoring hydrogen yield, microbial growth, and the influence of non-ideal gas components compared to pure CO-N_2 systems.

Following confirmation of the organism's functionality with syngas, efforts will focus on scaling up to bioreactor-level fermentations to determine if laboratory findings can be replicated at a larger scale. Lastly, the role of gas partial pressure is being examined, as elevated partial pressures can enhance the solubility and availability of gases in the liquid fermentation medium. However, high concentrations of CO may also pose toxicity risks that could inhibit microbial activity and hydrogen production. The influence of increased CO, H_2, and N_2 partial pressures on the hydrogenogenic capability of *P. thermoglucosidasius* will be investigated, focusing on solubility effects, toxicity thresholds, and potential inhibitory impacts.

By addressing these key aspects, this research aims to evaluate the technological and biological feasibility of deploying *P. thermoglucosidasius* DSM 6285 in a robust, scalable, and renewable biohydrogen platform. The results will provide critical insights into the potential of this system for industrial integration and contribute to the advancement of sustainable, carbon-neutral energy solutions.

2. Fermentation process optimization

This chapter is based on the publication:

Batch and semi-continuous fermentation with *Parageobacillus thermoglucosidasius* DSM 6285 for H_2 production. Magda S. Ardila, Habibu Aliyu, Pieter de Maayer, Anke Neumann. Biotechnology for Biofuels and Bioproducts (2025), 18:3. https://doi.org/10.1186/s13068-024-02597-z

Author's Contributions:

Magda Ardila	Conceptualization and design of the experiments, analysis of the data, writing the original draft, reviewing and editing visualization
Habibu Aliyu	Conceptualization and design of the experiments, reviewing and editing, project administration
Pieter de Maayer	Reviewing and editing, project administration, funding acquisition
Anke Neumann	Conceptualization and design of the experiments, reviewing and editing, project administration, funding acquisition

2.1 Introduction

Currently, there is an extensive drive for the development of carbon-neutral technologies for energy production, mitigating the negative environmental effects and overreliance on finite fossil fuel reserves [31]. Hydrogen (H_2) has emerged as an attractive and versatile energy carrier with a high energetic yield, producing only water during combustion [2,3,6,7]. Given the high costs and non-carbon-neutral nature of current industrial H_2 production strategies, increasing research has focused on the development of biological means for production [31]. Explored approaches include direct and indirect bio-photolysis, microbial electrolysis cells, and photo- and dark fermentations [7,8]. More recently, research has focused on hydrogenogenic carboxydotrophic microorganisms that can produce H_2 using carbon monoxide (CO) as an energy and/or carbon source [35,88]. These make use of two metalloenzymes namely a nickel-containing carbon monoxide dehydrogenase (NiFe-CODH) and an energy-conserving NiFe-hydrogenase to catalyze the water-gas shift (WGS) reaction, where CO reacts with water to produce hydrogen and carbon dioxide (CO_2) [20,28,35,37,89]. CO is an inexpensive compound, present not only in syngas but in other waste gases, and hence, using this substrate for biohydrogen production has the added benefit of reducing carbon emissions [28].

Parageobacillus thermoglucosidasius is a thermophilic, Gram positive, rod shaped bacterium in the family Anoxybacillaceae and the phylum Bacillota, which has previously been shown to produce H_2 gas from CO using the WGS reaction, using a unique carbon monoxide dehydrogenase (CODH) hydrogenase enzyme complex [52,60,90,91]. Unlike most other hydrogenogenic carboxydotrophs, which are strict anaerobes, this taxon is a facultative anaerobe, that can grow in the presence of atmospheres containing air and CO, but then shifts to the WGS reaction once oxygen has been consumed [60,91]. A lag phase between O_2 depletion and the beginning of H_2 production has been described, and different parameters were optimized to reduce this lag phase in batch experiments with *P. thermoglucosidasius* DSM 6285 [52].

This study aimed to further increase H_2 yield and reduce the lag phase before H_2 production with *P. thermoglucosidasius* DSM 6285. To achieve this, two-phase semi-continuous fermentations containing an aerobic and anaerobic step were performed in 2.5 L stirred tank reactors and compared to a batch fermentation strategy.

2.2 Materials and methods

2.2.1 Microorganism and Media

Parageobacillus thermoglucosidasius DSM 6285 was obtained from the Deutsche Sammlung von Mikroorganismen und Zellkulturen (DSMZ, Braunschweig, Germany) and was conserved in glycerol (80%) stocks at − 80 °C. Routine cultivation of *P. thermoglucosidasius* DSM 6285 was performed in mLB (modified Luria–Bertani) medium containing tryptone (10 g/L), yeast extract (5 g/L), NaCl (5 g/L), 1.25 mL/L NaOH (10 g/L) and 1 mL/L of each of the filter-sterilized stock solutions 1.05 M nitrilotriacetic acid, 0.59 M $MgSO_4 \cdot 7H_2O$, 0.91 M $CaCl_2 \cdot 2H_2O$ and 0.04 M $FeSO_4 \cdot 7H_2O$, as described before [52]. The reactor medium used was mASM (modified ammonium sulfate) medium, containing 8.7 mM citric acid, 20.2 mM MgSO4, 10 mM K_2SO_4, 22.6 mM NaH_2PO_4, 0.8 mM $CaCl_2$, 25 mM $(NH4)_2SO_4$, 4.162 mM glucose, and the trace elements in the final concentration of 0.012 mM H_2SO_4, 0.002 mM $CuSO_4$, 0.004 mM $CoSO_4$, 0.010 mM $ZnSO_4$, 0.046 mM $FeSO_4$, 0.006 mM $NiSO_4$, 0.018 mM $MnSO_4$ and 0.002 mM H_3BO_3 [60,62].

2.2.2 Inoculum preparation

A volume of 300 µL of glycerol stock was added to 200 mL of mLB medium in 500 mL shake flasks and grown under aerobic conditions at 60 °C and rotation at 120 rpm in an Infors Thermotron (Infors Thermotron, Infors AG, Bottmingen, Switzerland). The shake flask were closed using stoppers and covered with aluminum foil, which helped to reduce evaporation of the media, in addition to the short incubation time. After 14 h, a calculated volume of the inoculum was added to the reactors to achieve an initial absorbance (OD_{600}) of 0.1 for a total volume of 1 L.

2.2.3 Experimental Setup

Batch fermentation

Batch fermentation was performed in two bioreactors of 2.5 L capacity (Minifors, Infors AG, Bottmingen, Schweiz) with a 1 L working volume for 11 days. The stirrer speed was set to 500 rpm, temperature to 55 °C and pH to 6.8; the pH was routinely monitored using a pH probe (model, manufacturer country) and controlled with NaOH (1 M) and H_2SO_4 (1 M) via a peristaltic pump connected to the reactor system. The fermentation was performed in two phases. First, fermentation was performed using a continuous flow rate of 4.46 mmol min^{-1} of air and CO for 24 hours. This was performed by sparging the liquid through the microsparger present in the reactor. Subsequently, the headspace gas was exchanged with 3.57 mmol min^{-1}

of a mixture of 20% CO and 80% nitrogen. During the gas exchange, the headspace of the reactor was flushed for 10 min with N_2 at a flow rate of 0.1 L min^{-1} to reduce the oxygen content in the reactor.

Semi-continuous fermentation

The semi-continuous fermentation was performed following the set-up described for the batch fermentation. During each feed, 60 mL of fresh mASM medium was fed while removing the same volume of media at a rate of 1 mL min^{-1}. For each reactor, a liquid sample (1 mL) was collected in triplicate at each sampling time to evaluate growth by absorbance and the metabolic profile through an HPLC analysis. An additional sample of 5 mL was withdrawn to evaluate the CODH activity

2.2.4 Analytical methods

The gas composition of the bioreactor head space was evaluated online with a 3000 Micro GC gas analyzer (Inficon, Switzerland) connected with Molsieve columns and PLOT Q for data acquisition. The absorbance (OD_{600}) was measured using the Ultrospec 1100 pro spectrophotometer (Amersham Biosciences, Uppsala, Sweden). The samples for HPLC analysis were diluted 1:5 with ddH_2O; prior to storage at -20 °C. After thawing for the analysis, samples were transferred into 1.5 mL HPLC vials. A 5 mM H_2SO_4 solution was used as the mobile phase, 55 °C was selected as the column temperature, and samples were analyzed at a flow rate of 0.6 mL min^{-1} flow rate for 40 min per sample and injection volume of 10µL. HPLC was undertaken using the Agilent 1100 series HPLC system (Agilent Technologies, Waldbronn, Germany) was used, equipped with a wavelength detector and refractive index detector with a 50 mm long pre-column (model Rezex ROA-Organic Acid H^+ 8% Guard Column) and a 300 mm long separation column (model Rezex ROA-Organic Acid H^+ 8%). Data acquisition and analysis were performed with the software Chemstation (Agilent Technologies). The gas composition was calculated according to the ideal gas law, as described before [59]. The electron selectivity was used to show the electron flux in the process. This was calculated from the electron mole (e^- mol) of each compound. Additional information on the calculations can be found in Additional File 1 (Supplementary material 1).

2.2.5 CODH enzyme assay

CODH enzyme activity was evaluated using a colorimetric enzyme assay based on reducing methyl viologen (MV) under anaerobic conditions [92,93]. The reduction of 10 mM MV^{2+} dichloride solution in 50 mM Tris-HCl to MV^+ along the oxidation of CO to CO_2 results in the

change of color of the solution to dark violet color (Equation 1). One unit of CO dehydrogenase activity is defined under these conditions as that amount required to catalyze the reduction of 1 µmol min^{-1} methyl viologen.

$$CO + H_2O + 2\,MV^{2+} \leftrightarrows CO_2 + 2MV^{+} + 2H^{+}$$

The reaction was performed by filling a glass cuvette (Synthetic quartz glass, Hellma Analytics) with 1 mL of MV dichloride solution (pH 8) in a vinyl anaerobic chamber (Type B with incubator, Coy Laboratory Products, Inc.); each cuvette was closed with a rubber stopper and flushed with CO for 3 min (0.1 bar). Subsequently, 2-5 µL of Titanium (III) citrate solution (2 M Na_2CO_3, 0.4 M $Na_3C_6H_5O_7$, 15% $TiCl_3$) was added, followed by 100 µL of the sample supernatant. Absorbance was measured for 30 minutes at 578 nm (Ultrospec 2100 pro, Amersham Biosciences).

2.6 Results

2.6.1 The effects of semi-continuous fermentation on hydrogen production rates and yield

Batch fermentations were first performed, where *P. thermoglucosidasius* DSM 6285 was grown in duplicate STR bioreactors containing defined modified Ammonium Sulphate Medium (mASM) [62] and fed with a continuous flow of CO. Consumption of CO started on day 2 concomitant with the production of H_2 in the reactors. A maximum hydrogen production rate (HPR) of 0.144 ± 0.002 mmol min^{-1} was observed on the fourth day of fermentation (Figure 4A), followed by decreased H_2 production throughout the remainder of the fermentation, plausibly due to the growth-limiting conditions imposed by the complete consumption of glucose and build-up of toxic metabolites. The semi-continuous approach, undertaken in the same STR reactors, involved the feeding of the bioreactors with 60 mL d^{-1} mASM medium containing 5.5 mM glucose every 24 or 48 hours. Similar to the batch fermentation, the gas flow was kept constant throughout the fermentation.

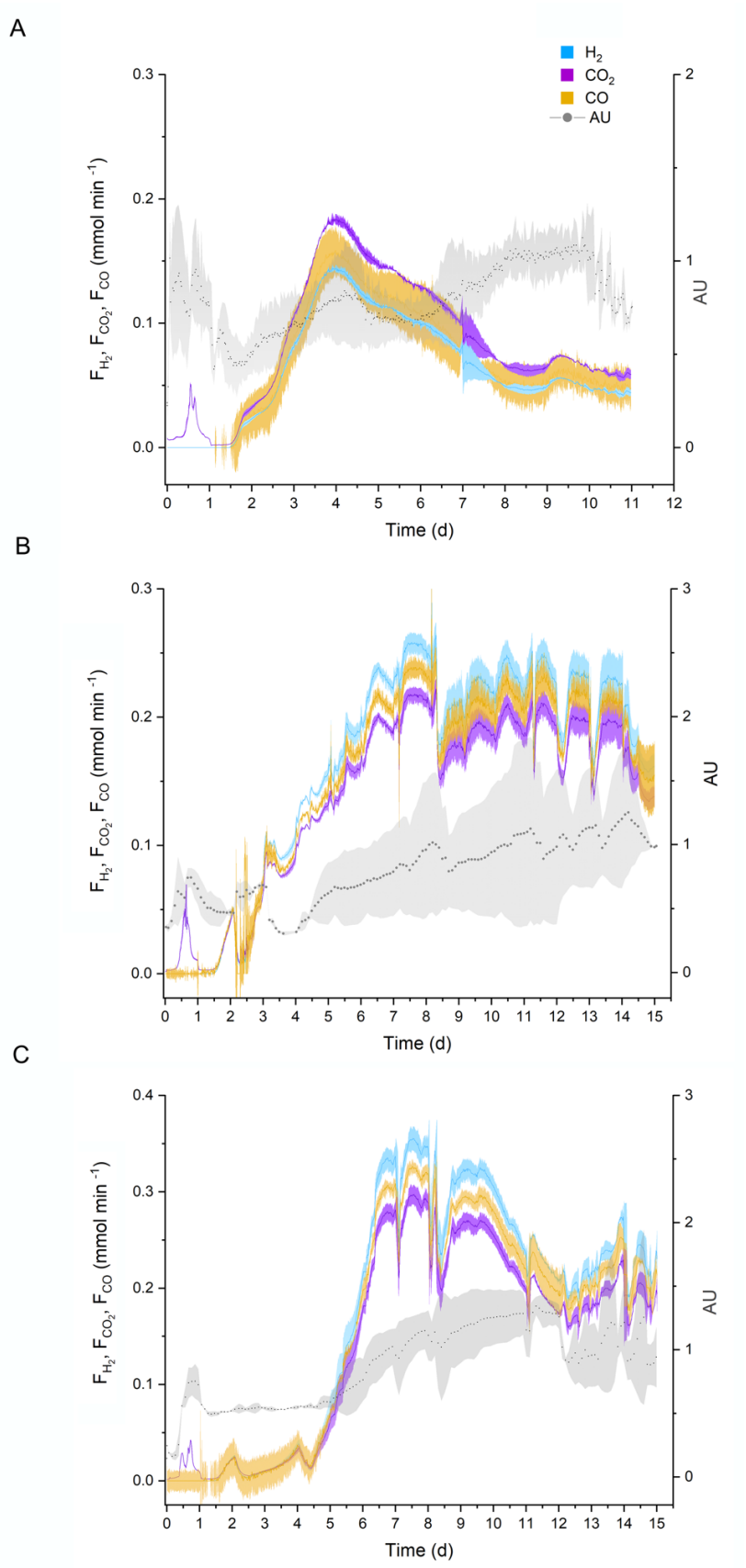

Figure 4. Fermentations in mASM medium. *P. thermoglucosidasius* DSM 6285.

The H_2 and CO_2 production rate (mmol min^{-1}) and the CO consumption rate (mmol min^{-1}) are the average of two bioreactors, with the standard deviation indicated by the colored regions. The biomass, measured as absorbance units (AU), is depicted as a grey line. The aerobic phase ends after 24 h with gas exchange. a) Batch fermentation over 11 days. b) Semi-continuous fermentation with feeding every 24 hours, starting from day 2. c) Semi-continuous fermentation with feeding every 48 hours starting from day 2 (Figure adapted from the published version for improved clarity).

The 24-hour interval feeding proportionated the first stable hydrogen production after six days of fermentation. Hydrogen production started from the second day, increasing to 0.26 ± 0.01 mmol min^{-1} by day 7, a volumetric HPR of 7.98 L H_2 L^{-1} d^{-1}, with a hydrogen yield of 0.22 mmol H_2/mmol CO of a flow rate of 0.71 mmol CO min^{-1}. CO consumption increased from the second until seventh day, and remained stable throughout the rest of the fermentation (Figure 4B). With the 48-hour interval feeding, H_2 production was delayed to day 7 of the fermentation, when it increased to an HPR of 0.32 ± 0.01 mmol min^{-1} and a volumetric HPR 11.91 L H_2 L^{-1} d^{-1} (Figure 4C). Subsequently, instability in the H_2 production profile was observed, decreasing to 0.23 ± 0.02 mmol min^{-1} on day 8, followed by recovery 0.32 ± 0.01 mmol min^{-1} by day 9, before decreasing to a minimum HPR of 0.188 ± 0.01 mmol min^{-1} (7.65 L H_2 L^{-1} d^{-1}) by day 13. This was likely due to the formation of foam, which caused changes in the CO uptake rate from day 11.

2.6.2 Relationship between HPR and CODH activity

To determine whether H_2 production and enzyme activity were correlated, CODH activity was measured for the batch and semi-continuous fermentations using previously described spectrophotometric assays based on methyl viologen reduction [92,93]. For the batch fermentation, the activity was measured from the second day of fermentation, after the gas exchange, as H_2 production started. The maximum activity, 599 U mL^{-1}, was achieved on the fourth day of fermentation and corresponded to the peak of H_2 production with an HPR of 0.144 mmol min^{-1} and a volumetric HPR of 4.62 L H_2 L^{-1} d^{-1} (Figure 5A). From day 5 to day 11, a reduction of the CODH activity was observed, in parallel with the drop on HPR during batch fermentation.

CODH activity was lower than 10 U mL^{-1} for both 24-hour and 48-hour interval fed fermentations on day 3, but increased substantively throughout the remainder of the fermentations. The activity was measured for both intervals from day 3 of the fermentations until day 14. Overall, CODH activity was higher with the 48-hour interval feeding, and reaching a maximum activity of 1651 U mL^{-1} on day 14 (Figure 5C). The lag phase prior to H_2 production was longer with the 48-hour interval feeding and this correlates with a lag in CODH activity. The CODH activity also remained more stable in the semi-continuous fermentation with 24-hour feeding interval, at around 200 U mL^{-1} from day 6 to 10, which was also a period of stable H_2 production. By contrast with the 48-hour interval feeding, peaks and troughs in H_2 production were observed, which can also be correlated to peaks and troughs in the WGS enzymatic machinery. For example, a low HPR (0.287 mmol min^{-1}) on day 8 of the fermentation is associated with a low CODH activity of 316 U mL^{-1}. It should be noted that for each feeding interval, at some sampling points, extensive differences in CODH activity were noted between the duplicate bioreactors for each feeding strategy, which could, in the future, be addressed by performing additional sampling. When comparing the batch with the semi-continuous fermentations, CODH activity is constant after the highest point of H_2 production during the batch and the 24-hour interval fermentations, suggesting that the enzyme is active throughout fermentation.

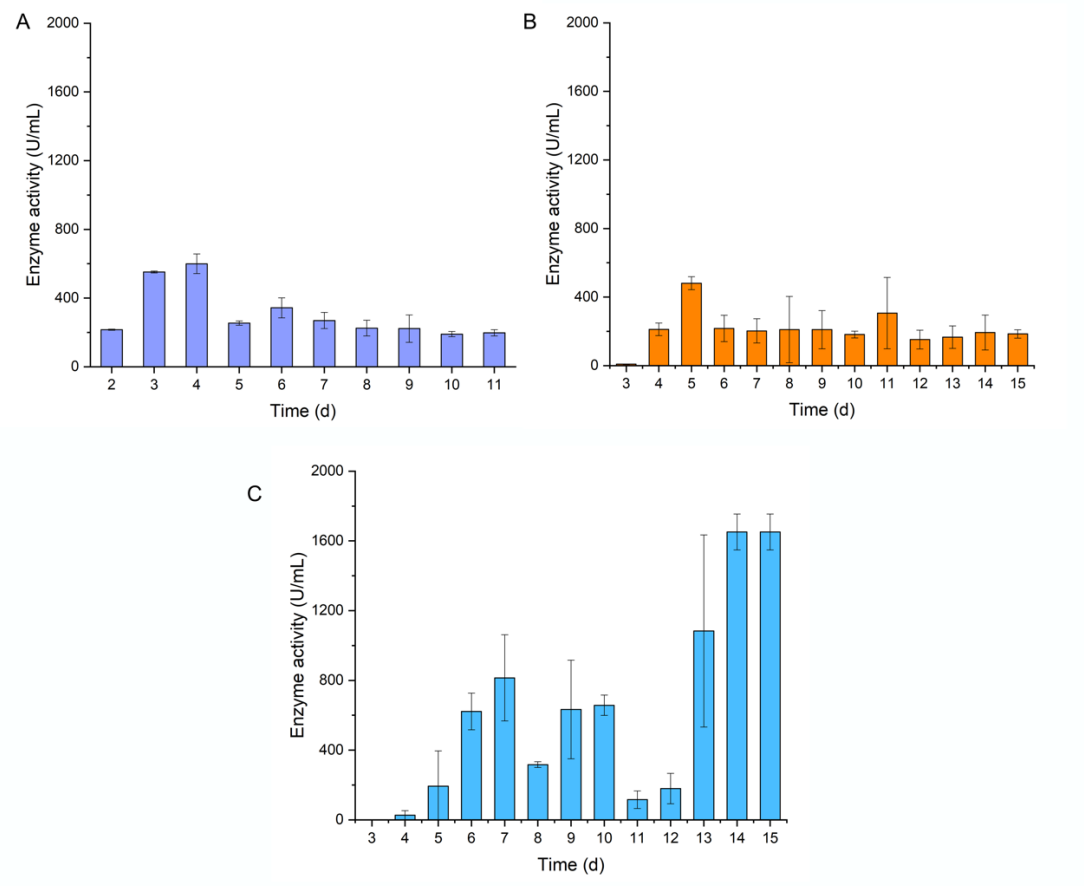

Figure 5. CODH enzyme activity for a) batch fermentation, b) feeding every 24 h, and c) 48 h. The enzyme activity for the semi-continuous fermentations was measured from the third day of fermentation.

2.6.3 Metabolites analysis during the fermentations

The metabolic profiles of *P. thermoglucosidasius* DSM 6285 during the batch and both 24-hour and 48-hour interval feeding semi-continuous fermentations were evaluated using High Performance Liquid Chromatography (HPLC) analysis. Under aerobic conditions, *P. thermoglucosidasius* produces acetate, lactate, succinate, glyoxylate and a spectrum of other metabolites, while when growing anaerobically in a CO-containing atmosphere, more extensive acetate production has been reported [62]. As observed in Figure 6, four key metabolites were observed in the batch and semi-continuous fermentations, formate, acetate, lactate, and propionate, while other metabolites such as butyrate, glyoxylate, ethanol, valerate, and citrate were below the detection limit of the HPLC method (<0.1 g L^{-1}). After glucose and acetate depletion in the batch fermentation, at day 4, is possible that citrate is consumed, which could

explain the increase in growth from day 7 to 10. However, this has not been described before. It is also known that *P. thermoglucosidasius* has genes linked to the citrate cycle [60].

Formate was the primary metabolic product observed in both batch and semi-continuous fermentations. The second most prevalent metabolite, acetate was produced primarily in line with glucose consumption in the batch fermentation and subsequently tapered off, while in the semi-continuous fermentation it continued to increase largely in parallel with glucose addition. Key differences were observed between the batch and semi-continuous fermentations in terms of propionate and lactate production. Limited propionate production was observed in the semi-continuous fermentations with 48-hour feeding interval. Similarly, while negligible lactate production was observed in the batch fermentations, large amounts of lactate up to 18.3 mmol and 9.5 mmol by 15 days were produced in both semi-continuous fermentations. This could be due to the additional glucose in the media that routes the metabolism to organic acid production, and the consumption of acids after each feeding reduces accumulation that can be detrimental for the microorganism growth.

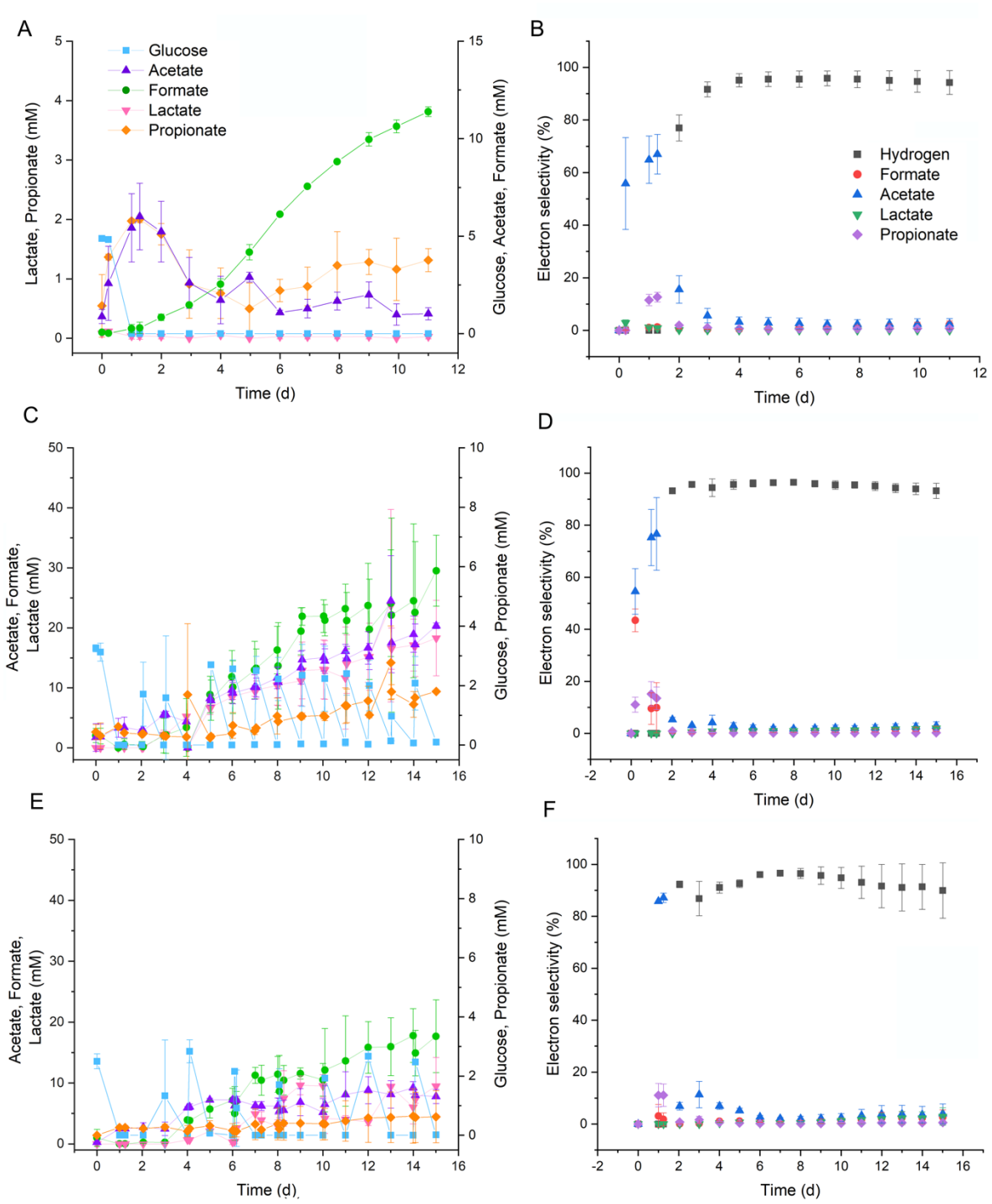

Figure 6. Metabolites during the two-phase fermentations in mASM medium. The aerobic phase ends after 24 h with gas exchange. *P. thermoglucosidasius* DSM 6285 was cultivated at 55°C, 500 rpm, and pH 6.8. The concentration of the metabolites is the average of two bioreactors, with error bars indicating standard deviation. Metabolite concentration for the a) Batch fermentation, c) 24-hour feeding and e) 48-hour feeding. Electron selectivity for the b)

batch, d) 24-hour feeding, and f) 48-hour feeding semi-continuous fermentations, respectively (Figure adapted from the published version for improved clarity).

Formate production rate was constant throughout the fermentation with the 24-hour feeding strategy, reaching a maximum of 2.41 ± 0.16 mmol d^{-1}. Acetate reached a maximum production rate of 9.15 ± 0.55 mmol d^{-1} by 0.2 days and 1.36 ± 0.03 mmol d^{-1} by the end of the fermentation. Lactate had a maximum production rate of 1.82 ± 0.23 mmol d^{-1} on day 13 and later reduced to 1.22 ± 0.41 mmol d^{-1} by day 15. Propionate had a maximum production rate of 1.52 ± 0.15 mmol d^{-1} on day 1, but throughout the fermentation, the production rate was lower than 1 mmol d^{-1}. Glucose was consumed by the first day of fermentation, and it increased after the glucose-containing feeding and depleted by the next day. The 48-hour feeding strategy also had formate as the main metabolic product, with production rate 1.61 ± 0.18 mmol d^{-1} by day 7. Acetate had a maximum production rate of 2.51 ± 0.37 mmol d^{-1} on day 1. Lactate started to be produced from day 4 and had a maximum production rate of 1.07 ± 0.17 mmol d^{-1}. The propionate production rate was below 0.5 mmol d^{-1} throughout the entire fermentation. Glucose consumption was observed one day after the feeding, as observed with the 24-hour feeding strategy.

The production of metabolites is significantly shifted to more reduced products, such as H_2. This is also shown in the electron selectivity, as at the beginning of the fermentations, the electrons coming from glucose were routed into acetate. As soon as the gas exchange was performed on the first day of fermentation, most of the electrons coming from CO and glucose shifted primarily towards H_2 production.

2.7 Discussion

Continuous fermentation has several advantages over batch fermentation, which is often hampered by substrate limitation and product inhibition, shorter microbial exponential growth phase, and the additional time and cost of cleaning and sterilization of the reactor, ultimately leading to lower productivity [94]. Here we employed both batch and semi-continuous fermentations to evaluate their effect on WGS-driven hydrogenogenesis by the facultative anaerobic thermophile *P. thermoglucosidasius*. Furthermore, two distinct feeding intervals, 24 hourly and 48 hourly, were evaluated for the semi-continuous mode.

In our study, the semi-continuous mode with feeding every 24 hours increased H_2 yield by 18% compared with batch fermentation, and the process could be extended to a longer period. Hydrogen yields declined after 4 days in the batch fermentation, while sustained H_2 production was achieved over the evaluated period of 15 days with the 24-hour interval feeding semi-continuous fermentations. Similarly maintained H_2 production has been observed in experiments with a dark fermentative microbial consortium grown with cheese whey permeate that was replaced 12 and 24 hourly [80].

Foam formation hampered the 48-hour feeding interval semi-continuous fermentations, where the foam can affect the gas transfer to the liquid phase, creating a barrier in the headspace [95]. This precluded meaningful comparison of the effect of different feeding intervals on *P. thermoglucosidasius* hydrogenogenesis. Although there are many strategies to minimize foam, such as defoaming agents and mechanical disruption, the constant change of the medium in fed-batch fermentations is also an alternative [96], as observed with the 24-hour feeding interval employed in the study.

While the 24-hour feeding interval semi-continuous fermentation facilitated stable hydrogen production for more than 7 days, variations were observed between duplicate bioreactors with both feeding intervals. A broad range of operating parameters, such as gas composition, inoculum size, temperature, pH, stirring rate, and media composition [52], can affect H_2 production. As such, additional bioreactor and inoculum parameters will need to be evaluated to optimize the semi-continuous fermentation and its reproducibility.

The semi-continuous supplementation with glucose affected the fermentative metabolism of *P. thermoglucosidasius* in several ways. Primarily, in the semi-continuous fermentations substantive acetate and lactate were produced in line with glucose consumption, while these were negligible byproducts of the batch fermentation. Acetate was consumed, once glucose was depleted during the aerobic phase via the presumably TCA cycle, also described by [62]. Once the gas exchange step reduces oxygen of the gas phase, CO consumption through the WGS reaction commences and H_2 production starts, however as glucose is added to the feeding, there is a flux of electrons to the production of organic acids mainly acetate, formate, and lactate from pyruvate following glucose metabolism pathways [62]. Under anaerobic metabolism, glucose is oxidized into two molecules of pyruvate, while NAD^+ is reduced to NADH, afterwards, pyruvate is converted into acetate, and NAD^+ is regenerated, maintaining glucose oxidation [97]. In our work, all fermentations produced acetate, formate, and lactate suggesting this

metabolic route. In addition to glucose, or lack thereof, amino acids in the ASM media such as L-alanine and L-cysteine could be metabolized into pyruvate generating NADH [98]. *P. thermoglucosidasius* DSM 6285 can produce H_2 via the WGS reaction, catalyzed by the CODH [52]. CODH is sensitive to oxygen at the protein levels [99]. The regulation of the CODH genes is still unclear [60]. The presence of two uptake hydrogenases and one H_2-evolving hydrogenase in *P. thermoglucosidasius* makes this microorganism distinctive from others, even more so that it has an anaerobic CODH [59]. Spectrophotometric assays based on methyl viologen reduction were used to evaluate CODH activity as proxy for hydrogenase activity in the batch and semi-continuous fermentations [93,100,101].

We observed that the CODH activity was constant in both batch and semi-continuous fermentations after reaching the highest H_2 production. When comparing the feeding intervals, it was noticed that during the 24-hour, CODH activity remained stable alongside a period of stability in H_2 production, while when evaluating the enzymatic activity with the 48-hour interval feeding, the overall instability of the H_2 production reflected the observed variability in the spectrophotometric assays. Nevertheless, certain drawbacks must be taken into consideration. This is evidenced by the differences in CODH activity between the duplicate reactors at several time points, due to the sensitivity of the CODH activity assay to oxygen [99]. Although methyl viologen acts as an artificial electron donor and shares similarities with the natural electron donor, it is not identical [102]. Additionally, variations in reaction conditions and redox potential have a pronounced effect on the reliability and reproducibility of the assay [103,104].

In conclusion, enhanced HPR and extended operational stability were attained using semi-continuous fermentation with a 24-hour feeding strategy. Persistent challenges with the 48-hour feeding interval, however, underscore the need for further optimization of the semi-continuous fermentation approach for WGS-driven hydrogenogenesis with *P. thermoglucosidasius.* Further evaluation of different feeding rates, environmental conditions and better control and monitoring of foam formation, can mitigate operational challenges to the semi-continuous strategy and concomitantly improve hydrogen productivity over extended fermentation periods.

Acknowledgments

We acknowledge support by Mona Urich from the Karlsruhe Institute of Technology, Germany.

3 Oxygen perturbation and syngas as substrate

This chapter is based on the publication:

The effects of synthesis gas feedstocks and oxygen perturbation on hydrogen production by *Parageobacillus thermoglucosidasius*. Michael Mol, Magda S. Ardila, Bronwyn Ashleigh Mol, Habibu Aliyu, Anke Neumann, and Pieter de Maayer.
Microbial Cell Factories, 2024.

Author's Contributions:

Michael Mol	Planning of experiments, collection and analysis of the data, stadistical analysis of the data, preparation of figures, tables and additional files, draft the manuscript.
Magda Ardila	Planning of experiments, collection and analysis of the data, draft the manuscript.
Bronwyn Ashleigh	Stadistical analysis of the data.
Habibu Aliyu	Planning of experiments, draft the manuscript.
Pieter de Maayer	Planning of experiments, draft the manuscript.
Anke Neumann	Planning of experiments, draft the manuscript.

3.1 Introduction

Increasing energy demands and dwindling fossil fuel reserves are driving the development and implementation of environmentally friendly energy production technologies, using renewable resources [105]. Hydrogen (H_2) gas is regarded as an ideal energy carrier, with carbon neutral combustion characteristics and high energy density [106]. While H_2 gas is currently produced almost exclusively through the reformation of non-renewable fossil fuels, various alternative renewable H_2 gas production processes have and are currently being developed [107].
Numerous microbial taxa are capable of producing H_2 gas from a wide spectrum of organic and inorganic feedstocks in an environmentally friendly and energetically favourable manner [108,109]. These are subdivided into light dependent and independent processes with those incorporating dark-, photo-, and hybrid-fermentative processes having dominated mainstream research [108].

Despite yielding promising results, these processes are hindered by limitations such as cost, feedstock availability/suitability, turnover rate and scalability, that restrict their industrial application [107]. Less well-explored hydrogenogenic processes such as the biological water–gas shift (WGS) reaction, are promising alternatives to the aforementioned systems.
The reversible WGS reaction involves the oxidation of carbon monoxide to carbon dioxide and the reduction of water to molecular hydrogen at an equimolar ratio ($CO + H_2O \rightarrow CO_2 + H_2$ $\Delta G^{O\prime} = -20$ kJ/mol CO) [35]. The potential to conduct the WGS reaction has been identified in more than twenty-five bacterial species spanning the phyla Proteobacteria, Firmicutes and Dictyoglomi and among four archaeal species in the phyla Crenarchaeota and Euryarchaeota [110]. The biological WGS reaction has been best characterised in the mesophilic proteobacterium *Rhodospirillum rubrum*, the thermophilic Firmicutes *Carboxydothermus hydrogenoformans* and *Parageobacillus thermoglucosidasius* and the hyperthermophile *Thermococcus onnurineus* in the phylum Euryarchaeota [59,108,111,112]. The reaction proceeds via a carbon monoxide dehydrogenase (CODH)/H2 evolving hydrogenase enzyme complex [88,113,114]. Both the CODH and H_2 evolving hydrogenase enzymes are highly sensitive to O_2, greatly restricting their industrial applicability [114,115]. Although several hydrogenases demonstrate greater O_2-tolerance, they exhibit poorer H_2 gas turnover efficiencies [116]. As such, the majority of bacterial taxa capable of conducting the WGS reaction are strict

anaerobes. One exception, however, is the facultatively anaerobic thermophile *P. thermoglucosidasius*, which carries a Ni-CODH/NiFe group 4a hydrogenase complex and is capable of the WGS reaction following oxygen depletion [59,60,91,117].

By optimising growth medium composition and pH, fermentation temperatures and CO concentration, H_2 gas production yields have been improved [52], but further developments towards industrial application are necessary. Key foci include progression of the process towards more continuous operation and evaluation of system efficiency when utilising gas feedstocks more reflective of industrially/commercially available waste gases. Industrial waste gasses or synthesis gases (syngas) are highly variable, typically comprising CO, H_2 and CO_2. Impurities including tars, particulate carbon, light hydrocarbons, inorganic compounds (sulfur-, nitrogen-, halogen- and metal-incorporated compounds) and O_2 are also typically found at low levels [118,119].

Here we investigated the effects of gas feedstocks, with compositions more reflective of industrial waste gases, on H_2 gas production by *P. thermoglucosidasius* through bioassays in conjunction with GC and HPLC analysis of select gases and metabolites. Furthermore, as optimal *P. thermoglucosidasius* growth is observed under aerobic atmospheres, balancing aerobic conditions conducive to sustained biomass accumulation and anaerobic conditions obligatory for H_2 production is necessary for more advanced continuous/semi-continuous hydrogenogenic operation. Therefore, the impacts of temporal and volumetric O_2 perturbations (as would occur with industrial and syngas) on *P. thermoglucosidasius* DSM 6285 hydrogenogenesis were further evaluated in this study.

3.2 Materials and methods

3.2.1 Strains and media

P. thermoglucosidasius DSM 6285 was maintained and cultured routinely in modified Luria Bertani medium (mLB) [59]. Experimental cultures were grown in modified ammonium sulphate medium (mASM) [62].

3.2.2 Experimental setup

Pre-cultures were grown in 100 mL mLB in 500 ml baffled shake flasks, inoculated with 40 µL of glycerol stock and incubated aerobically at 55 °C for 14 h at 120 rpm in an Infors HT Thermotron (Infors AG, Bottmingen, Switzerland). Following incubation, appropriate volumes of pre-culture were used to inoculate experimental cultures to an initial OD_{600} of ~ 0.1. Experimental cultivations were conducted in 250 ml serum bottles sealed with a rubber stopper, containing 50 mL ASM with differing gas headspace compositions at atmospheric pressure. To investigate the effects of variable industrial syngas mixtures on the *P. thermoglucosidasius* DSM 6285 WGS reaction, the strain was cultured in several gas headspace atmospheres (Table 3). Four sets of experimental cultures were cultivated in triplicate. The first set served as an aerobic control grown under an optimal gas atmosphere composed of 50% air and 50% CO. The second set served as an anaerobic control, with a gas headspace composed of 50% N_2 and 50% CO. This was achieved by flushing bottle headspaces with N_2 for 5 min at a flow rate of 0.2 L/minute, followed by injection of the bottles with CO to an overpressure of 1 bar, with subsequent equilibration to atmospheric pressure. The third culture set was cultured under an initial gas headspace comprising 50% N_2 and 50% synthetic syngas mixture (Table 3; Air Liquide, Düsseldorf, Germany). This was achieved by flushing bottle headspaces with N_2 for 5 min at a flow rate of 0.2 L/minute, then injecting the bottles with the synthetic gas mixture to an overpressure of 1 bar, followed by subsequent equilibration to atmospheric pressure. The fourth culture set was cultivated under a 100% atmosphere of the synthetic syngas mixture. Following inoculation, bottles were incubated at 55 °C for 134 h at 120 rpm.

Table 3. Composition of synthetic syngas stock and initial gas headspace mixtures

	Gas Component (%)								
Atmosphere	CO_2	CO	CH_4	N_2	H_2	C_4H_{10}	C_2H_6	C_3H_8	O_2
Synthetic syngas stock	~43.99	36.90 ± 0.07	6.22 ± 0.12	5.07 ± 0.10	3.64 ± 0.07	2.42 ± 0.05	1.03 ± 0.02	0.73 ± 0.01	0
Aerobic Control	0.42 ± 0.03	48.61 ± 0.11	0	39.73 ± 0.10	0	0	0	0	9.93 ± 0.73
Anaerobic (N_2) Control	0.31 ± 0.05	45.51 ± 0.36	0	52.90 ± 0.44	0	0	0	0	0

Syngas 50% mixture*	17.08 ± 1.64	17.28 ± 0.77	3.91 ± 0.37	59.37 ± 2.02	1.05 ± 0.01	~1.21	~0.52	~0.37	0
Syngas 100% mixture*	41.65 ± 1.60	38.01 ± 0.92	6.30 ± 0.09	9.68 ± 0.50	3.11 ± 0.00	2.42 ± 0.05	1.03 ± 0.02	0.73 ± 0.01	0

*Theoretical composition inferred from dilution of stock gas.

To investigate the influence of O_2 addition on WGS reaction-driven hydrogenogenesis, two experiments were conducted. In all cases, the serum bottle gas headspace of each stoppered replicate was reconstituted to an ideal initial atmosphere of 50% air and 50% CO prior to inoculation [62]. This was achieved by flushing bottles with CO to an overpressure of 1 bar, then equilibrating the headspace to atmospheric pressure. O_2 was injected into the gas headspace of bottles containing actively fermenting cultures at various stages of the fermentation. Four time points (post-inoculation) were selected for O_2 addition, reflective of distinct periods of the WGS reaction fermentation profile [60]. These included the mid aerobic phase (14 h), the commencement of the anaerobic phase (24 h), the early-mid hydrogenogenic phase (38 h) and the late hydrogenogenic phase (48 h). The experiment was carried out in two batches, comprising three sets of cultures, one control and two experimental cultures, respectively. In each batch, cultures were cultivated in triplicate with one set serving as a control where no O_2 was added at any timepoint. The two remaining culture sets in each batch were designated a time point where a defined volume of O_2 was injected. O_2 volumes injected were ~ 5% of the initial serum bottle gas headspace volume, calculated as $vO_2 = v_t - v_m - v_i$, where vO_2 = volume O_2 added, v_T = total serum bottle volume, v_m = volume of the liquid culture medium and v_i = inoculum volume. Following inoculation, bottles were incubated at 55 ˚C for 120 h at 120 rpm, with O_2 being added to the appropriate replicate set at the designated time points.

Finally, the influence of different volume O_2 additions on the WGS system at a single time point was investigated. A 38-h post-inoculation timepoint, representative of the peak hydrogenogenic period, was selected based on the fermentation profiles of the previous experiments. Five sets of experimental cultures were cultivated in triplicate under a gas atmosphere of 50% air and 50% CO, with one set serving as a control where no O_2 was added. Each of the four remaining culture sets were designated an O_2 volume to be injected at 38 h, either ~ 1, 3, 5 or 10% of the initial serum bottle gas headspace volume, calculated as described

above. Following inoculation, bottles were incubated at 55 ˚C for 120 h at 120 rpm, with the appropriate O_2 volumes being added to the respective replicate sets at 38 h.

3.2.3 Sampling and analytics

Liquid culturing medium and gas headspace sampling was conducted at various time points for each experiment. For the experiment where different syngas mixtures were evaluated, samples were taken at 0, 14, 24, 38, 48, 62, 72, 86, 96, 110, 120 and 134 h post-inoculation. For the first oxygen supplementation experiment, where a fixed O_2 volume was supplemented at various timepoints in the WGS reaction fermentation, sampling points were 0, 10, 14, 24, 34, 38, 48, 58, 72, 84, 96, 110 and 120 h post-inoculation. Sampling points for the final experiment, where variable O_2 volumes were supplemented during the peak hydrogenogenic period were 0, 14, 24, 38, 41, 44, 48, 62, 72, 86, 96, 110, 120, and 134 h post-inoculation. In both O_2 addition experiments, prior to the addition of O_2 at applicable time points, both a liquid and gas sample were taken and immediately followed by a second gas sampling post-O_2-addition. A volume of 3 mL gas headspace was drawn at each time point and analyzed using a 300 Micro GC gas analyzer (Inficon, Switzerland), with argon and helium as carrier gases connected with Molsieve 5 Å and PLOT Q columns for data acquisition. Gas composition was calculated based on the ideal gas law as previously described [59]. Headspace pressure was determined before sampling using a manometer (GDH 14 AN, Greisinger electronic, Regenstauf, Germany) and temperature was maintained at 60 ˚C. A volume of 1 mL of liquid culture medium was sampled at each sampling point for growth and used for subsequent HPCL analysis. Growth was estimated using absorbance (OD_{600}) values using an Ultrospec 1100 pro spectrophotometer (Amersham Biosciences, Uppsala, Sweden) and pH was measured using a Profilab pH 597 (Xylem Analytics, Weilheim, Germany).

Following absorbance and pH measurement, samples were centrifuged at 16,000 × g for 10 min and supernatants transferred to a clean 1.5 mL microcentrifuge tube for storage at − 20 ˚C. Thawed supernatants (100 µL) were dispensed in 1.5 mL HPLC autosampler vials fitted with micro-inserts. Glucose and twelve central carbon metabolites (1-propanol, acetate, butyrate, ethanol, formate, glyoxylate, iso-butyrate, iso-valerate, lactate, propionate, succinate and valerate) were monitored over 0–2.0 g/L concentration ranges. Samples were analyzed using an Agilent 1100 series HPLC system (Agilent Technologies, Waldbronn, Germany) connected

to a wavelength detector and refractive index detector with a 50 mm long pre-column (model Rezex ROA-Organic Acid H+ 8% Guard Column) and a 300 mm long separation column (model Rezex ROA-Organic Acid H+ 8%). Analysis was conducted using a 5 mM H2SO4 mobile phase, 50 ˚C column temperature, 0.6 mL/min flow rate for 40 min per sample and injection volume of 20 µL. Data acquisition and handling was conducted using Chemstation (Agilent Technologies) and datasets were summarized and figures plotted using R v. 4.3.2 [120,121]. Statistical analysis Statistical analysis for the Gas chromatography and HPLC was performed in R v. 4.3.2 [120,121]. To determine significant changes in gas headspace and metabolite profile compositions between the controls and experimental cultures, one way analysis of variance (ANOVA) was conducted between the respective constituents within each experiment, followed by post-hoc Tukey Honest Significant Difference (HSD) tests. To determine significant changes in H_2 following O_2 addition in both the temporal and volumetric experiments, H_2 levels at each sampling point within culture sets were subjected to one way ANOVA, followed by post-hoc Tukey HSD tests.

3.3 Results

3.3.1 Anaerobic synthesis gas mimetic feedstocks promote earlier onset of hydrogenogenesis at the expense of biomass accumulation.

Previous studies have characterised the fermentation profile of *P. thermoglucosidasius* DSM 6285 under various aerobic and anaerobic CO enriched headspaces, citinga 50% CO/50% air atmosphere as an ideal balance between suitable growth conditions and facilitating downstream WGS reaction conditions [52,60,62] Here we observed distinct fermentation profiles between the aerobic and anaerobic control, syngas (50%) and syngas (100%) atmospheres (Figure 9).

The aerobic control growth profile corresponded with previously observed patterns. This included an initial sharp increase in absorbance during the aerobic phase, peaking at 0.327 ± 0.008 by 48 h (coincidental with peak WGS reaction activity), followed by gradual decreases towards the end of fermentation (Figure 9). All anaerobic atmospheres exhibited significantly poorer growth throughout the fermentations (Supplementary material 2, Additional file 1:Table S1). Slight, albeit much less pronounced increases were observed for the anaerobic control (50%) and syngas (50%) atmospheres during the first 14 h of the experiment. This growth was not, however, shared by the syngas (100%) atmosphere replicates, which increased negligibly,

plateauing similarly to the N_2 and synthetic syngas (50%) atmosphere replicates at 0.111 ± 0.007. Growth of the syngas (100%) atmosphere replicates was also atypical, exhibiting a granular flocculant-type of growth compared to the turbid/cloudy appearance observed in the other atmospheres (results not shown).

In the early phases of each fermentation, pH values decreased across all atmospheres to varying extents (Figure 7). The aerobic control reached a low of 5.82 ± 0.02 by 14 h, accompanied and likely accounted for by concerted acetate production observed in this period. Anaerobic atmospheres demonstrated similar pH profiles to the aerobic control, however, reaching significantly lower pH values of 5.31 ± 0.04 by 38 h (Supplementary material 2, Additional file 1: Table S1).

These atmospheres exhibited strong concurrent production of lactate, formate and acetate which plateaued in conjunction with pH stabilisation and were likely responsible for the observed pH fluctuations. Following initial decreases, pH stabilized across all atmospheres, with the aerobic control stabilizing at a final value of 5.87 ± 0.02 and the anaerobic atmospheres at 5.37 ± 0.03. H_2 production was observed within 14 h in the anaerobic atmospheres (Figure 7), while the aerobic control only showed H_2 production by 24 h. Notably, H_2 production in the aerobic control was observed with concurrent O_2 levels of 0.95 ± 0.06%. Peak H_2 productivity for the aerobic control was much higher than the anaerobic atmospheres with peak productivity observed between 38 and 48 h at 0.0137 ± 0.0048 mmol h^{-1}. For the anaerobic control and syngas (100%) atmospheres, lower peak productivity was observed earlier between 24 and 38 h at 0.0063 ± 0.0005 mmol h^{-1} and 0.0047 ± 0.0016 mmol h^{-1} respectively, while the syngas (50%) atmosphere exhibited the earliest peak productivity between 14 and 24 h at 0.0055 ± 0.0005 mmol h^{-1}. Notably for the anaerobic atmospheres, H_2 production appeared to coincide with mixed acid fermentation, suggesting concurrent operation of these processes (Figure 7).

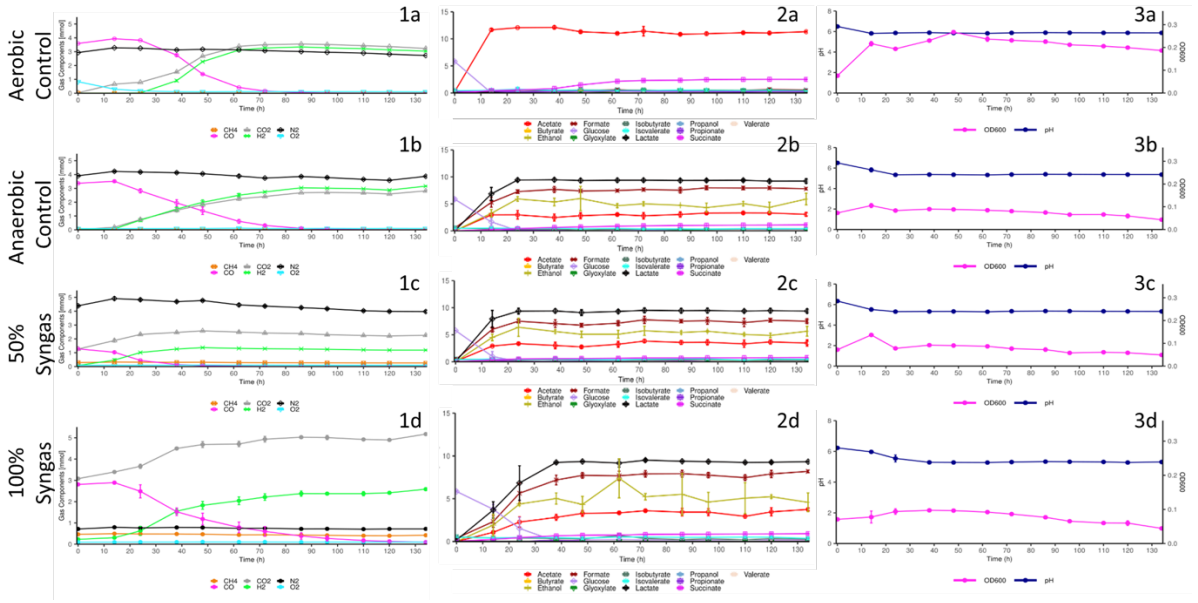

Figure 7. Gas composition (1) and growth- and pH-profiles (2) for *P. thermoglucosidasius* DSM 6285 cultured under 50% CO/50% Air- (a) 50% CO/50% N_2(b) 50% synthetic syngas- (c) and 100% synthetic syngas- (d) -gas headspaces.

H_2 mol yields per CO mol consumed (H_2/CO) across the fermentations varied between the points where CO was completely consumed and the endpoints of the fermentations at 134 h. Each atmosphere, except for the syngas (100%) atmosphere showed complete CO consumption within 134 h. Unsurprisingly, due to its comparatively low initial CO levels, the syngas (50%) atmosphere demonstrated the earliest CO depletion (84 h), followed by the aerobic control (110 h), then the anaerobic control (120 h). By 134 h, 1.06 ± 0.63% CO remained in the syngas (100%) atmosphere gas headspace. At the points where CO was completely consumed, the aerobic and anaerobic controls and the syngas (50%) atmosphere exhibited significantly different H_2/CO yields from one another (Supplementary material 2, Additional file 1: Table S2), of 89.48 ± 0.83%, 85.40 ± 0.14% and 93.62 ± 0.31% respectively. However, by the end point of the fermentations, yields fluctuated further, with both the aerobic control and syngas (50%) atmospheres having exhibited decreases of 4.92 ± 0.47% and 6.73 ± 0.85% respectively.

Conversely, the anaerobic control H2/CO yield increased by 8.48 ± 0.43%. By 134 h, despite not having depleted CO, the H_2/CO yield of the syngas (100%) atmosphere stood at 83.83 ± 1.42%, similar to that of the aerobic control but significantly lower than those of the anaerobic control and syngas (50%) atmospheres (Supplementary material 2, Additional file 1: Table S2).

Analysis of the metabolite profile with HPLC showed that lactate, formate and ethanol were, in descending order, the most prevalent metabolites produced under anaerobic atmospheres, while only negligible amounts of formate and ethanol were observed for the aerobic atmosphere (Figure 7). Lactate, formate and ethanol levels across the anaerobic atmospheres stabilized at 9.3442 ± 0.2808 mmol, 7.6075 ± 0.4817 mmol and 5.2032 ± 1.0371 mmol after 38 h levels despite the syngas (100%) atmosphere having exhibited significantly lower productivity of each acid between 0–14 h (Supplementary material 2, Additional file 1: Table S1).

Acetate was the central metabolite detected through HPLC in the aerobic atmosphere, rising rapidly and peaking at 12.1255 ± 0.2620 mmol by 38 h (Figure 7). Slight decreases in acetate levels were observed between 38 and 62 h to 11.0224 ± 0.1368 mmol but remained relatively stable thereafter. Acetate accumulation in the anaerobic atmospheres was significantly lower than the aerobic atmosphere (Supplementary material 2, Additional file 1: Table S1), accumulating to only a third of that of the aerobic control. The aerobic control also exhibited significant increases in succinate production between 38 and 72 h (Supplementary material 2, Additional file 1: Table S1), reaching a final level of 2.5111 ± 0.0606 mmol, while the anaerobic atmospheres showed negligible succinate accumulation. Glucose was completely consumed within 14 h post-inoculation in the aerobic control. Low levels of glucose, below the 0.1 mg L−1 HPLC method detection limit, were observed throughout all three anaerobic fermentations. However, most of the initially available glucose (> 99%) was consumed by 24 h in the N2 control and syngas (50%) atmospheres and by 38 h in the syngas (100%) atmosphere.

3.3.2 Pre-hydrogenogenic phase O_2 perturbations extend the lag phase prior to H_2 production

Oxygen addition at the various timepoints resulted in distinct fermentation profiles. Oxygen additions at 14 h and 24 h (Figure 8) exhibited markedly different influences on the various fermentation profiles compared to the control and 38 h and 48 h O_2 additions (Figure 9). For all O_2 additions, significantly higher peak and final absorbance (OD_{600}) values were observed compared to the controls following O_2 addition (Supplementary material 2, Additional file 1: Tables S3 and S4). In the cases of the 38 h and 48 h O_2 additions, which coincided with the hydrogenogenic phase, severe

reductions in H_2 production were observed, implying the growth observed was primarily the result of O_2 addition and not supplemented through the WGS reaction. While the control OD600 values declined following peak levels at 48 h, the 38 h and 48 h O_2 additions exhibited further significantly elevated peak OD_{600} values of 0.332 ± 0.011 and 0.302 ± 0.006 at 48 h and 58 h respectively following oxygen addition (Supplementary material 2, Additional file 1: Tables S3 and S4).

Steep declines in pH to lows of 5.78 ± 0.01 (Figure 8) and 5.93 ± 0.02 (Figure 9) within 14 h were observed across the fermentation batches in the aerobic phase, reflective of the observed acetate, formate and lactate accumulation. In the controls, these declines were followed by slight increases alongside near complete and complete consumption of formate and lactate, stabilizing at final pH values of 5.88 ± 0.02. Similar profiles were observed until either the addition of O_2 in the 14 h and 24 h O_2 addition replicates or 34–38 h in the 38 h and 48 h O_2 additions replicates. O_2 addition resulted in the significant increase in pH compared to the controls (Supplementary material 2, Additional file 1: Tables S3 and S4), until the final sampling point, likely the result of decreases in observed acetate levels. H_2 gas was first detected across all samples within 38 h. The highest O_2 level detected with concurrent H_2 production was 2.49 ± 0.06% O_2.

O_2 additions elevated O_2 levels an average of 4.51 ± 0.35%. Peak H_2 productivities were experienced between 34 and 38 h at 0.0297 ± 0.0004 mmol h^{-1} (Batch 1 control), 0.0205 ± 0.0045 mmol h^{-1} (Batch 2 control) and 0.0130 ± 0.0052 mmol h^{-1} (38 h O_2 addition). The 48 h O_2 addition replicates demonstrated peak H_2 productivity between 38 and 48 h at 0.0143 ± 0.0006 mmol h^{-1}, whilst both the 14 h and 24 h O_2 additions showed more delayed peak productivities of 0.0133 ± 0.0004 mmol h^{-1} and 0.0123 ± 0.0002 mmol h^{-1}, respectively, between 48 and 58 h. H_2 productivity decreased gradually as CO was depleted, eventually consumption of H_2, with a maximal H_2 consumption rate of 0.0030 ± 0.0002 mmol h^{-1} across all replicate sets.

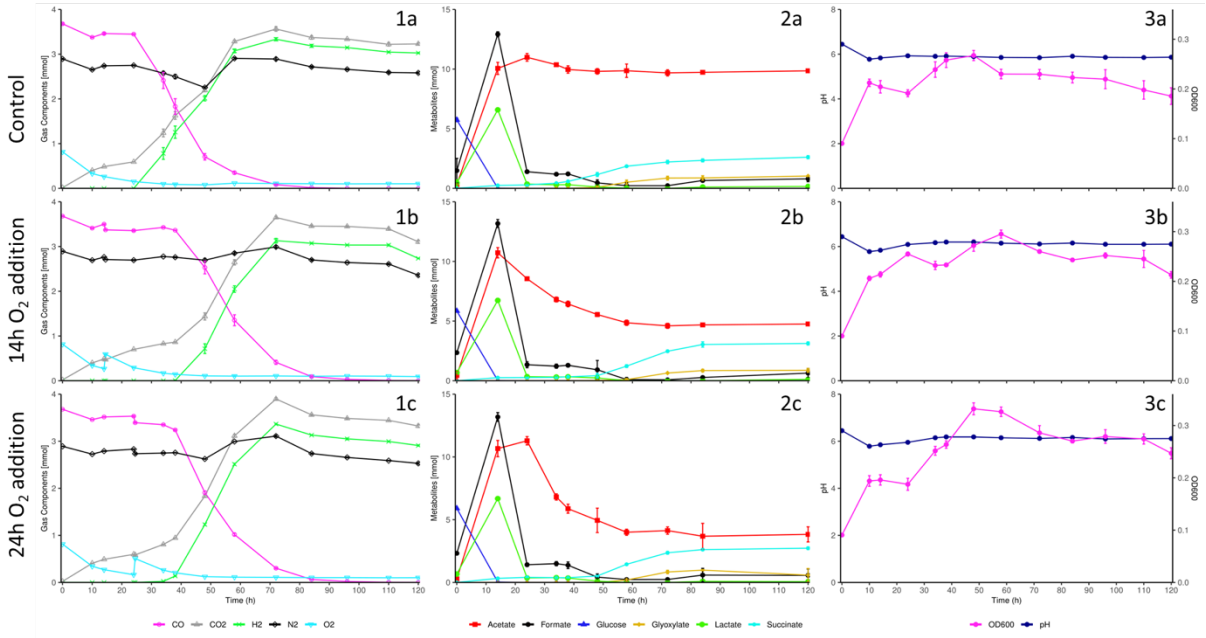

Figure 8. Gas composition (1), metabolite- (2) and growth- and pH-profiles (3) for *P. thermoglucosidasius* DSM 6285 cultured under a 50% CO/50% Air with no O_2 addition (a), 14h O_2 addition (b) and 24h O_2 addition (c).

Significant increases in H_2 levels were observed in both controls between 24-72h (Supplementary material 2, Additional file 5; Table S5). In each instance where O_2 was added, significant disruptions to H_2 production were observed (Supplementary material 2, Additional files 3 and 4; Tables S3 and S4). H_2 production was delayed following O_2 addition at 14h and 24h and resulted in significantly lower final H_2 levels (2.7351 ± 0.0058 mmol and 2.9094 ± 0.0127 mmol respectively) compared to the control (3.0260 ± 0.0112mmol). H_2 productivity was significantly lower between both O_2 additions and the control between 24h-38h. Notably, the 24h O_2 addition replicates showed earlier and more intensive H_2 production than the 14h O_2 addition replicates, with comparably higher H_2 levels and H_2 productivities during the majority of the fermentation (Supplementary material 2, Figure 8; Additional files 3 and 4; Tables S3 and S4). Following O_2 addition for the 38h and 48h O_2 addition replicate sets, both H_2 levels and H_2 productivities were significantly lower than the control for the subsequent 10h period (Supplementary material 2, Additional files 3 and 4; Tables S3 and S4). However, weak H_2 production was still observed across this period, with H_2 productivities of 0.0011 ± 0.0004 mmol h^{-1}. Following this period, however, significant increases in H_2 levels were observed for the 38h and 48h O_2 addition replicates between 48-84h and 58-84h respectively (Supplementary

material 2, Additional file 5; Table S5). However, H_2 levels for both O_2 ¬additions remained significantly lower than the control following O_2 addition.

Both controls and pre-hydrogenogenic phase 14h and 24h O_2 additions showed complete utilisation of CO, with trace amounts of CO remaining in the 38h and 48h O_2 addition replicates (Figure 8). H_2/CO yields at the points of complete CO depletion were 83.26 ± 1.19% (Controls), 74.35 ± 0.07% (14h O_2 addition) and 79.10 ± 0.26% (24h O_2 addition), respectively. These were all significantly different from one another (Supplementary material 2, Additional file 2; Table S2). Yields of 80.35 ± 0.13% and 81.33 ± 0.30% were observed for the 38h and 48h O_2 addition replicates by 120h. Both yields were significantly lower than the respective control but not significantly different from one another (Supplementary material 2, Additional file 2; Table S2).

HPLC analysis detected fluctuations in acetate and succinate profiles following oxygen addition. Acetate levels across all samples increased dramatically from the onset of the fermentations and peaked either prior to O_2 addition or within 34h post-inoculation (Figure 8). In the controls, after reaching peak acetate levels of 11.4257 ± 0.5833 mmol, a low-level net consumption of acetate was observed, gradually reducing acetate levels to a final concentration of 10.4132 ± 0.6191 mmol. In each case where O_2 was added, significantly lower acetate levels were observed throughout the remainder of the fermentations compared to the respective controls (Supplementary material 2, Additional files 3 and 4; Tables S3 and S4). Correspondingly, significantly higher acetate consumption levels were observed between all O_2 addition replicates and the controls immediately following O2 addition. This was observed between 14-34h (14h O_2 addition), 24-38h (24h O2 addition), 38-82h (38h O_2 addition) and 38-72h (48h O_2 addition), respectively post-O_2 addition.

Although succinate levels were observed to increase gradually from the start of all fermentations, prominent increases were only observed after 24h in the controls, peaking at 2.544 ± 0.1405 mmol (Figure 8). O_2 addition at 14h and 24h delayed succinate accumulation, presenting significantly lower succinate levels than the control between 34-58h and 38-58h respectively (Supplementary material 2, Additional file 3; Table S3). Despite this, the 14h O_2 addition replicates accumulated significantly higher final succinate levels compared to both the

control and 24h O_2 addition replicates, peaking at 3.1261 ± 0.1344 mmol. Following O_2 addition at 38h and 48h, significantly lower levels of succinate were observed compared to the control between 48-58h (Supplementary material 2, Additional file 4; Table S4). Despite this delay in succinate production, there were no significant differences between the final accumulated succinate concentrations of the control, 38h and 48h O_2 additions, which averaged at 2.7774 ± 0.9710 mmol.

Glucose levels across all samples were almost completely consumed (>97%) 14h post-inoculation and were completely consumed within 34h. Large formate 12.9833 ± 1.0624 mmol and lactate 6.5760 ± 0.5515 mmol peaks were detected at 14h post-inoculation across each replicate set. Both compounds were almost completely consumed thereafter with only minor increases in formate below the detection limit (<0.1g/L) of the HPLC method.

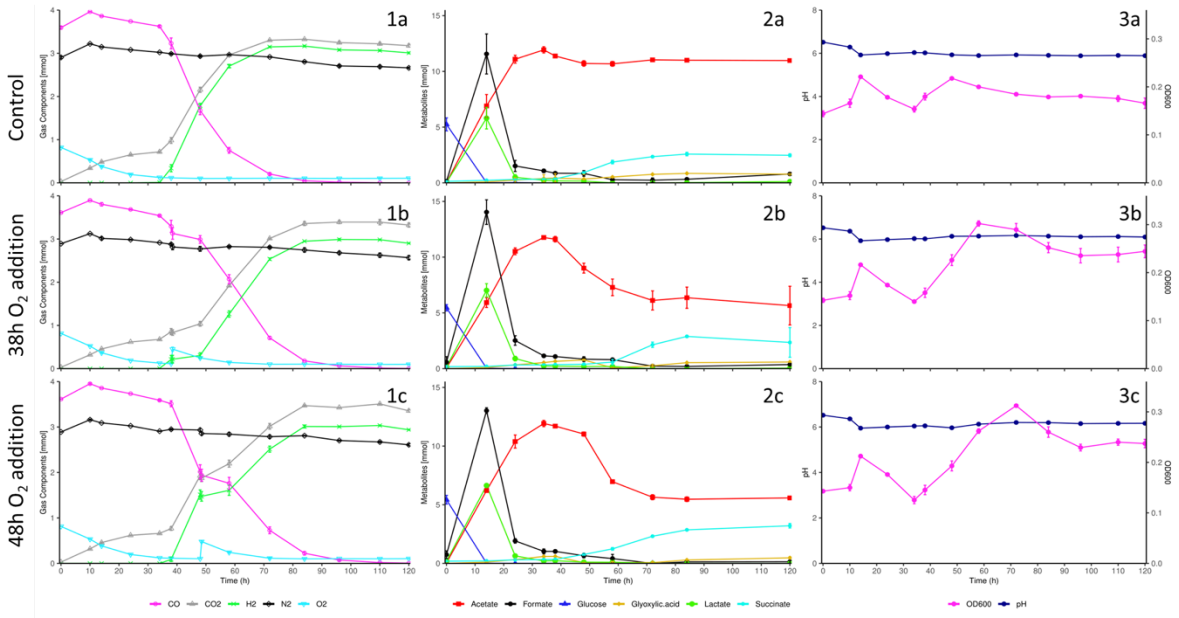

Figure 9. Gas composition (1), metabolite- (2) and growth- and pH-profiles (3) for *P. thermoglucosidasius* DSM 6285 cultured under a 50% CO/50% Air with no O_2 addition (a), 38h O_2 addition (b) and 48h O_2 addition (c).

3.3.3 Minor O_2 perturbation during peak-hydrogenogenesis minimally disrupts H_2 production in *P. thermoglucosidasius* DSM 6285

Prior to oxygen addition, the 38h varied O_2 volume addition fermentations demonstrated the same trends in growth, pH, gas composition and HPLC metabolite profiles as observed

previously (Figure 7; Figure 8). Following varied oxygen additions, however, disruptions in these profiles were scaled accordingly with the volumes of oxygen supplemented (Figure 10). O_2 levels post-O_2 addition were 0.90 ± 0.22% (1% O_2 addition), 2.83 ± 0.07 % (3% O_2 addition), 4.70 ± 0.14% (5% O_2 addition) and 9.08 ± 0.14% (10% O_2 addition), respectively.

Following O_2 addition OD_{600} values increased in accordance with volumes of O_2 added, with larger O_2 volume additions resulting in greater peak OD_{600} values achieved (Figure 10). The 1% O_2 addition prompted the weakest response, but exhibited significantly higher values compared to the control from 48h onwards (Supplementary material 2, Additional file 5; Table S5). The 3% O_2 addition showed a slightly more delayed increase in OD_{600} values, with significantly elevated OD_{600} values compared to the control from 62h onwards. The 5% and 10% O_2 additions both exhibited a slight decrease in OD_{600} values following O_2 addition between 38-41h, however, showed a steep increase thereafter. From 44h onwards, the 5% O_2 addition maintained significantly higher OD_{600} values compared to the control. The 5% O_2 addition also maintained significantly higher OD_{600} values than those of the 1% and 3% O_2 additions over the majority of the fermentation and was similar to the 10% O_2 addition. Although the 10% O2 addition exhibited the greatest increase in OD_{600} values, peaking at 0.395 ± 0.006 at 72h, OD_{600} values appeared to decrease sooner than those of the 5% O_2 addition.

Larger O_2 volume additions correspondingly resulted in larger sustained increases in pH, likely the result of the observed reduction in acetate levels following O_2 addition (Figure 10). Apart from the 1% O_2 addition, which displayed no significant difference from the control, all other O_2 additions prompted significant increases in pH values 6h post-O_2 addition (Supplementary material 2, Additional file 5; Table S5). pH values stabilized in each case after ~62h, alongside plateaus in acetate consumption and OD600 peaks, with the 10% O_2 addition almost returning to starting pH values, reaching as high as 6.35±0 (Figure 10).

H_2 was first detected at 38h across all replicate sets at elevated levels (Figure 10). The control exhibited a H_2 productivity of 0.0460 ± 0.0013 $mmol.h^{-1}$ between 38-41h. Comparatively, H_2 productivities of the O_2 addition replicates were all significantly lower than the control in this period (1%: 0.0137 ± 0.0062 $mmol.h^{-1}$; 3%: 0.0002 ± 0.0003 $mmol.h^{-1}$; 5%: 0.0005 ± 0.0012 $mmol.h^{-1}$; 10%: 0.0009 ± 0.0003 $mmol.h^{-1}$; Supplementary material 2, Additional file 5; Table

S5). In the case of the 1% O_2 addition, no significant difference in H_2 productivity with the control was detected after 41h (Supplementary material 2, Additional file 6; Table S6), with H_2 productivity between 38-48h (0.0101 ± 0.0013 mmol.h^{-1}), the peak H_2 productivity period, only slightly lower than that of the control (0.0150 ± 0.0006 mmol.h^{-1}). However, unlike the control, no significant increase in H_2 levels were observed between 38-41h (Supplementary material 2, Additional file 5; Table S5). Significant increases in H_2 levels were only detected in the 1% O_2 addition replicates between 41-62h (Supplementary material 2, Additional file 5; Table S5), when O_2 levels were below 0.79 ± 0.13%. Despite this, no significant difference in H_2 concentration was detected between the 1% O_2 addition and the control over this period (Supplementary material 2, Additional file 6; Table S6). However, following complete CO consumption, the 1% O_2 addition replicates exhibited significantly lower final H_2 levels (2.8999 ± 0.0788 mmol) than the control (3.1277 ± 0.0874 mmol; Supplementary material 2, Additional file 6; Table S6).

Following O_2 addition, significantly lower levels of H_2 were detected between the 3%, 5% and 10% O_2 addition replicates and the control until the endpoints of the fermentations (Supplementary material 2, Additional file 6; Table S6). Lower final H_2 levels were observed accordingly with higher volumes of O_2 added (Control: 3.0525 ± 0.0110 mmol, 1% O_2 addition: 2.8290 ± 0.0097 mmol, 3% O_2 addition: 2.8038 ± 0.0084 mmol, 5% O_2 addition: 2.7613 ± 0.0085 mmol, 10% O_2 addition: 2.7657 ± 0.0096 mmol). However, no significant differences in final H_2 levels were observed between the 1% and 3%- and between the 5% and 10% -O_2 addition replicates (Supplementary material 2, Additional file 6; Table S6). Following the reduction in H_2 productivity experienced by the 3%, 5% and 10% O_2 addition replicates between 38-41h, H_2 consumption was observed for each of these O_2 additions between 41-44h at rates of 0.0002 ± 0.0005 mmol.h-1, 0.0019 ± 0.0002 mmol.h-1 and 0.0018 ± 0.0005 mmol.h-1 respectively (Figure 10). H_2 productivity for these replicates remained significantly lower than the control between 38-48h for 3% and 5% O_2 addition replicates and 38-62h for the 10% O_2 addition replicates (Supplementary material 2, Additional file 6; Table S6). However, H_2 productivity increased following 44h with the 10% O_2 addition replicates demonstrating significantly higher ($P<0.01$) H_2 productivity than the control between 62-96h (Supplementary material 2, Additional file 6; Table S6). Consequently, significant increases in H_2 levels were only detected between 48-62h for the 3% and 5% O_2 addition replicates and between 62-72h

for the 10% O_2 addition replicates (Supplementary material 2, Additional file 5; Table S5). Following O_2 addition, O_2 levels at the first point where a significant increase in H2 was observed (Supplementary material 2, Additional file 6; Table S6), were 0.03 ± 0.06% (3% O_2 addition), 0.17 ± 0.09% (5% O_2 addition) and 0.97 ± 0.1% (10% O_2 addition).

CO was completely consumed across each condition by 134h (Figure 10). The control exhibited CO depletion first (110h) alongside the 1% O_2 addition replicates, then the 3% O_2 addition replicates (120h) and the 5% and 10% O_2 addition replicates (134h). The control exhibited the highest H_2/CO yield both at the first point of CO depletion (88.56 ± 0.62%) and by the end of the fermentation (83.86 ± 0.62%). In both instances yields were significantly higher than all O_2 addition yields (Supplementary material 2, Additional file 2; Table S2), despite exhibiting a decrease in yield following CO depletion. Although producing significantly different yields at the first points of CO depletion (82.26 ± 0.25% and 85.26 ± 0.30% respectively), the 1% and 3% O_2 additions showed no significant difference in H_2/CO yield by the endpoint of the fermentation (Supplementary material 2, Additional file 2; Table S2), with final yields of 77.82 ± 0.00%. In both cases, however, reductions in H_2/CO yields of 4.70 ± 0.41% and 8.30 ± 0.94%, respectively, were observed between the two points. The 5% followed by 10% O_2 additions exhibited the lowest H_2/CO yields at 134h, with yields of 76.51 ± 0.20% and 75.89 ± 0.24%, respectively.

Acetate levels across all samples increased dramatically from the onset of the fermentations and peaked prior to O_2 addition (Figure 10). Peak acetate levels of 12.5025 ± 0.1713 mmol were observed by 24h, followed by net reduction, with the control reaching a final acetate concentration of 11.1013 ± 0.6522 mmol. The 1% O_2 addition showed almost no differences in acetate levels compared to the control (Supplementary material 2, Additional file 6; Table S6). In the cases of the 3%, 5% and 10% O_2 additions, significantly lower acetate levels were observed after 48h, 44h and 48h, respectively, with final acetate levels of 8.5019 ± 0.5227 mmol (3% O_2 addition), 5.3856 ± 0.3675 mmol (5% O_2 addition) and 2.2098 ± 1.0733 mmol (10% O_2 addition). Greater degrees of acetate consumption were observed in accordance with greater volumes of O_2 added, with the most noteworthy decreases in acetate observed by the 10% O_2 addition, followed by the 5%, 3% and finally 1% O_2 additions, with the latter showing no significant difference from the control (Supplementary material 2, Additional file 6; Table S6).

Succinate levels increased gradually from the start of all fermentations (Figure 10), although prominent increases in succinate were staggered. Whilst there was no significant difference in succinate productivity immediately following O_2 addition between the 1%, 3% and 5% O_2 additions and the control, the 10% O_2 addition exhibited net succinate consumption following O_2 addition, between 38-48h and significantly lower succinate productivity until 62h post-inoculation (Supplementary material 2, Additional file 6; Table S6). All O_2 additions exhibited significantly higher succinate productivity compared to the control between 62-84h. Compared to the control which exhibited final succinate levels of 2.7534 ± 0.1376 mmol, the 5% O_2 addition replicates accrued significantly higher levels of 3.2737 ± 0. mmol by the end of the fermentation. Glucose levels across all samples were almost completely consumed (>97%) within 14h and were completely consumed within 34h. Formate and lactate peaks were detected at 14h post-inoculation across each replicate set, however, both compounds were almost completely consumed thereafter with only minor increases in formate below the detection limit (<0.1g/L) of the HPLC method.

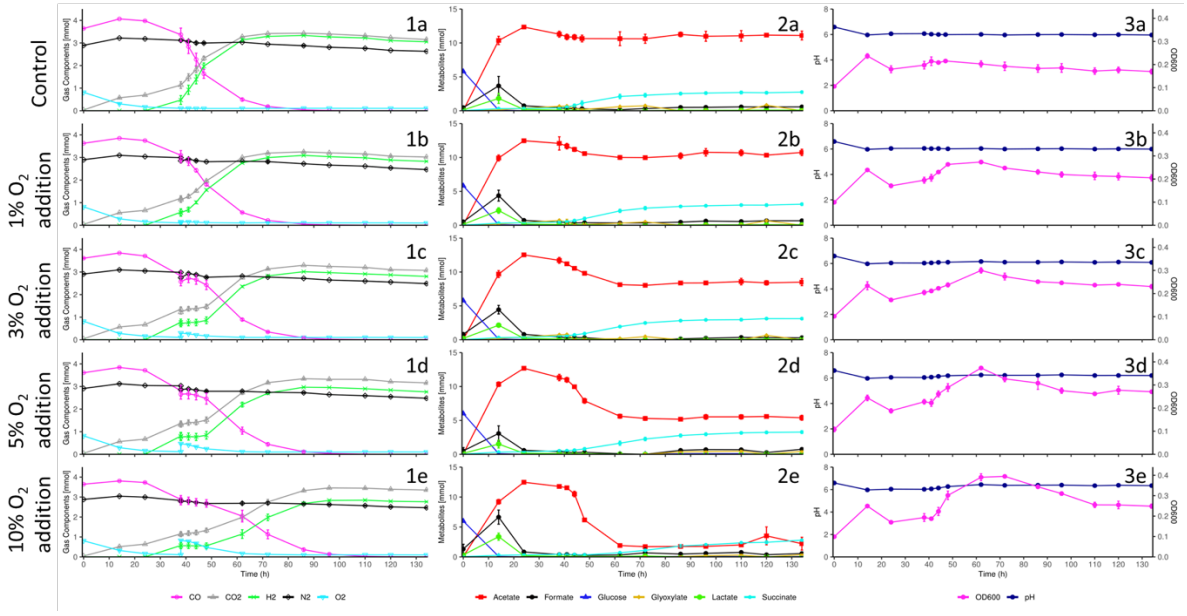

Figure 10. Gas composition (1), metabolite- (2) and growth- and pH-profiles (3) for *P. thermoglucosidasius* DSM 6285 cultured under a 50% CO/50% Air with no O_2 addition (a) and 1%- (b) 3%- (c), 5%- (d) and 10%-(e) –O_2 addition at 38h.

3.4 Discussion

Syngas fermentation provides the opportunity for microbial conversion to various value-added products from industrial waste gases [122]. Here we explored the effects of synthetic syngas mixtures on the *P. thermoglucosidasius* WGS reaction. Our analyses showed that *P. thermoglucosidasius* grown in anaerobic syngas atmospheres, with highly varied CO and CO_2 compositions and impurities including methane, ethane, propane and butane, was able to produce H_2, being limited only by CO availability. However, cultivation in these anaerobic atmospheres severely hampered biomass accumulation.

Poor biomass accumulation was likely due to the distinct bioenergetics associated with aerobic and anaerobic respiration as well as fermentation. Anaerobic atmospheres exhibited distinct mixed acids fermentation profiles favouring lactate, formate, ethanol and acetate production, which could account for the more marked reductions in pH observed across these conditions [123–126]. The aerobic control exhibited pronounced acetate production prior to commencement of H_2 production, alongside concerted succinate production which coincided with O_2 depletion and onset of the WGS reaction. As well as serving as a means for balancing cell redox levels and potentially as an alternative carbon pool, it has been suggested that elevated acetate levels increase the CO uptake capacity of CO consumers [62,126]. Notably, two-fold greater H_2 production rates were observed under an aerobic atmosphere, where acetate levels were also several fold higher than anaerobic/microaerobic atmospheres.

In the syngas atmospheres, varying CO levels influenced growth and metabolism to a large extent, impacting downstream H_2 production. H_2 production in these atmospheres showed considerably shorter lag phases between inoculation and onset of the WGS reaction, similar to the anaerobic control and previous anaerobic cultivations that have exhibited reductions to within 4h post-inoculation [117]. The 50% syngas, atmosphere, with the lowest CO level (~17%), exhibited pronounced earlier onset of fermentative metabolism and H_2 production compared to the anaerobic control (CO level ~46%) and the syngas (100%) atmosphere (CO level ~38%). From previous aerobic studies the opposite was anticipated as atmospheres with enriched CO levels facilitated more prolific growth responses and correspondingly greater hydrogenogenic activity [52,62]. We observed distinct conversion efficiencies between the first observed points of CO depletion and the fermentation end-points, with general yield decreases towards the end. Given the absence of known CO producing pathways, this was most likely the

result of H_2 consumption by one or both of two putative NiFe-uptake hydrogenases encoded on the genome of *P. thermoglucosidasius* DSM 6285 [91]. The consumption of H_2 by group 1d uptake hydrogenases is coupled with aerobic respiration or respiratory reduction of anaerobic oxidants like fumarate, NO^{3-}, SO_4^{2-} and CO_2 [88]. Group 2a uptake hydrogenases are involved in aerobic respiration and recycling H_2 produced through nitrogenase activity or fermentative pathways in aerobic soil and Cyanobacteria [88]. It is plausible that these enzymes couple H_2 oxidation with an anaerobic electron transport chain, however, this requires further validation. Despite showing accelerated commencement of H_2 productivity, anaerobic cultivation greatly reduced biomass accumulation, inadvertently reducing H_2 production potential. It can be reasoned that sustained active biomass accumulation and consequently O_2 availability are important considerations for developing this system towards more continuous operation. It would also be beneficial to balance maximally anaerobic conditions to minimally disrupt or delay WGS reaction onset, but maintain O_2 supply to sustain catalytically active biomass. As such we further explored the impacts, both temporally and volumetrically, of O_2 perturbation of the *P. thermoglucosidasius* DSM 6285 WGS reaction system at different key phases.

O_2 addition across the different phases of the *P. thermoglucosidasius* DSM 6285 fermentation negatively impacted H_2 production at all stages. O_2 addition prior to commencement of H_2 production delayed H_2 production to a greater extent than O_2 addition during the anaerobic phase, likely by extending more energetically efficient aerobic respiration [127]. O_2 addition in the anaerobic phase likely prompted resumption of aerobic respiration, although, with a more limited pool of reducing agents in higher oxidation states, required more rapid commitment to the WGS reaction for energy conservation, as observed for the WGS system in other taxa [113,128–131].

Later O_2 additions in the hydrogenogenic phase showed stark reductions in H_2 production alongside strong and extended gains in biomass accumulation, indicative of redirection of *P. thermoglucosidasius* towards aerobic metabolism, which offers greater potential energy yields. Expectedly, increasing volume O_2 additions saw more pronounced disruptions to H_2 production, however H_2 production resumed, albeit at lower rates, following O_2 depletion. As CO availability was not a limiting factor, this was likely the combined result of the extended

effects of O_2 induced inhibition of the WGS components and the shift towards maximizing use of the oxidative respiratory chain [115,130,132,133].

The Ni-CODH and group 4a NiFe-hydrogenase responsible for conducting the *P. thermoglucosidasius* DSM 6285 WGS are both classed as highly O_2 sensitive [88,115,130], although the tolerance of the *P. thermoglucosidasius* WGS system to O_2 disruptions have not previously been investigated. Here we observed the initial commencement of WGS activity in the presence of 2.49 ± 0.06% O_2 in the gas headspace and resumption of H_2 production following O_2 disruption once O_2 levels dropped below 0.97 ± 0.1%.

Although 1% O_2 addition initially reduced H_2 productivity between 38-41h, there were only minor observable differences in productivity of the 1% O_2 addition condition (0.0101 ± 0.0013 $mmol.h^{-1}$) compared to the control (0.0150 ± 0.0006 $mmol.h^{-1}$) over the peak period of H_2 productivity (38-48h). Productivity remained positive throughout, despite O_2 addition, demonstrating a final H_2 yield with no significant difference to the control. Conversely, reductions in H_2 levels were observed in the 3-10% O_2 additions, most likely due to the activity of one or both of the two putative O_2-tolerant NiFe-uptake hydrogenases, which potentially couple H_2 oxidation with aerobic respiration.

The lag in growth experienced post 5% and 10% O_2 addition coincided with relatively low increases in CO_2, despite rapid consumption of O_2, likely the result of the sudden pronounced oxidative stress. This phenomenon has been observed previously in *Klebsiella aerogenes* and *Escherichia coli*, where similar stimuli resulted in apparent uncoupling between growth and energy conservation, resulting in a switch towards energetically wasteful oxidation pathways [134,135]. In conjunction with the O_2 susceptibility of the WGS machinery, this may have effected lower H_2 production and yields following both temporally and volumetrically diverse O_2 perturbations.

Large increases in acetate, formate and lactate were detected early in all fermentations (Fig 1-4), resulting in pH decreases. These compounds likely served as overflow metabolites, acting as electron sinks to reduce the backlog of NADH generated from CO disrupted aerobic metabolism, at the expense of energetic efficiency [62,124,136]. Subsequently, shortfalls in

ATP generation were likely compensated by acetate kinase-mediated acetate production. Accumulation of these acids have also been attributed to the development of microoxic conditions developed in the media during O_2 consumption [137,138]. Subsequent consumption of lactate was likely through the putative LutA-C protein complex encoded by *P. thermoglucosidasius*, proteins associated with aerobic lactate utilisation in *Bacillus subtilis* [62,139]. Notably, formate was almost completely consumed by the onset of the WGS. Formate consumption is associated with concomitant CO_2 and H_2 production, however, no concomitant H_2 production was observed in this period, suggesting diversion of electrons towards another oxidant or electron transport chain. It remains unclear as to how formate was metabolised in these circumstances and represents an area for further investigation.

Strong acetate production in the aerobic phase resembled previous *P. thermoglucosidasius* fermentations and likely compensated for detraction of potential ATP production by lactate and formate production [62,124]. Acetate production was likely also bolstered through mixed acids fermentation to the detriment of ethanol-directed fermentation, which aligns with the insubstantial levels of ethanol detected here and in a previous study [124].

Following O_2 addition at all timepoints strong acetate consumption accompanied by slightly delayed growth responses, increasingly so for larger volume O_2 additions.
Notably, greater degrees of CO_2 than H_2 were evolved between O_2 addition and concerted resumption of WGS activity. Furthermore, following O_2 addition, increases in succinate were observed towards the tail-end of acetate consumption, where O_2 levels were approaching depletion. Together these factors suggest that a portion of the acetyl-CoA derived from the acetate consumed may have integrated into the TCA cycle and been incorporated into biomass via the glyoxylate shunt, as suggested previously[120,140], however confirmation of this requires further validation. Following O_2 depletion, acetate consumption ceased, indicating a necessity for O_2 for concerted acetate consumption in *P. thermoglucosidasius*. Further investigation into the metabolism of *P. thermoglucosidasius* under these conditions may further yield a greater understanding of the dynamics and interplay between the WGS reaction and alternative metabolic pathways.

3.5 Conclusions

Cultivation of *P. thermoglucosidasius* DSM 6285 under anaerobic synthetic syngas atmospheres induced faster onset of H_2 production than previously identified ideal aerobic gas mixtures, however, this was at the expense of biomass accumulation. This in turn severely hampered H_2 turnover. O_2 supplementation at all stages of the fermentation hindered H_2 production to greater extents accordingly with the volume of O_2 supplied, however, also supported reinvigorated biomass accumulation. Furthermore, upon depletion of the supplemented O_2, hydrogenogenic activity was rapidly resumed following a negligible lag period. Supplementation with 1% O_2 negligibly impacted H_2 production, however, still gave some support to growth. Notably, with elevated (10%) O_2 supplementation, H_2 consumption was observed briefly. This was potentially due to the two putative uptake hydrogenases encoded by *P. thermoglucosidasius* DSM 6285, which may present appealing targets for knockout mutagenesis. H_2 conversion efficiency was also reduced accordingly with the level of O_2 administered. The tolerance of the system to O_2 perturbations may be linked with the metabolism of accumulated acetate, where O_2 addition induces strong acetate consumption to support cell growth at all stages of the fermentation, including during the aerobic/microaerobic phase. It may be possible to incorporate this capacity for O_2 induced acetate consumption and the relative flexibility of the *P. thermoglucosidasius* DSM 6285 WGS reaction to O_2 perturbation to facilitate cyclical/fed batch hydrogenogenic fermentations on syngas at a larger scale. Additionally, focusing the strain towards concerted acetate production through inactivation of formate or lactate production pathways may facilitate concentrated acetate production to further supplement downstream acetate dependent growth.

4 Syngas and acetate fermentation in bioreactor

This chapter is based on the publication:

Evaluation of lab-defined syngas and acetate as substrates for H_2 production with *Parageobacillus thermoglucosidasius* DSM 6285. Magda S. Ardila, Habibu Aliyu, Pieter de Maayer, Anke Neumann.
Manuscript submitted.

Author's Contributions:

Magda Ardila	Conceptualization, investigation, data curation, writing the original draft, visualization
Habibu Aliyu	Conceptualization, supervision, reviewing and editing.
Pieter de Maayer	Conceptualization, supervision, reviewing and editing, project administration, funding acquisition.
Anke Neumann	Conceptualization, supervision, reviewing and editing, project administration, funding acquisition.

4.6 Introduction

Dwindling fossil fuel reserves and the increase in atmospheric CO_2 emissions as a result of their combustion are driving the development of alternative energy sources to meet growing global energy demands [141]. Renewable production approaches, such as electrolytic, thermolytic and photo-electrolytic water-splitting technologies, as well as biological (biomass) transformations, may provide a sustainable means for the production of H_2, an attractive fossil fuel alternative [7,8,28]. The latter involves the use of bacteria and algae to produce H_2 photolytically (from water and sunlight), or through dark fermentation, using biomass or organic acids through hydrogenase or nitrogenase enzyme systems [7,8]. In addition to the existing biological processes for H_2 production, carboxydotrophic microorganisms that produce H_2 and CO_2 through water-gas shift (WGS) reaction, using carbon monoxide (CO) and water as substrates, are a potential option for CO-based H_2 production [28,59]. The thermophilic facultatively anaerobic bacterium *Parageobacillus thermoglucosidasius* is a metabolically versatile, biotechnologically relevant microorganism, that can perform the WGS reaction in the presence of low levels of oxygen [52,59,142]. Syngas, gas mixtures comprised primarily of CO, H_2 and CO_2 are produced through the industrial gasification of coal, biomass or natural gas and may serve as a good source for WGS-driven hydrogenogenesis, but often contain traces of oxgen, making *P. thermoglucosidasius* an attractive candidate for syngas-derived hydrogen production [142]. Previous studies have shown that this bacterium was able to perform the WGS reaction with complex syngas mixtures and that this gas substrate led to a shorter lag phase before the commencement of hydrogenesis [142], compared to when more purified (CO and N_2) gas mixtures were used [62].

In previous work, we evaluated the effect of increasing CO, N_2, and H_2 partial pressures at bottle scale, concluding that the increase of CO partial pressure to 3.0 bar was inhibiting for H_2 production while rising N_2 and H_2 partial pressures had a positive effect [143]. Pressure was evaluated as a process parameter, as the experiments allowed to assess the total pressure of the system and compare the different partial pressures of the gas mixtures used [143]. In comparison, the present work aimed to evaluate the effects of increased CO and H_2 partial pressures (pCO and pH_2) in a gas mixture containing CO, CO_2, and H_2, at ambient pressure on hydrogenogenesis at the bioreactor scale with a continuous gas flow and pH regulation. The

process control over parameters such as pH, temperature, and gas flow rates is difficult to achieve in bottle fermentations. Furthermore, the gas-liquid mass transfer can be enhanced through mixing and sparging systems in bioreactors, whereas in bottles, the gas diffusion is achieved solely by stirring [144,145].

In addition to syngas being a replacement for pure CO used for bioreactor scale fermentations, the glucose in the media needs to be exchanged for a sustainable the scale-up process. Acetate, or more specifically its protonated form acetic acid, can be found in biomass gasification waste streams [146]. Microorganisms such as acetogenic bacteria that metabolize syngas often produce acetate as an intermediate or end product, such as acetogenic bacteria, which can convert CO and CO_2 into acetate via the Wood-Ljungdahl pathway [147,148]. This organic acid is also produced by *P. thermoglucosidasius* as metabolite during fermentation following glucose depletion and is later consumed during the fermentation [62]. Therefore, a set of fermentations was designed to evaluate acetate as carbon source and its effects on H_2 production in *P. thermoglucosidasius*.

4.7 Materials and methods

4.7.1 Microorganisms and Media

P. thermoglucosidasius DSM 6285 was acquired from the Deutsche Sammlung von Mikroorganismen und Zellkulturen (DSMZ, Braunschweig, Germany) and was conserved in glycerol (80%) stocks at – 80 °C. Routine cultivation of *P. thermoglucosidasius* DSM 6285 was performed in modified Luria Bertani (mLB) medium [52]. Bioreactor fermentations were undertaken in modified ammonium sulfate medium (mASM) [88,149]. For the acetate fermentations, glucose (1 g/L) was replaced with acetate at the same concentration (16.7 M = 1 g/L).

4.7.2 Inoculum preparation

A volume of 300 µL of glycerol stock was added to 200 mL of mLB medium in 500 mL shake flasks and grown under aerobic conditions at 60 °C and rotation at 120 rpm in an Infors Thermotron (Infors Thermotron, Infors AG, Bottmingen, Switzerland). After 14 h, a calculated

volume of the inoculum was added to the reactors to achieve an initial absorbance (OD_{600}) of 0.1 for a total volume of 1 L.

4.7.3 Experimental Setup

Each fermentation was performed in two bioreactors of 2.5 L capacity (Minifors, Infors AG, Bottmingen, Schweiz) with a 1 L working volume. The growth conditions were maintained as reported previously [149], with stirrer speed set to 500 rpm, temperature to 55 °C and pH to 6.8; pH was controlled using a pH probe (Easyferm plus, Hamilton, Switzerland) and with the help of a peristaltic pump connected to the reactor system providing NaOH (1 M) and H_2SO_4 (1 M). For the syngas fermentation, an anaerobization step was performed to ensure no oxygen was present in the reactors before inoculation. This was achieved by flushing the reactors overnight with nitrogen (N_2) gas. Two hours prior to the addition of the inoculum, the gas mixture was set through mass flow controllers, with a flow rate of 200 mL min^{-1} and the gas compositions outlined in Table 4. The two-phase fermentation using acetate as an additional substrate was performed as described before [149]. The aerobic phase (Acetate P1) had a continuous flow rate of 100 mL min^{-1} of air and CO for 24 h, while the anaerobic phase (Acetate P2) had an 80 mL min^{-1} flow of a mixture of 80% nitrogen and 20% CO (Table 4).

Table 4. Gas mixtures for each fermentation, with increasing CO (1-3) and H_2 (4-6) percentages.

Fermentation	H_2 (%)	CO (%)	CO_2 (%)	N_2 (%)
CO-1	15	10	15	55
CO-2	15	30	15	35
CO-3	15	50	15	20
H_2-4	5	20	15	60
H_2-5	12	20	15	53
H_2-6	20	20	15	45
Acetate P1*	-	10	-	-
Acetate P2	-	20	-	80

*in Acetate P1 there was also 90% air.

4.7.4 Analytical methods

Online measurement of the gas content in the headspace of the reactor was performed using a 3000 Micro GC gas analyzer (Inficon, Switzerland) connected with Molsieve and PLOT Q columns for data acquisition. Liquid samples were withdrawn daily and absorbance (OD_{600}) readings were confirmed using an Ultrospec 1100 pro spectrophotometer (Amersham Biosciences, Uppsala, Sweden). HPLC analyses were performed on the liquid samples using the Agilent 1100 series HPLC system (Agilent Technologies, Waldbronn, Germany), equipped with a 50 mm pre-column (model Rezex ROA-Organic Acid H+ 8% Guard Column) and a 300 mm separation column (model Rezex ROA-Organic Acid H+ 8%), together with a wavelength detector and refractive index detector. Operational parameters were: 55°C for column temperature, flow rate of 0.6 mL min^{-1}, injection volume of 10µL, a mobile phase of 5 mM H_2SO_4 and a duration of 40 min per sample. Chemstation software (Agilent Technologies) was used for data acquisition and analysis. Gas composition was calculated according to the ideal gas law, as described before [59]. The electron selectivity was used to show the electron flux in the process. This was calculated from the electron mole (e^- mol) of each compound, calculated from the quantities of each compound (mmol), and a conversion factor to electrons based on the oxidation state of each element. Additional information on the calculations can be found in Additional File 1 (Supplementary material 3).

4.8 Results

4.8.1 Effects of different CO concentrations on H_2 production

The increase of CO was performed to evaluate possible inhibition on the hydrogen production rate (HPR) by a high CO percentage within the gas mixture. The HPR is given in liter of H_2 produced per liter of growth media and day. Evaluation of the HPRs at the three different CO percentages showed that at a 50 % CO, hydrogenesis was delayed by 24 hours, while at 10 and 30%, hydrogenesis was observed after 26 and 36 hours, respectively (Figure 11A). Furthermore, lower HPRs were consistently observed throughout the 96-hour evaluation with 50% CO, compared to when 10% and 30% CO were added. By contrast, with 30% CO, the HPR was higher than with 10% and 50% CO addition up to 72h post-inoculation, while similar HPRs of 11.8, 9.7, and 10.8 L H_2/L/d were observed 96 hours post-inoculation. The CO

consumption rate reflected the production of H_2 and CO_2 independent from the CO concentration evaluated (Supplementary material 3, Figure 1).

Analysis of the electron balance showed that at 30 % CO, CO consumption was the highest at 72 hours, as 88-90% of electrons coming from CO were converted into H_2, with acetate as the second main product, followed by formate (Figure 11B). The 30% CO had the highest H_2 proportion (90%), followed by 5% acetate. At the lowest percentage (10% CO), 6% of electrons were converted into acetate, while for the highest (50% CO), 5.5% of electrons went into acetate production. Other metabolites such as lactate, butyrate, propionate, and valerate were produced in lower proportions (<1%).

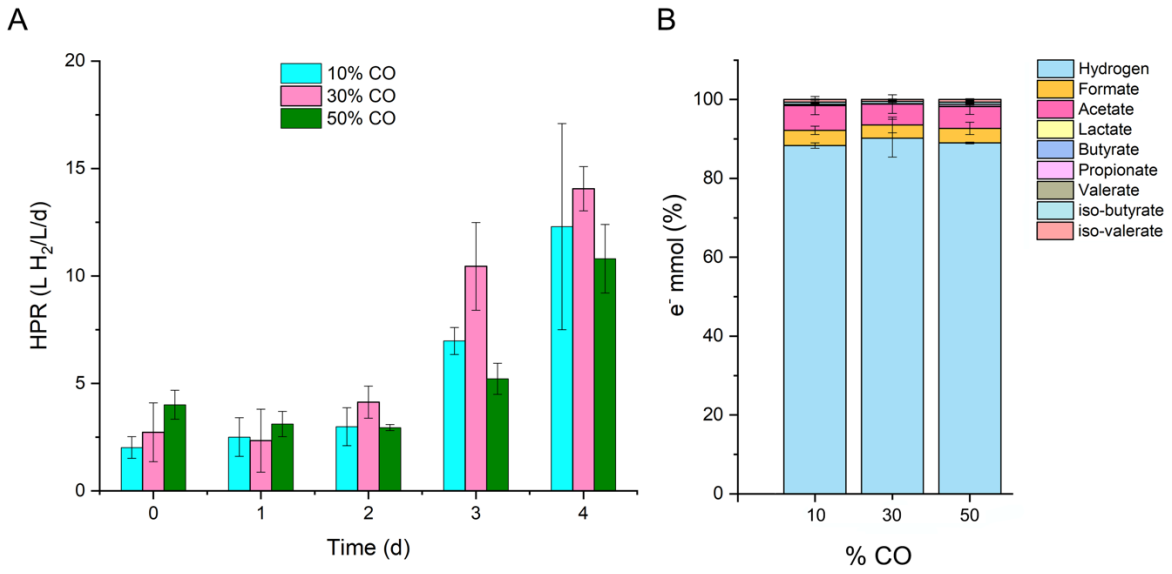

Figure 11. A) HPR with increasing percentage of CO. B) Selectivity of the process in terms of electron balance at 96 hours.
The represented data is the average between two reactors and the error bars indicate the standard deviation.

Glucose (5.5 mM) was fully consumed by the first day of fermentation at all three CO levels, while formate was cumulatively produced, reaching 19.7 mM in the fermentation with 10% CO (Figure 12A). Acetate production peaked at 11.6, 12.4, and 12.2 mM at 10, 30, and 50% CO, respectively, by 48 hours, before being almost completely consumed by the end of the fermentation. In comparison, lactate accumulated to 5.2 and 6.6 mM at CO levels of 10 and

30%, respectively, before being consumed within 48 hours. A distinct lactate production pattern was observed at 50% CO, where it reached 1.1 mM at 72 hours and remained stable for the remainder of the fermentation.

The greatest biomass (OD_{600}) was attained at 30% CO (with the highest HPR). After a long lag phase of nearly 24 hours, the absorbance started to increase, reaching a maximum of 1.5 at 96 hours post-inoculation (Figure 12B). At a 10% CO, absorbance started to increase from 4 hours post-inoculation and reached an OD_{600} of 0.9 by the end of the fermentation (96 hours). After 24 hours, the absorbance at 50% CO increased to 0.1, and reached 0.4 at 48 hours of fermentation, remaining constant until 96 hours.

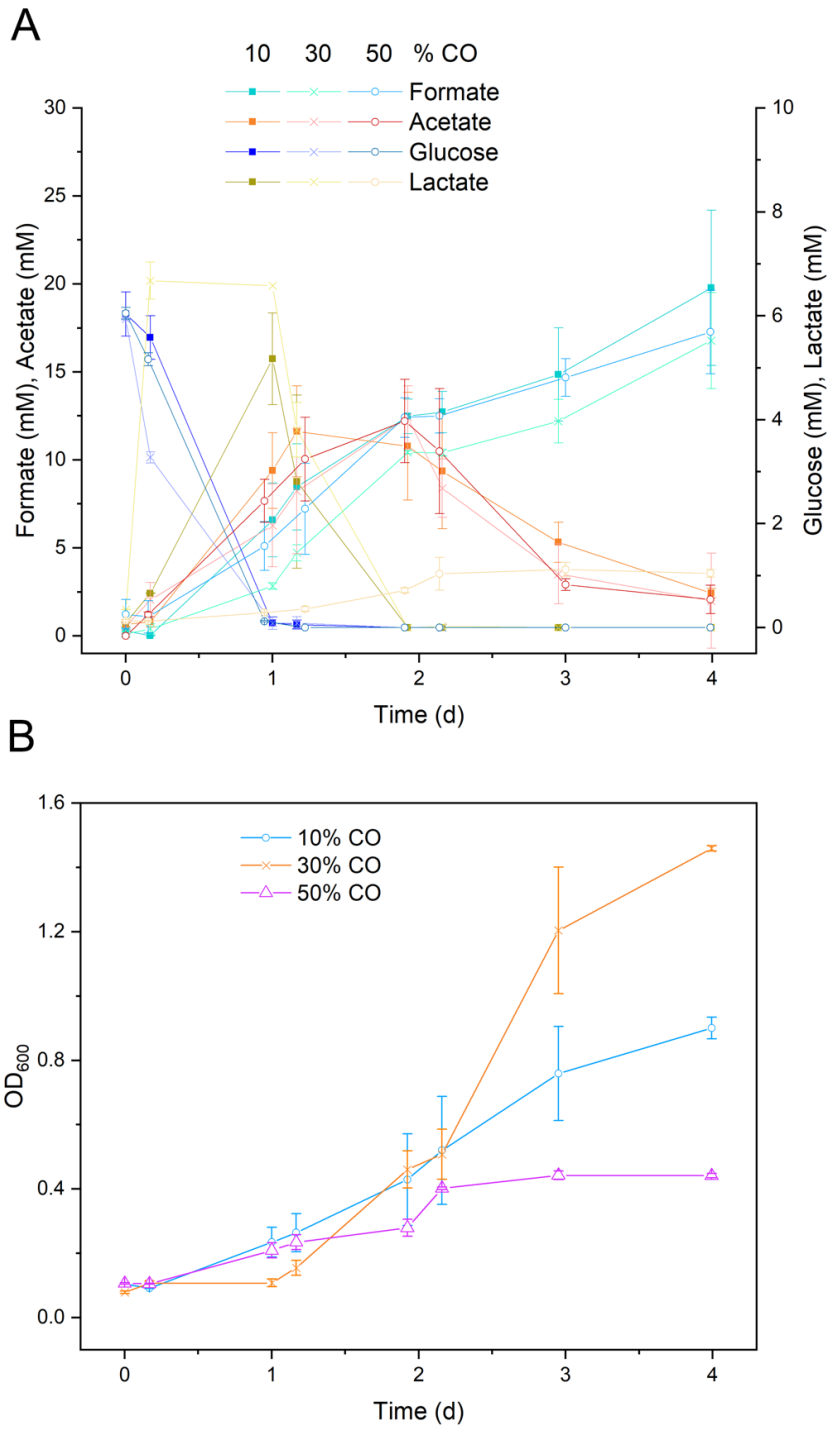

Figure 12. A) Metabolite concentration during the fermentations at increasing CO percentages. B) Growth of *P. thermoglucosidasius* in terms of absorbance (OD_{600}).

The data shown represent the average of two reactors, with error bars indicating the standard deviation.

4.8.2 Effects of increased H_2 percentages in the gas mixture on H_2 production

Overall, increasing H_2 had a positive effect on the HPR. While there were no noticeable differences in hydrogen production 48 hours post-inoculation (Supplementary material 3, Figure 2). At 72 hours post-inoculation 33% and 36% higher HPRs were achieved with 12% (12.4 L H_2/L/d) and 20% (13.1 L H_2/L/d) of H_2 added to the gas mixture, respectively, compared to the gas mixture containing 5% H_2 (8.3 H_2/L/d) (Figure 13A). By 96 hours, the HPR decreased, and similar HPR values were observed, with 7.8, 9.7, and 9.1 L H_2/L/d, for 5, 12, and 20% H_2, correspondingly.

As observed for the experiments with increasing CO, most of the electrons from CO went to H_2 production (Figure 13B). When H_2 was increased from 5 to 20%, the proportion of acetate changed from 3.7 to 5.8%. In contrast, formate decreased from 4.1 to 2.9% when changing the percentage from 12 to 20%.

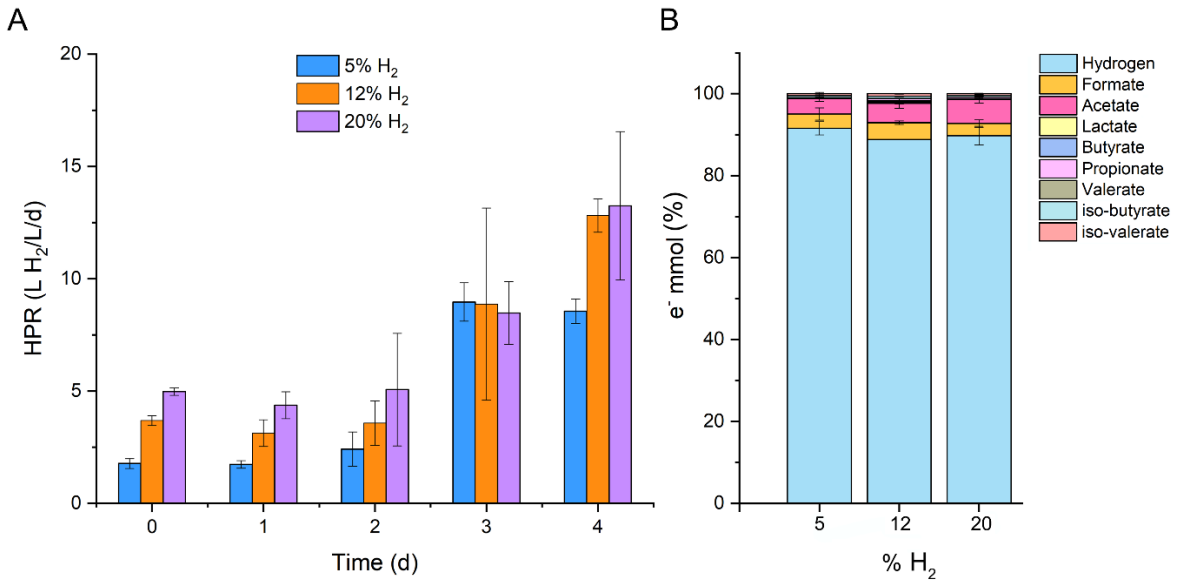

Figure 13. A) HPR with increasing H_2 percentage. B) Selectivity of the process in terms of electron balance at 96 hours.
The represented data is the average between two reactors and the error bars indicate the standard deviation.

Similar to the trend observed with increasing CO, glucose was consumed (5.5 mM) on the first day when H_2 was increased. Formate accumulated to 17.9 and 17.5 mM at 5 and 12% H_2,

respectively, while at 20%, it increased to 20 mM. Acetate production peaked at 11.9 and 47.7 mM at 5 and 12% H_2 within 24 hours before being consumed by 96 hours (Figure 14A). In contrast, at the highest H_2 level (20%), acetate increased to 15.6 mM at 48 hours and was gradually consumed from that point onward. Maximum lactate production reached 2.9, 1.1, and 0.5 mM at 5, 12, and 20% H_2, respectively.

Similar biomass accumulation was observed at 5 and 12% H_2. Even though with 20% H_2 an OD_{600} value 50% lower than that with a 5% H_2 was observed 48 hours post-inoculation, all the H_2 levels evaluated resulted in similar OD_{600} values (~1.2) by 96 hours post-inoculation (Figure 14B).

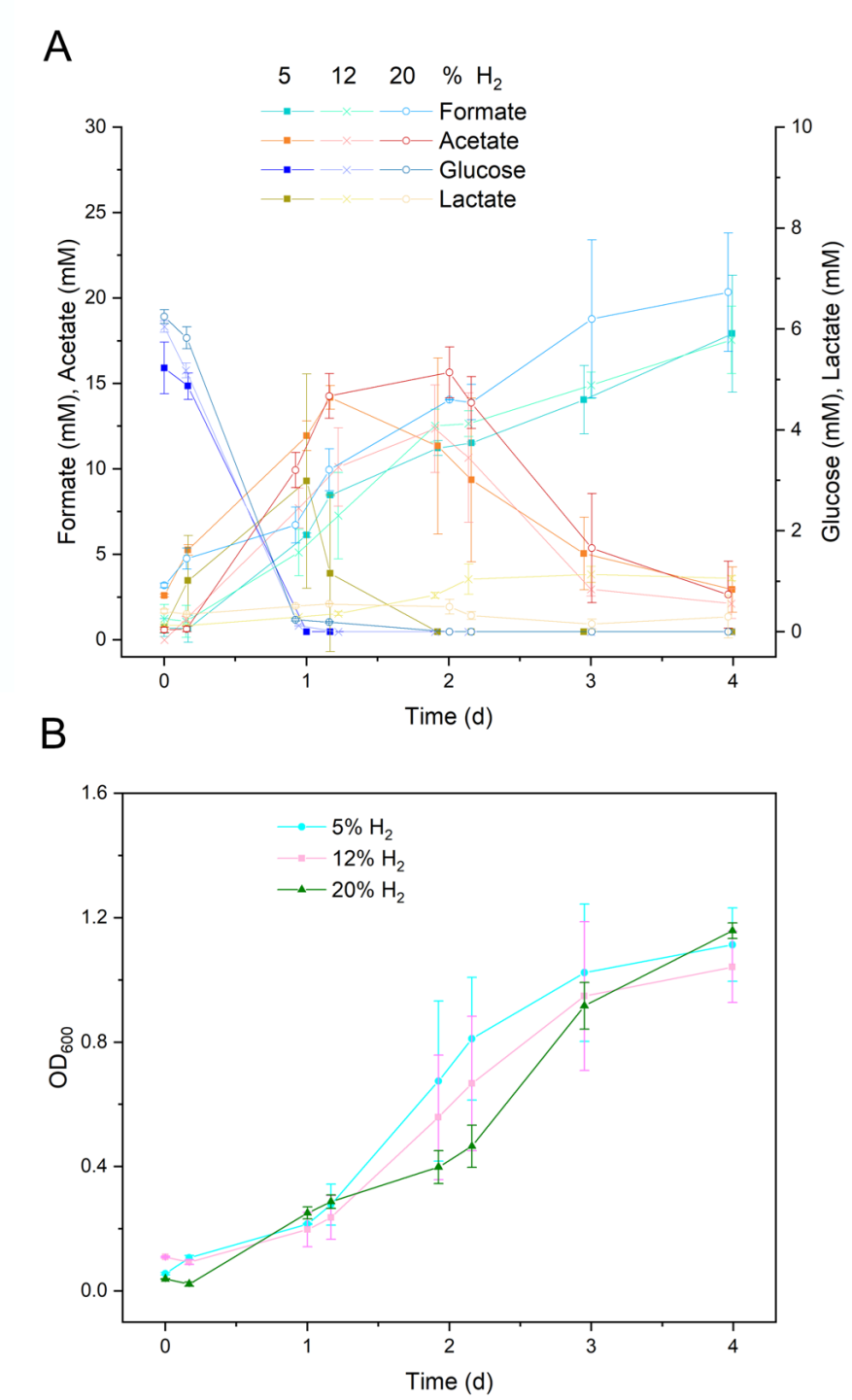

Figure 14. A) Metabolite concentration during the fermentations at different H_2 percentages. B) Growth of *P. thermoglucosidasius* in terms of absorbance (OD_{600}).

The data shown represent the average of two reactors, with error bars indicating the standard deviation.

4.8.3 Acetate as substrate for *P. thermoglucosidasius*

In batch fermentations using acetate as an additional carbon source, CO uptake followed a slightly delayed pattern (Figure 15A). Additionally, *P. thermoglucosidasius* biomass decreased from an absorbance (OD_{600}) of 1.0 ± 0.1 to 0.37 ± 0.01 after gas exchange. However, the OD recovered in correlation with H_2 production, which began 36 hours post-inoculation and continued until the end of fermentation (Figure 15B). The decrease in OD observed after the gas exchange has been observed before, as the microorganism needs to adapt to the anaerobic conditions and start CO consumption [149].

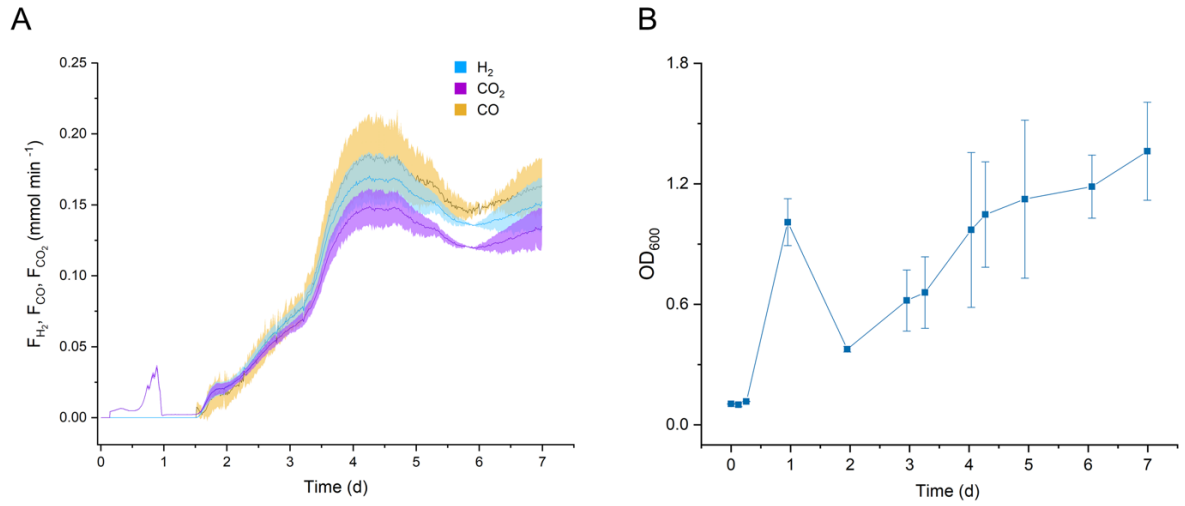

Figure 15. Batch fermentation with acetate as substrate A) H_2 and CO_2 production rate (mmol min^{-1}) and CO consumption rate (mmol min^{-1}) with the standard deviation indicated by the colored regions. Gas exchange is indicated by the drop of CO on the first day of fermentation. B) Growth indicated by absorbance OD_{600}.
The data shown represent the average of two reactors, with error bars indicating the standard deviation

Acetate consumption began around 24 hours into the fermentation, but CO uptake was only initiated at approximately 36 hours (12 hours after gas exchange). H_2 production increased gradually in this case, reaching its peak HPR of 0.167 ± 0.017 mmol min^{-1} at 96 hours. In contrast, when glucose was the additional carbon source, *P. thermoglucosidasius* began consuming CO on the second day of fermentation, following gas exchange. H_2 production via the WGS reaction started concurrently, reaching a maximum HPR of 0.144 ± 0.002 mmol min^{-1}

by 96 hours. This indicates that although the onset of WGS activity was slower with acetate, it led to a slightly higher maximum HPR.

The metabolite production profiles differed significantly between glucose and acetate fermentations. The acetate fermentation resulted in markedly reduced production of most organic acids (Figure 16A). Notably, butyrate became the predominant product once acetate consumption began, reaching a peak production rate of 0.2 mmol d^{-1} within just four hours. This suggests a more efficient metabolic response, with carbon flux favoring butyrate and hydrogen production over a wider spread of by-products. On the other hand, in the glucose batch fermentations, *P. thermoglucosidasius* produced a broad of organic acids, particularly formate, lactate, acetate, and propionate. Formate was the dominant product, and acetate production was closely associated with glucose metabolism, decreasing once the substrate was depleted.

Electron selectivity analysis revealed important differences in how electrons from CO and the carbon substrate were distributed. During acetate-fed fermentations, 91.4% electron selectivity toward H_2 was reached by 48 hours and maintained thereafter (Figure 16B). However, acetate fermentation also channeled a small but notable portion of electrons—around 8.3%—into butyrate production at 48 hours. This tighter distribution of electron flow toward fewer end-products implies a more efficient conversion of substrates into targeted outputs, particularly hydrogen and butyrate. A similar trend was observed in the glucose fermentation, electrons were initially routed toward acetate, then shifted toward H_2 production following gas exchange. By 48 hours, 79% of electrons were directed toward H_2 production, and this value remained stable at around 90% by 72 hours.

Carbon recovery during acetate fermentation—calculated based on the carbon from the substrates (CO and acetate) incorporated into product formation—exceeded 80%, indicating that the majority of the carbon was successfully converted into products such as formate, lactate, butyrate, propionate, valerate, iso-butyrate, and iso-valerate (Supplementary material 3, Figure 3). The ratio of CO_2 produced to CO consumed ranged from 0.8 to 1.0, suggesting that most of the carbon derived from CO was converted into CO_2 (Supplementary material 3, Figure 4). Additionally, the data indicate that acetate was primarily converted into biomass and other

organic acids, including formate, lactate, butyrate, propionate, valerate, iso-butyrate, and iso-valerate.

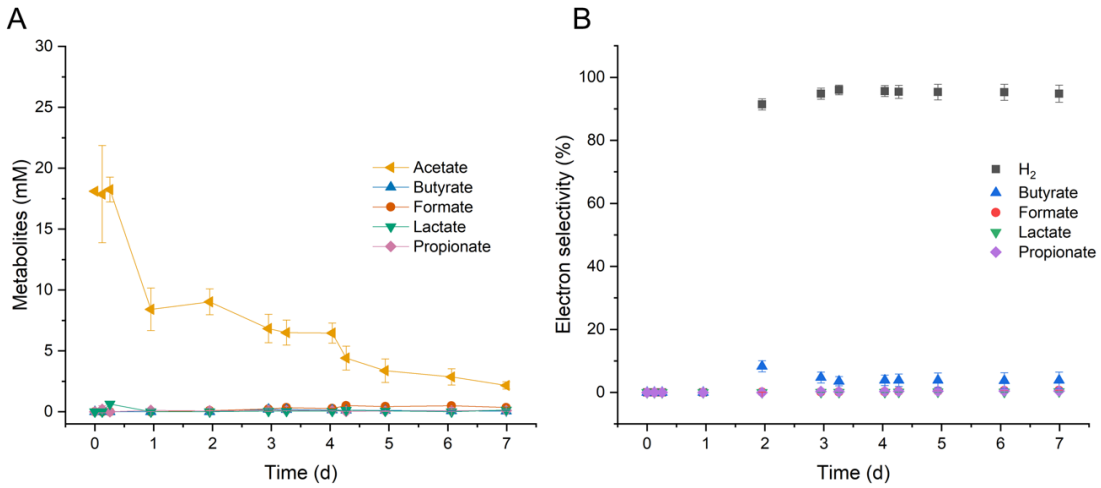

Figure 16. A) Metabolites concentration during the fermentation with *P. thermoglucosidasius* DSM 6285. B) Electron selectivity along the fermentation. The error bars indicate the standard deviation.

The data shown represent the average of two reactors, with error bars indicating the standard deviation.

4.9 Discussion

Understanding the impact of gas composition on microbial growth and metabolism is crucial for optimizing fermentation processes. While the total gas flow in our experiments remained constant, the partial pressure of individual gases (pCO, pH_2) was varied to assess potential substrate or product inhibition. An increase in CO positively influenced the growth rate up to 30% CO. However, further increasing CO to 50% led to a 42% reduction in growth rate by 72 hours. A recent study investigating *Rhodospirillum rubrum* in a bioreactor found that pCO became inhibitory at 1.0 atm, where the growth rate decreased from 0.058 to 0.040 h^{-1} as pCO increased from 0.2 to 1.0 atm. Despite this, H_2 production improved significantly, rising from 1.81 to 4.88 mol under the same conditions [150].

Raising CO to 50% within a gas mixture resulted in reduced CO uptake and delayed onset of H_2 production compared to lower CO conditions. This observation aligns with our previous study, which examined syngas fermentation in bottle experiments using different gas

compositions [142]. In that study, CO depletion occurred earlier with a gas mixture containing 17.28% CO, whereas a higher CO concentration (38.01%) left residual CO in the headspace. Although this did not completely inhibit H_2 production, it delayed the onset of hydrogenogenesis [142]. One of the parameters to improve H_2 production at the bioreactor scale would be to evaluate different CO flow rates or adapting *P. thermoglucosidasius* to higher CO percentage in syngas. In an adaptive laboratory evolution study with *R. rubrum*, the evolved strains showed up to 50% additional H_2 production and a reduced lag phase, compared to the parental strain, demonstrating their adaptation to gas photofermentation [151]. Contrarywise, this could also cause a decrease in the conversion efficiency, as described for *Carboxydothermus hydrogenoformans* [111]. It has been reported that the CO mass transfer can be a limiting step in growth [152]. This has to be considered when conditioning syngas with higher CO amounts.

Increasing H_2 to 20% in a gas mixture containing CO and CO_2 was not detrimental to H_2 production, with a maximum HPR of 13.6 L H_2/L/d at 72 hours at this H_2 percentage. In another study, increasing pH_2 up to 1.52 bar increased ethanol production and hydrogen uptake rate in a syngas fermentation performed with *Clostridium ljungdahlii* [153]. However, further increase of H_2 had negative effects, possibly due to inhibition of an enzymatic reaction above a critical equilibrium concentration of H_2 in the liquid phase [153].

Previous anaerobic fermentations with *P. thermoglucosidasius* DSM 6285, showed that the onset of the WGS reaction was faster and had shorter lag phases for H_2 production when syngas was used compared to pure mixtures of CO and N_2 [142]. This was also encountered in our fermentations using syngas compared to previous work with a two-phase system to change from aerobic to anaerobic conditions, where CO consumption started after 12 hours from the gas exchange on a batch fermentation, reaching a maximum consumption rate at 96 hours [149]. A possible reason could be the additional time cells need to adapt to the shift from the aerobic to the anaerobic phase. In contrast, syngas fermentation may allow for a more seamless metabolic transition due to its composition, reducing the lag phase. Additionally, the presence of H_2 in the syngas mixtures can lead to enzyme activation and metabolic adaptation from the strain [154].

As demonstrated by the fermentations with the different CO and H_2 levels (this study) and previous experiments [62], acetate is the primary metabolite when glucose is used as carbon source for hydrogenogenic fermentation. Here we evaluated the use of acetate to serve as carbon source (alongside CO). Previous evaluation with glucose achieved a maximum HPR of 0.144 ± 0.002 mmol d^{-1} [149]. Using 16.6 mM acetate, an HPR of 0.167 ± 0.017 mmol d^{-1} was achieved, translating into a 13% increase in the HPR with the latter substrate.

High acetate concentrations can inhibit microbial growth due to the uncoupling effect of organic acids, i.e., acetic acid can diffuse across the cell membrane and affect the osmotic pressure [155]. Therefore, process optimization, evaluating different substrate concentrations, gas flow rates, and agitation speeds is required when using acetate as a carbon source in a semi-continuous fermentation or a chemostat [156]. Gradual feeding of acetate or using acetate-tolerant strains can be a solution for further upscaling strategies [157].

4.10 Conclusions

Higher percentages of CO led to a delayed onset of hydrogenogenesis, while elevated H_2 levels enhanced hydrogen productivity toward the end of the fermentation. H_2 presence in different compositions had no inhibitory effect on HPR, therefore H_2 does not inhibit the water-gas shift reaction. Electron flow was primarily directed toward hydrogen production, with the remainder contributing to the formation of organic acids. The use of a clean, syngas-like gas mixture, free from common microbial inhibitors such as tars, ammonia, hydrogen sulfide, particulates, among others [119], provided a controlled baseline for evaluating microbial performance and scaling up the process. However, gas-liquid mass transfer of CO remains a limiting factor, as poor solubility can reduce CO availability and ultimately lower hydrogen yields. Additionally, acetate proved to be an effective alternative to glucose for biomass production during the aerobic phase, offering several advantages due to its direct entry into central metabolism and its lower cost. These characteristics make acetate a promising substrate for hydrogenogenic fermentation.

4.11 Acknowledgments

We acknowledge support from Tommy Fischer from Karlsruhe Institute of Technology.

5 Effect of increasing partial pressures

This chapter is based on the publication:

Effect of different partial pressures on H_2 production with *Parageobacillus thermoglucosidasius* DSM 6285. Magda S. Ardila, Habibu Aliyu, Pieter de Maayer, Anke Neumann.
Fermentation, 2024.

Author's Contributions:

Magda Ardila	Conceptualization, investigation, data curation, writing the original draft, visualization.
Habibu Aliyu	Conceptualization, reviewing and editing, project administration.
Pieter de Maayer	Conceptualization, supervision, reviewing and editing, project administration, funding acquisition.
Anke Neumann	Conceptualization, supervision, reviewing and editing, project administration, funding acquisition.

5.6 Introduction

Hydrogen (H_2) is a versatile energy carrier, with the highest energy content per unit weight (142kJ/g). Furthermore, it can be transported and is safer to handle than natural gas, and its zero-carbon nature makes it a promising energy alternative to dwindling fossil fuels [2,3,6,7,35]. Current industrial H_2 production practices are hampered by high costs and are often non-carbon neutral, and hence there has been increasing research on the development of biological means for H_2 production, with focus on improving the yield and the emergent renewable technologies [31,158]. Biological H_2 production strategies of interest include direct and indirect bio-photolysis, microbial electrolysis cells, and photo and dark fermentations, and combined systems such as photo-electrochemical electrolysis [6,7,159,160]. Recently the biological water-gas shift (WGS) reaction has been added to this group of processes [6,35,159]. This area of biohydrogen production research centers on the use of hydrogenogenic carboxydotrophic mesophilic or thermophilic microorganisms capable of performing the WGS reaction, where carbon monoxide (CO) reacts with water under anaerobic conditions to produce hydrogen and CO_2 [28,88]. A waste gas, forming part of synthesis gas from various industrial process, CO expands the substrate range for carbon-neutral biological H_2 production [35,159]. In particular, the Gram-positive thermophile *Parageobacillus thermoglucosidasius* presents a robust microorganism for WGS-driven hydrogen production [52] and it is a versatile microorganism with industrial significance able to degrade starch, hemicellulose, cellulose and lignocellulose [161]. Unlike other hydrogenogenic carboxydotrophs, which are strict anaerobes, this bacterium is a facultative anaerobe, and has even been observed to undertake the WGS reaction under low oxygen levels [59,142]. Various parametric optimizations have been investigated to improve the hydrogen yield from CO oxidation by *P. thermoglucosidasius*, including factors such as temperature, media composition, pH, inoculum size, and age of the inoculum [59]. One parameter that has received limited attention is the effect of pressure on *P. thermoglucosidasius* hydrogenogenesis and how it affects H_2 production, as well as the microorganism metabolism.

When considering gas fermentations, Henry's law applies, where a proportional relationship exists between the concentration of the gases in the liquid phase (where the microorganism resides) and the total headspace pressure [162]. This suggests that more CO would be available for the microorganism to use as substrate and concomitantly increase the H_2 yield. However,

this represents a challenge, as the toxicity of CO to microbial cells also tends to increase [27]. *P. thermoglucosidasius* has been shown to cope with toxicity, as CO is present during initial aerobic growth [62]. Alternatively, a lower hydrogen partial pressure in the headspace facilitates the mass transfer of hydrogen from the liquid to the gas phase [162].

Understanding the effects of different partial pressures of gases on the WGS process could therefore be used to increase H_2 yield and thereby optimize the biohydrogen process. In this study, the effect of increasing CO, H_2, and N_2 partial pressures (pCO, pH_2, and pN_2) on WGS-driven H_2 production by *P. thermoglucosidasius* was evaluated.

5.7 Materials and methods

5.2.1. Microorganism and Media

P. thermoglucosidasius DSM 6285 was obtained from the Deutsche Sammlung von Mikroorganismen und Zellkulturen (DSMZ, Braunschweig, Germany) and was conserved in glycerol (80%) stocks at – 80 °C. The cultivation of *P. thermoglucosidasius* DSM 6285 was performed in modified Luria Bertani (mLB) medium containing, yeast extract (5 g/L), NaCl (5 g/L), tryptone (10 g/L), 1.25 mL/L of NaOH (10 g/L) and 1 mL/L of each of the stock solutions of nitrilotriacetic acid (1.05 M), $MgSO_4 \cdot 7H_2O$ (0.59 M), $CaCl_2 \cdot 2H_2O$ (0.91 M) and $FeSO_4 \cdot 7H_2O$ (0.04 M), previously filter-sterilized. *P. thermoglucosidasius* was cultured at 60 °C as described below in the inoculum preparation. For the subsequent fermentations, a modified ammonium sulfate medium (mASM) was used, with the following content: citric acid (8.7 mM), $MgSO_4$ (20.2 mM), K_2SO_4 (10 mM), NaH_2PO_4 (22.6 mM), $CaCl_2$ (0.8 mM), $(NH_4)_2SO_4$ (25 mM),, and 1 mL each of the filter-sterilized trace elements: H_2SO_4 (6 mM), $CuSO_4$ (0.1 mM), $CoSO_4$ (0.2 mM), $ZnSO_4$ (0.5 mM), $FeSO_4$ (2.29 mM), $NiSO_4$ (0.3 mM), $MnSO_4$ (0.9 mM) and H_3BO_3 (0.1 mM). The pH was adjusted to 6.8 with 4 M NaOH. The ASM medium was supplemented per liter with 0.02 mM biotin (Carl Roth, Karlsruhe, Germany), 20 mL 50x-MEM amino acids solution, 10 mL 100x-MEM non-essential amino acids solution, and 10 mL 100x-MEM vitamin solution (Thermo Scientific, Schwerte, Germany), all supplementary solutions were previously filter-sterilized, and added after the main components of the media were autoclaved. Finally, glucose was added (1 g/L final concentration).

5.2.2. Inoculum preparation and bottle fermentation

Precultures were prepared by adding 300 µL of glycerol stock to 200 mL of mLB medium in 500 mL shake flasks, which were then incubated at 60 °C and 120 rpm under aerobic conditions in an Infors Thermotron (Infors AG, Bottmingen, Switzerland). After 14 h, a calculated volume of 30 mL of the inoculum was added to 1.5 L stainless steel bottles (DURAN® GL 45) containing 600 mL mASM. Initially, the bottles were prepared with an atmosphere of 50% CO, 50% air at standard pressure (1 bar), afterwards, the pressure in the bottles was increased by adding up either CO, H_2, or N_2, up to a given partial pressure for each gas (Table 5). The bottles were then incubated at 60°C and 120 rpm in the Infors Thermotron (Infors AG, Bottmingen, Switzerland). The fermentations were evaluated over a duration of 168 hours.

Table 5. Gas composition for the different experiments.

Experiment	**Initial partial pressure (bar)**					**Total pressure (bar)**
	CO	**N_2**	**H_2**	**O_2**	**CO_2**	
No overpressure	0.523	0.482	0	0.133	0.001	1.139
CO (1 bar)	0.976	0.803	0	0.226	0.001	2.006
CO (2 bar)	1.524	0.870	0	0.238	0.002	2.634
CO (3 bar)	2.102	1.201	0	0.329	0.002	3.634
N_2 (1 bar)	0.508	1.390	0	0.129	0.001	2.028
N_2 (2 bar)	0.496	2.429	0	0.123	0.001	3.049
N_2 (3 bar)	0.436	3.073	0	0.138	0.002	3.650
H_2 (1 bar)	0.541	0.487	0.999	0.136	0.001	2.164
H_2 (2 bar)	0.573	0.362	1.908	0.139	0.001	2.983
H_2 (3 bar)	0.675	0.213	2.777	0.111	0.002	3.778

5.2.3 Analytical methods

The gas composition was evaluated at different time points in each fermentation by drawing 3 mL samples of gas from the headspace and injecting each sample in a 3000 Micro GC gas

analyzer (Inficon, Switzerland) connected with 10 m Molsieve and 10 m PoraPLOT Q columns. Gas compositions were calculated according to the ideal gas law as previously described [59]. To evaluate the growth of *P. thermoglucosidasius* and metabolites production during the fermentation, 1 mL liquid samples were collected through the bottle stoppers. The absorbance (OD_{600}) of each sample was measured using the Ultrospec 1100 pro spectrophotometer (Amersham Biosciences, Uppsala, Sweden). The remain liquid samples were centrifuged at 13000 rpm for 10 min and the supernatants were transferred into 1.5 mL HPLC vials to evaluate the presence of glucose, acetate, ethanol, formate, lactate, succinate, propionate, butyrate, and valerate. HPLC was performed to quantify the metabolies present in each sample with an Agilent 1100 series HPLC system (Agilent Technologies, Waldbronn, Germany) equipped with a wavelength detector and refractive index detector with a 50x7.8 mm long pre-column (model Rezex ROA-Organic Acid H^+ 8% guard column) and a 300x7.8 mm, 8 µm long separation column (model Rezex ROA-Organic Acid H^+ 8% column). A sample volume of 10µL was injected, with a 0.6 mL min^{-1} flow rate for 40 min per sample. A 5 mM H_2SO_4 solution was used as the mobile phase, and a column temperature of 55 °C was selected. Data acquisition and analysis were performed with the software Chemstation (Agilent Technologies). The electron selectivity for the different partial pressures experiments was calculated as explained in the Supplementary material 4.

5.8 Results

5.8.1 Effect of increased CO partial pressure on H_2 production

The pCO was increased in the fermentations to evaluate its enhancing or inhibitory effect on hydrogenogenesis. H_2 production commenced after 24 hours in the fermentation with no overpressure (pCO: 0.523 bar) and reached a maximum of 16.2 mmol H_2 corresponding to a pCO of 0.574 bar after 72 hours (Figure 17A). Increase of pCO invariably resulted in a delay in the start of H_2 production. Increasing pCO to 1 bar resulted in the commencement of hydrogenogenesis after 48 hours. However, due to higher availability of CO in the headspace, the production of H_2 increased to 63 mmol, corresponding to a pH_2 of 1.39 by 96 hours post-inoculation (Figure 17A).

A further increase of pCO to 2 bar, delayed the start of H_2 production to 52 hours, post-inoculation, with H_2 reaching a concentration of 26.6 mmol after 168 hours, with a pH_2 of 1.42

bar. At the highest pCO (3 bar), no evident CO consumption or hydrogen production was observed (Figure 17A). Hydrogen production rate reached a maximum of 0.21 mmol d^{-1} at 96 hours with 1 bar pCO, while at the same time, it reached 0.03 mmol d^{-1} with 2 bar pCO (Supplementary material 4, Figure 1.). The volumetric H_2 production rate was 7.44 and 1.08 L H_2 L^{-1} d^{-1} for 1 bar and 2 bar pCO, respectively. On the other hand, oxygen was depleted in all experiments, within the first 24 hours of fermentation except for the 3 bar pCO, and it remained constant from 24 to 120 hours (Supplementary material 4, Figure 2.).

Changes in the metabolite profiles were also observed with increased pCO. With a pCO of 1 bar, acetate production was the highest, while for 2 and 3 bar pCO, formate and lactate, respectively, were prominently produced (Figure 17B). More specifically, with 1 bar pCO, acetate production commenced after 24 hours, and increased to a maximum of 14.17 mM after 120 hours. Formate production stayed below 0.66 mM, while lactate peaked (0.71 mM) after 24 hours, and subsequently decreased to 0.02 mM (Figure 17B). With 2 bar pCO, 22.4 mM of formate was observed after 72 hours and subsequently remained constant, while lactate (0.25 mM) and acetate (0.73 mM) production reached their maximum after 120 hours and 72 hours, respectively (Figure 17B).

Under 3 bar pCO, formate (8.6 mM) and acetate (2.5 mM) reached their relatively low maxima after 72 hours and 24 hours, respectively, while fermentation with this partial pressure resulted in the highest amount of lactate being produced, reaching 3.2 mM after 24 hours and remaining stable throughout the remainder of the fermentation (Figure 17B). For all the fermentations, the glucose in the media was depleted by 24 hours post-inoculation, except for the highest pCO (3 bar), where glucose content decreased to 4 mM and remained constant until the end of the fermentation. This correlates with the lack of consumption of CO under this partial pressure, underlying the inhibition in the fermentation (Supplementary material 4, Figure 3). Additionally, it further correlates relates with the slight O_2 concentration observed with 3 bar pCO, as normally, both oxygen and glucose consumption, should occur in parallel.

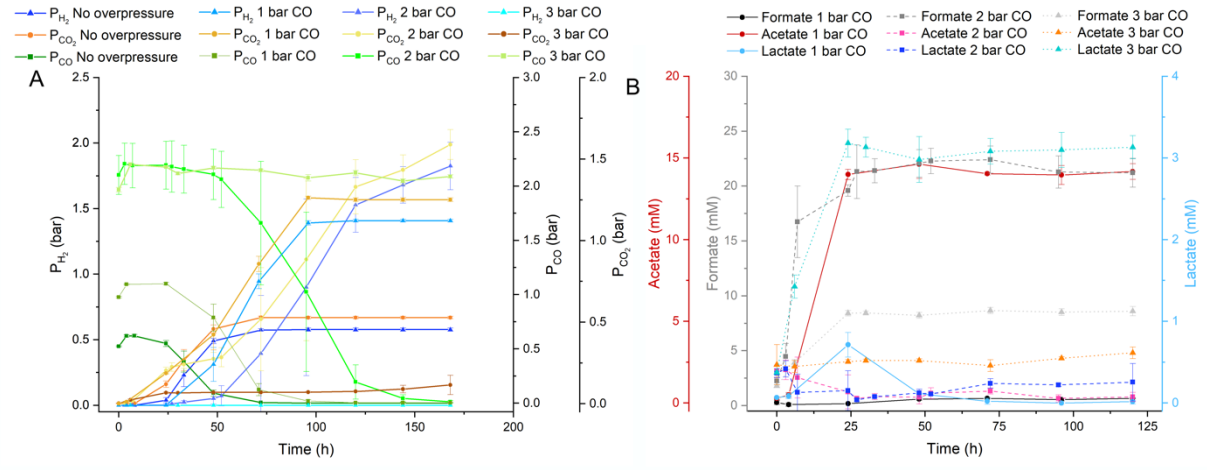

Figure 17. A) Gas partial pressures during fermentations with different pCO. The blue lines denote H_2 production, while the green and orange represent CO and CO_2. **B)** Formate, acetate, and lactate production in the different pCO. Formate, acetate, and lactate are indicated in grey, red, and blue, respectively.

5.8.2 Effect of increased N_2 partial pressure on H_2 production

To understand the effects of overall gas pressure on hydrogenogenesis, pN_2 was increased by adding up to 3 bar of pressure. Under no overpressure, H_2 production was observed after 24 hours, with 1.0 mmol (pH_2: 0.03 bar), increasing up to 16.4 mmol by 96 hours (pH_2: 0.5 bar). With 1 bar pN_2, H_2 production was first observed after 24 hours, with 7.9 mmol (pH_2: 0.2 bar) and 22.1 mmol (pH_2: 0.5 bar) of H_2 produced after 29 hours and 72 hours of fermentation, respectively (Figure 18A). Increasing the pressure in the system to 2 bar pN_2, produced 6.8 mmol (pH_2: 0.2 bar) and 17.6 mmol (pH_2: 0.5 bar) of H_2 at the same time points. At the highest pN_2 (3 bar), H_2 production commenced earlier, 5.7 mmol of H_2 (pH_2: 0.3 bar) already observed after 24 hours of fermentation, reaching a peak of 9.2 mmol H_2 (pH_2: 0.6 bar) after 48 hours and afterward remaining stable. The maximum hydrogen production rate was observed at 48 hours with 0.13, 0.11, and 0.07 mmol d^{-1} corresponding to 1, 2, and 3 bar pN_2 (Supplementary material 4, Figure 1.). Similarly, the volumetric H_2 production rate was 1.58, 0.94, and 0.40 L H_2 L^{-1} d^{-1} for the increasing pN_2 of 1, 2, and 3 bar. Increased pN_2 also affected the growth of the microorganism; the specific growth rate was reduced from 0.145 to, 0.116, 0.090, and 0.075 h^{-1}, with 1, 2, and 3 bar pN_2, respectively.

Lactate and formate production increased in line with the increase in pN_2. Whereas formate accumulated to 0.79 mM at the end of fermentation with 1 bar pN_2, it reached 0.96 mM and 1.19 mM with 2 and 3 bar pN_2, respectively (Figure 18B). Maximum lactate production was observed after 24 hours for all evaluated pN_2 levels, with 2.05 mM, 2.88 mM and 3.14 mM produced with 1, 2 and 3 bar of pressure, respectively. Afterwards, lactate production decreased by 1 mM in all the pN_2 levels and remained stable. By contrast, acetate production was highest (6.15 mM after 120 hours) with 1 bar pN_2, and the lowest (4.14 mM after 120 hours) with 3 bar pN_2.

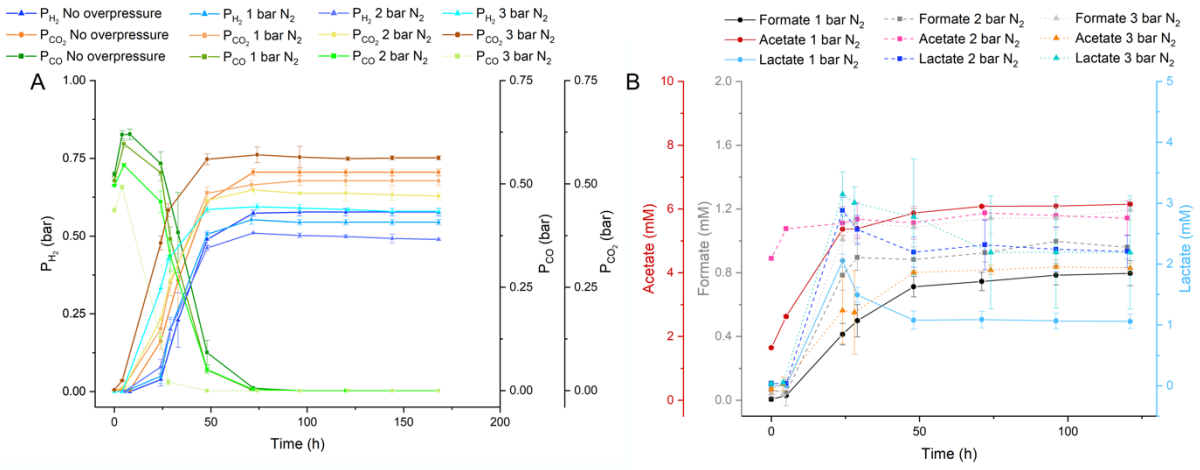

Figure 18. A) Gas partial pressures during fermentations with different pN_2. The blue lines denote H_2 production, while the green and orange represent CO and CO_2. **B)** Formate, acetate, and lactate production in the different pCO. Formate, acetate, and lactate are indicated in grey, red and blue, respectively.

5.8.3 Effect of H_2 partial pressure on H_2 production

Increasing pH_2 up to 3 bar allowed us to evaluate product inhibition. With 1 bar pH_2, an increase in H_2 from an initial amount of 37.8 mmol to 46.2 mmol (an increase of 8 mmol) was observed after 24 hours, while increases of 11.9 mmol and 15.1 mmol of H_2 were observed with 2 bar (initial 69.1 mmol H_2) and 3 bar (initial 97.9 mmol H_2) pH_2, respectively. The highest amount of H_2, 130 mmol after 120 hours with 3 bar pH_2. Production of hydrogen commenced already on the 4 hours of fermentation, with 0.39, 0.70, and 0.97 mmol d^{-1}, for 1, 2, and 3 bar pH_2, respectively (Supplementary material 4, Figure 1.). A similar trend was observed with the volumetric H_2 production rate, with 1.03, 4.05, and 7.64 and L H_2 L^{-1} d^{-1} for the increasing pH_2

1, 2, and 3 bar. The specific growth rate was negatively affected by increased pH_2, reducing from 0.145 h^{-1} with no overpressure to 0.062 h^{-1} when increasing the pH_2 to 3 bar.

With 1 bar pH_2, acetate accumulated to 6.24 mM after 48 hours, then remained stable until 96 hours and subsequently decreased to 4.33 mM by 120 hours of fermentation. A similar trend was observed with 2 bar pH_2, where acetate accumulated to 6.85 mM by 48 hours, and remained relatively stable until 120 hours, with a production of 6.70 mM at this time point. A further increase of pressure to 3 bar pH_2 led to a decrease in acetate with the highest acetate amount (3.92 mM) after 72 h.

Formate production with 1 bar pH_2 increased to 0.89 mM after 24 hours and stabilized at a highest concentration of 1.09 mM after 72 hours. By contrast, with 2 bar pH_2, there was consumption of the initial amount (1.0 mM) of formate, decreasing to 0.54 mM after 24 hour. However, it subsequently recovered to a concentration of 1.01 mM after 120 hours. Formate trends with 3 bar pH_2 were similar to what was observed with 1 bar, as formate increased to 0.69 mM after 24 h, with the highest accumulation (0.92 mM) after 120 hours of fermentation. Production of lactate increased to 6.8 mM only after 4 hours of the fermentation with 1 bar pH_2, but then decreased to 1.62 mM after 120 hours of fermentation. Lower and later peaks of lactate production were observed with 2 and 3 bar pH_2.

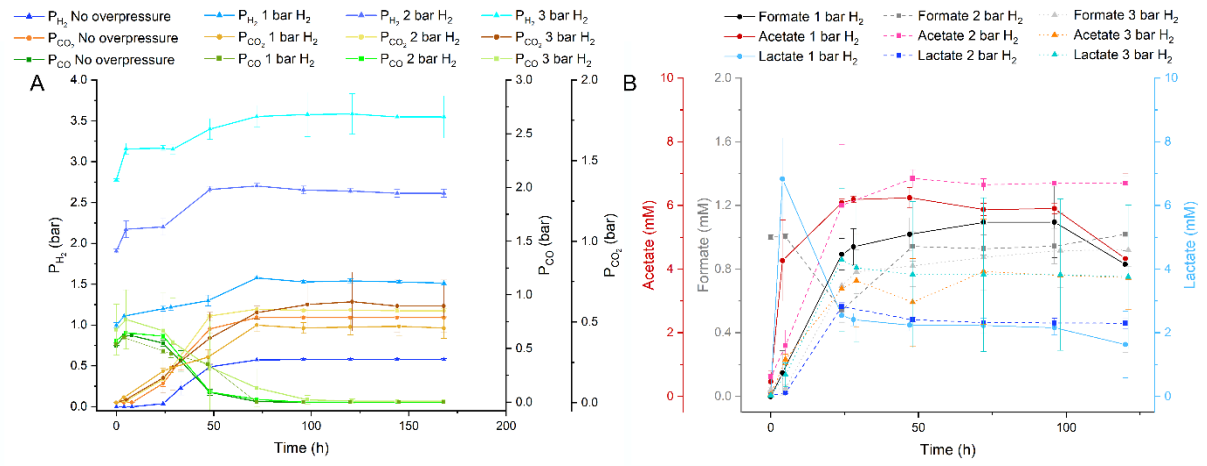

Figure 19. A) Gas partial pressures during fermentations with different pH_2. The blue lines denote H_2 production, while the green and orange represent CO and CO_2. **B)** Formate, acetate, and lactate production in the different pCO. Formate, acetate and lactate are indicated in grey, red and blue, respectively.

5.8.4 Selectivity of the WGS process with different CO, N_2, and H_2 partial pressures

The electron balances of the fermentation reactions with different pCO, pN_2, and pH_2 were evaluated. In the experiment with no overpressure, more than 98% of electrons from CO are directed into H_2. Similarly, for the experiments with increased pN_2 and pH_2, the fermentation process was highly selective towards H_2 production, where more than 95% of electrons derived from CO were converted into H_2, regardless of the level of partial pressure of the selected gas (Figure 20A and 20B). This is followed by acetate as the main metabolite, with less than 5% of electrons from CO and glucose being routed into organic acids. The same trend was observed with 1 and 2 bar pCO. However, when applying 3 bar pCO (Figure 20C), as H_2 production was inhibited, the electrons were primarily derived from glucose and acetate and routed into organic acids.

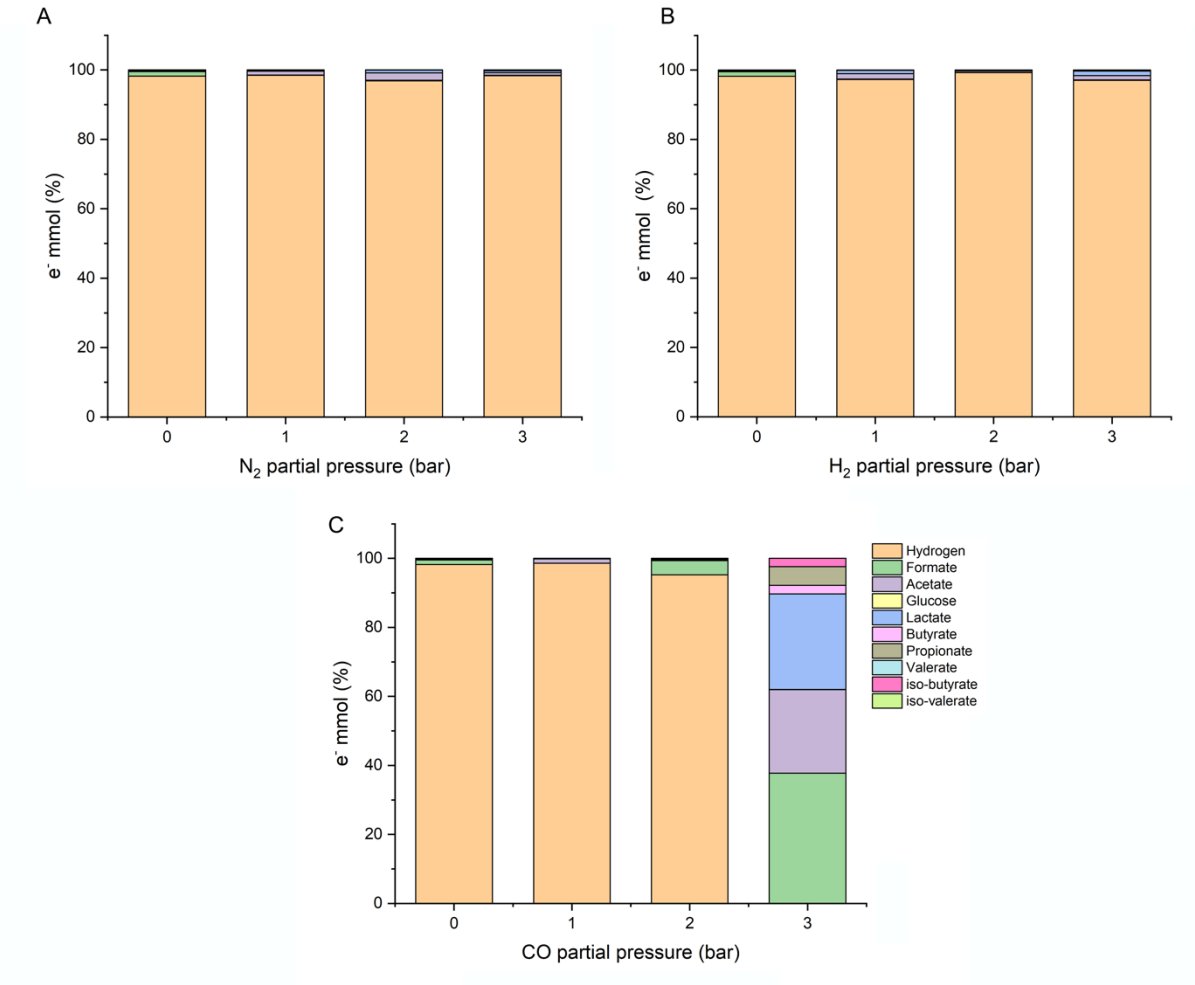

Figure 20. Electron selectivity for the different **A)** N_2 **B)** H_2 and **C)** CO partial pressures.

5.9 Discussion

5.9.1 Effect of increasing partial pressure of gases on H_2 production

The presence of H_2 could lead to product inhibition, as described for the thermophilic bacterium *Caldicellulosiruptor saccharolyticus,* where H_2 production ceased after reaching a pH_2 of 0.56 bar [163]. Similarly, an increase in pH_2 had a detrimental effect on H_2 yield and decreased sugar utilization efficiency by *Clostridium butyricum* TM-9A, where the total H_2 production decreased 2.6-fold when the pH_2 increased from 0.1 to 0.2 bar [27].

The increase of pH_2 up to 3 bar in our study had no inhibitory effect on H_2 production, and following the WGS reaction, all the CO present in the system was converted into H_2 with a selectivity higher than 95%. This agrees with a study where pH_2 up to 1.25 bar had no effect on *P. thermoglucosidasius* H_2 production [164]. In contrast, the increase of pH_2 in a study evaluating different gas release strategies (uncontrolled, intermittent, and constant) demonstrated that increasing pH_2 was inhibitory to dark fermentative H_2 production by a mixed anaerobic microbial consortium, and that the highest H_2 production was obtained with the constant gas release denoting the lowest pH_2 [165].

An increase in pH_2 primarily resulted in a reduction of acetate and formate, while lactate production was higher at 3 bar pH_2. Changes in the metabolite profile in response to high pH_2 have also been observed in *T. thermosaccharolyticum* W16 [166]. In anaerobic bacteria, the end product formation can be greatly affected by the pH_2, with a metabolic shift towards reduced metabolites such as ethanol and lactate [167]. This was also documented in a study with *Clostridium ljungdahlii*, where the increase of pH_2 to 1.52 bar, shifted the product ratio to ethanol, however, increase of pH_2 up to 3 bars caused a decrease in the gas consumption rates [153]. In *Chlamydomonas reinhardtii*, a high pH_2 caused inhibition of H_2 production, in addition to changes in metabolism towards reduced products, therefore a low pH_2 improved H_2 yields expotentially in the latter case [168].

The effect of total pressure on *P. thermoglucosidasius* hydrogenogenesis was evaluated by increasing the pN_2 up to 3 bar. A similar experiment with selected *Clostridium* spp. in an anaerobic biodisc reactor with a pressure increase of 0.18 above atmosphere pressure (0.89 bar) decreased H_2 yield by 19.5% [169]. In another experiment with *Clostridium acetobutylicum*, hydrogen yield declined by 40%, in comparison with a strategy releasing constant gas [170]. In our case, while no difference in CO consumption was observed in our study at pN_2 up to 3 bar,

slight decreases in H_2 production were noted, rather than the expected increase in yield. However, given the negligible effects, total pressures above 3 bar should be evaluated for effect on H_2 yield.

Increasing pCO positively affected cell growth and product (ethanol and acetate) formation in *Clostridium carboxidivorans* $P7^T$ [171]. In our study, increasing pCO up to 3 bar resulted in inhibition of hydrogenogenesis. Furthermore, the increase of pCO caused a decrease in the specific growth rate of *P. thermoglucosidasius* by 59.4% at a pressure to 1.0 bar and by 66.2% when the pCO reached 3.0 bar compared to when no overpressure was applied. Similarly, an increase of pCO from 0 to 0.5 atm was limiting on the specific growth rate of *Citrobacter* sp. Y19, reducing from 0.72 to 0.29 h^{-1} [172]. In *P. thermoglucosidasius*, the production of acetate and lactate increased at a pCO of 2 bar. This may serve as a means for this bacterium to cope with CO toxicity, as there is a shift in the flow of reducing equivalents away from terminal oxidases with increased CO concentration [62]. Furthermore, the conversion of pyruvate to lactate is a well-established mechanism used to restore the balance of NAD^+/NADH during bacterial growth on glucose [173]. A relationship between acetate and pCO was documented in *C. carboxidivorans* $P7^T$, where lower amounts of acetate were produced at higher pCO [171]. An opposite effect was shown in this work, where the increase of pCO caused an overall decrease of acetate from 14.17 mM to 2.5 mM, with 1.0 and 3.0 bar pCO, respectively. It has been observed that CO conversion rate is limited by the gas-liquid mass transfer when evaluating high biomass concentrations, additionally, the dissolved CO concentration affects the specific CO uptake [174].

5.9.2 Future perspectives

Increasing the pH_2 up to 3 bar did not have an inhibitory effect on *P. thermoglucosidasius* hydrogenogenesis. Future studies, where pH_2 is increased to pressures higher than this could help to understand the limits of product inhibition on the WGS reaction and changes in *P. thermoglucosidasius* metabolism. A study performed with *Clostridium acetobutylicum* showed that when increasing pH_2 up to 14.59 bar, the yield of butanol and ethanol increased by 18 and 13% [68]. In the latter study, the high H_2 concentration caused the hydrogenase system to be inhibited, while the oxidoreductase system received a higher flow of electrons to produce ethanol [68]. The increase of pH_2 up to 25 bar with a mixed culture was evaluated in a series of batch fermentations; when evaluating the partial pressures of 20 and 25 bar, these were

inhibiting due to the increase in the dissolved gas tension, which could be detrimental for the microorganisms [175]. However, to evaluate higher pressures in the presented study, would require a different system, such as a high-pressure resistant reactor.

Influence of CO_2 partial pressure in the present study was not evaluated, however, it has been reported that CO_2 sparging, which increases CO_2 partial pressure is beneficial for H_2 production when working under gas mixtures. In a study performed with *Thermoanaerobacterium thermosaccharolyticum* W16, it was observed that under high CO_2 partial pressure the microorganism could produce H_2 while with increasing H_2 partial pressure had a negative effect [166]. Future studies should therefore also consider the effect of increased pCO_2 on *P. thermoglucosidasius* hydrogenogenesis.

5.10 Conclusions

With the exception of 3 bar pCO, *P. thermoglucosidasius* DSM 6285 was capable of producing H_2 under conditions of increased pCO, pN_2, and pH_2. Increasing pCO up to 2 bar, in particular, had a positive effect on hydrogen production, likely due to increased WGS substrate availability. Finetuning of the pCO should be investigated further as a potential strategy for improved hydrogen yield. However, caution should be exercised as inhibition of hydrogenogensis was observed at pCO of 3 bar, suggesting a toxic CO limit for *P. thermoglucosidasius*. The application of higher pH_2 should also be investigated further as it could be crucial to understand the limit of inhibition of the WGS reaction, and the kinetics of distribution of the organic acids produced under such inhibition.

Regardless of the partial pressure applied, hydrogenogenesis via the WGS is a highly efficient process, with 95% electron recovery from CO and glucose in hydrogen gas, while other metabolites such as acetate, formate, and lactate represent minor electron sinks, suggesting that hydrogenogensis by *P. thermoglucosidasius* via the WGS reaction represents an attractive option for future biohydrogenogenesis approaches.

The potential for scaling up this process in bioreactors utilizing *P. thermoglucosidasius* remains to be fully assessed. While challenges exist, scaling this system up presents an open possibility for improving the biological hydrogen production platform. It is also important to evaluate the influence of different gas mixtures and a range of gas partial pressures to better understand the limitations observed in this study. Such evaluations could provide essential insights into

optimizing biohydrogen production. This study serves as a foundation for further research aimed at refining gas phase conditions to enhance hydrogen yields in biological systems.

Discussion

The evaluation of batch fermentations with *P. thermoglucosidasius* DSM 6285 supplemented with glucose led to the realization that an additional substoichiometric amounts of substrate was necessary to maintain biomass and H_2 production. The reduction of substrate inhibition and improvement of metabolic activity were achieved through a semi-continuous fermentation with optimized feed intervals, leading to a more stable and higher hydrogen yield with *P. thermoglucosidasius* compared to batch fermentation.

In this study, a 24-hour feed interval in semi-continuous mode led to an 18% increase in H_2 yield and sustained production over 15 days. In contrast, batch fermentation showed a decline in H_2 yield after just 4 days. Supplementing the feed with glucose helped maintain cell viability and prolonged H_2 production. While this feeding strategy promoted stability, variability between replicates suggests that additional process parameters, such as inoculum size, gas composition, and mixing, need optimization to ensure reproducibility [52].

A key metabolic distinction between semi-continuous and batch fermentations emerged in the pattern of byproduct formation. In batch fermentation, acetate production closely followed glucose consumption and was used once glucose was depleted. In contrast, during semi-continuous fermentation, acetate concentration continued to rise in parallel with each glucose addition, reflecting a sustained metabolic response. The glucose supplementation strategy used in the semi-continuous setup appeared to shift the metabolic balance toward mixed-acid fermentation, resulting in the accumulation of acetate, formate, and lactate, byproducts consistent with anaerobic glucose metabolism pathways [97]. These organic acids are formed as pyruvate is reduced, a process that regenerates NAD^+ and supports continued glycolytic activity under anaerobic conditions [97]. Notably, once glucose was depleted during the aerobic phase in both batch and semi-continuous fermentations, acetate concentrations decreased, suggesting its subsequent utilization, presumably through the tricarboxylic acid (TCA) cycle [62]. This observation highlights the metabolic flexibility of *P. thermoglucosidasius*, as well as the influence of feeding strategy on fermentation profiles and byproduct dynamics.

An alternative carbon source, acetate, was tested to evaluate its potential to replace glucose in a batch fermentation with continuous flow of CO. Acetate supported a 13% higher H_2 production rate than glucose under equivalent conditions. However, high concentrations can be inhibitory due to acetic acid's uncoupling effect, disrupting membrane potential and osmotic balance [155]. Strategies such as gradual feeding or strain adaptation will be necessary to implement acetate use in scale-up systems [157].

Raising CO concentration in bottle fermentations initially enhanced growth, but at 50% CO, the growth rate dropped by 42% after 72 hours. CO uptake was delayed, and H_2 production lagged significantly, indicating mass transfer limitations at elevated partial pressures. These findings align with prior studies where residual CO persisted in headspaces at high concentrations, despite active hydrogenogenesis, demonstrating that dissolved CO, rather than total headspace CO, is the limiting substrate. This was observed when evaluating syngas fermentation in bottle experiments using different gas compositions [142]. When evaluating two gas mixtures, one containing 17.28% CO and the other, 28.01% CO, there was residual CO in the headspace with the highest CO concentration, and CO depletion occurred earlier with the lowest CO (17.28%) [142]. Indicating that dissolved CO was independent of the total CO in the headspace.

However, increasing pCO to 3 bar significantly inhibited both growth and hydrogen production. Specific growth rate declined by over 66% under high CO pressure, with elevated acetate and lactate levels suggesting a shift toward fermentation byproducts as a stress response. This inhibition was attributed to CO toxicity.

Liquid–gas mass transfer is a critical constraint, particularly at higher biomass concentrations where CO demand outpaces solubility and transfer rate. CO low solubility and diffusivity in aqueous media means that increasing its partial pressure alone may not increase bioavailability due to transfer resistance [174]. Instead, improved agitation, gas sparging, or bioreactor design modifications may be required to enhance transfer coefficients (k_La) and overcome diffusion barriers.

Further experiments in bottle experiments confirmed that *P. thermoglucosidasius* is relatively tolerant to elevated H_2 levels (up to 3 bar), and H_2 accumulation did not inhibit production, with CO being fully converted to H_2 at selectivities over 95%. Similarly, nitrogen (N_2) pressures up to 3 bar did not improve hydrogen yield and showed only slight decreases in productivity, reinforcing that total system pressure alone is not beneficial unless it directly enhances gas solubility and transfer. Similarly, increasing total pressure on fermentations with *Clostridium ljungdahlii* revealed pressure-dependent declines in H_2 yield [153]. This emphasizes species-specific responses and the complex interaction between gas pressures and microbial metabolism.

Oxygen played a dual role in the fermentation process. While it disrupted hydrogen production, it also promoted biomass accumulation by enabling aerobic metabolism. The timing of O_2 addition significantly impacted H_2 production, with pre-fermentation oxygen exposure delaying hydrogenogenesis more than O_2 addition during anaerobic conditions. These findings suggest that strategic oxygen management could help sustain active cultures during prolonged fermentations, though excessive oxygen levels must be carefully controlled to avoid impairing H_2 yields.

Using syngas in anaerobic fermentation instead of pure CO-N_2 mixtures in a two-phase fermentation at bioreactor scale facilitated a more seamless shift from aerobic to anaerobic metabolism, reducing lag phases for H_2 production [142]. Similarly, when using the two-phase system and changing between aerobic to anaerobic conditions, CO consumption started only after 12 hours from the gas exchange [149]. This may be due to better metabolic adaptation under syngas conditions, and possibly enzyme activation by H_2 [154]. This again highlights the importance of gas composition and its transfer efficiency to microbial cells.

Mass transfer limitations were further evident during high CO partial pressure fermentations at bioreactor scale. While CO was present in the headspace, lower acetate and overall CO conversion at higher pressures indicated toxicity [174]. This underscores that the biological system is limited not by the presence of CO but by its physical transfer into the fermentation medium. The CO uptake rate depends on its dissolved concentration, which is governed by

Henry's law and influenced by temperature, pressure, solubility, salt concentration, and agitation.

The scale-up experiments in a bioreactor revealed that increasing CO partial pressure delayed hydrogen production. Raising pCO to 46 kPa resulted in a longer lag phase compared to 9 and 28 kPa. Conversely, increasing H_2 partial pressure did not inhibit production, with the highest H_2 yield (130 mmol) achieved at 3 bar pH_2. These findings highlight the importance of optimizing gas-phase conditions to maximize hydrogen yields while maintaining microbial activity.

Previous studies have similarly noted that CO transfer limitations dominate in high-density cultures, where microbial demand outpaces the gas supply rate. Enhancing k_La values through reactor design (e.g., improved impellers, gas dispersion strategies, or microbubble systems) is thus critical for industrial application of hydrogenogenic fermentations.

In conclusion, the enhancement of hydrogen production using *P. thermoglucosidasius* through semi-continuous feeding strategies and optimized gas mixtures is constrained by liquid–gas mass transfer, particularly for CO. While fermentation parameters such as feeding intervals, substrate selection, and environmental conditions are crucial, overcoming gas transfer limitations will be essential for process scale-up and industrial feasibility. Future work should focus on improving bioreactor gas delivery systems, increasing k_La values, and testing novel sparging or membrane technologies to ensure that the microbial demand for CO can be met in real-time, thereby maximizing hydrogen productivity.

Conclusions

Biological H_2 production emerges as an attractive and versatile energy carrier with a high energetic yield. The facultative anaerobic *Parageobacillus thermoglucosidasius* can produce H_2 using carbon monoxide as substrate via the WGS reaction. This thesis investigated the optimization of a fermentation process for H_2 production with *P. thermoglucosidasius* DSM 6285 in bioreactor scale. It also presented results on the evaluation of syngas as substrate and the effects of producing H_2 when increasing gas partial pressures.

Semi-continuous fermentation with a 24-hour feeding interval supplemented with glucose proved superior to batch fermentation, improving hydrogen yields and stability. This mode increased H_2 yield by 18% and sustained stable production over seven days, extending the fermentation period. The CODH activity strongly correlated with hydrogen production, emphasizing the importance of enzymatic stability. However, metabolic shifts under semi-continuous conditions introduced challenges such as lactate accumulation and foam formation.

When compared to a dark fermentation system, where glucose is the sole substrate, hydrogen yield is limited by metabolic pathways such as acetate or butyrate formation. In contrast, the carboxydotrophic system uses CO as the primary energy source, while glucose serves as a co-substrate to support biomass growth. As a result, the carboxydotrophic system achieves a higher hydrogen yield per gram of glucose, primarily due to CO being the main substrate utilized via the WGS reaction.

Additionally, *P. thermoglucosidasius* demonstrated the ability to produce H_2 under syngas atmospheres, with CO availability being the primary limiting factor. While syngas-based cultivation supported hydrogenogenesis, it also hindered biomass accumulation, suggesting a trade-off between cell growth and H_2 production.

Exploring pressures beyond 3 bar in bottle fermentation could provide insights into the limits of microbial tolerance and hydrogenogenesis kinetics. High-pressure systems, such as high-resistance bioreactors, are essential for these investigations. Furthermore, the role of CO_2, a key

component of the WGS reaction, warrants further study. CO_2 sparging could enhance H_2 production by improving gas-liquid interactions and driving the reaction forward.

For industrial applications, challenges such as gas mixing, pressure regulation, and reactor design must be addressed to scale up the process effectively. Optimizing these parameters could establish *P. thermoglucosidasius* as a viable candidate for commercial biohydrogen production. Genetic modifications, such as knocking out hydrogen-consuming enzymes, could further improve H_2 yields. Additionally, integrating this system with industrial processes that generate syngas offers a pathway to sustainable hydrogen production, reducing reliance on fossil fuels.
This study provides valuable insights into the metabolic responses of *P. thermoglucosidasius* under realistic conditions and highlights key factors influencing hydrogen production. It underscores the importance of gas partial pressures, fermentation modes, and metabolic adaptability in optimizing biohydrogen production. Future research should focus on overcoming mass transfer limitations, evaluating alternative reactor designs, and exploring metabolic engineering approaches to enhance hydrogen yields. With continued advancements, *P. thermoglucosidasius* could play a significant role in developing sustainable and carbon-neutral hydrogen production systems.

List of References

1. Ellabban, O.; Abu-Rub, H.; Blaabjerg, F. Renewable Energy Resources: Current Status, Future Prospects and Their Enabling Technology. *Renewable and Sustainable Energy Reviews* **2014**, *39*, 748–764, doi:https://doi.org/10.1016/j.rser.2014.07.113.
2. Cabrol, L.; Marone, A.; Tapia-Venegas, E.; Steyer, J.-P.; Ruiz-Filippi, G.; Trably, E. Microbial Ecology of Fermentative Hydrogen Producing Bioprocesses: Useful Insights for Driving the Ecosystem Function. *FEMS Microbiol Rev* **2017**, *41*, 158–181, doi:10.1093/femsre/fuw043.
3. Sherif, S.A.; Barbir, F.; Veziroglu, T.N. Wind Energy and the Hydrogen Economy—Review of the Technology. *Solar Energy* **2005**, *78*, 647–660, doi:https://doi.org/10.1016/j.solener.2005.01.002.
4. Ratnakar, R.R.; Gupta, N.; Zhang, K.; van Doorne, C.; Fesmire, J.; Dindoruk, B.; Balakotaiah, V. Hydrogen Supply Chain and Challenges in Large-Scale LH_2 Storage and Transportation. *Int J Hydrogen Energy* **2021**, *46*, 24149–24168, doi:https://doi.org/10.1016/j.ijhydene.2021.05.025.
5. Ishaq, H.; Dincer, I. Comparative Assessment of Renewable Energy-Based Hydrogen Production Methods. *Renewable and Sustainable Energy Reviews* **2021**, *135*, 110192, doi:https://doi.org/10.1016/j.rser.2020.110192.
6. da Silva Veras, T.; Mozer, T.S.; da Costa Rubim Messeder dos Santos, D.; da Silva César, A. Hydrogen: Trends, Production and Characterization of the Main Process Worldwide. *Int J Hydrogen Energy* **2017**, *42*, 2018–2033, doi:https://doi.org/10.1016/j.ijhydene.2016.08.219.
7. Nikolaidis, P.; Poullikkas, A. A Comparative Overview of Hydrogen Production Processes. *Renewable and Sustainable Energy Reviews* 2017, *67*, 597–611.
8. Balachandar, G.; Varanasi, J.L.; Singh, V.; Singh, H.; Das, D. Biological Hydrogen Production via Dark Fermentation: A Holistic Approach from Lab-Scale to Pilot-Scale. *Int J Hydrogen Energy* **2020**, *45*, 5202–5215, doi:https://doi.org/10.1016/j.ijhydene.2019.09.006.
9. Castelló, E.; Nunes Ferraz-Junior, A.D.; Andreani, C.; Anzola-Rojas, M. del P.; Borzacconi, L.; Buitrón, G.; Carrillo-Reyes, J.; Gomes, S.D.; Maintinguer, S.I.; Moreno-Andrade, I.; et al. Stability Problems in the Hydrogen Production by Dark Fermentation: Possible Causes and Solutions. *Renewable and Sustainable Energy Reviews* **2020**, *119*, 109602, doi:https://doi.org/10.1016/j.rser.2019.109602.

10. Dahiya, S.; Chatterjee, S.; Sarkar, O.; Mohan, S.V. Renewable Hydrogen Production by Dark-Fermentation: Current Status, Challenges and Perspectives. *Bioresour Technol* **2021**, *321*, 124354, doi:https://doi.org/10.1016/j.biortech.2020.124354.
11. Martins, M.; Pereira, I.A.C.; Pita, M.; De Lacey, A.L. Biological Production of Hydrogen BT - Enzymes for Solving Humankind's Problems: Natural and Artificial Systems in Health, Agriculture, Environment and Energy. In; Moura, J.J.G., Moura, I., Maia, L.B., Eds.; Springer International Publishing: Cham, 2021; pp. 247–273 ISBN 978-3-030-58315-6.
12. Ghimire, A.; Frunzo, L.; Pirozzi, F.; Trably, E.; Escudie, R.; Lens, P.N.L.; Esposito, G. A Review on Dark Fermentative Biohydrogen Production from Organic Biomass: Process Parameters and Use of by-Products. *Appl Energy* **2015**, *144*, 73–95, doi:https://doi.org/10.1016/j.apenergy.2015.01.045.
13. Castelló, E.; Braga, L.; Fuentes, L.; Etchebehere, C. Possible Causes for the Instability in the H_2 Production from Cheese Whey in a CSTR. *Int J Hydrogen Energy* **2018**, *43*, 2654–2665, doi:https://doi.org/10.1016/j.ijhydene.2017.12.104.
14. Adachi, Y.; Inoue, M.; Yoshida, T.; Sako, Y. Genetic Engineering of Carbon Monoxide-Dependent Hydrogen-Producing Machinery in *Parageobacillus thermoglucosidasius*. *Microbes Environ* **2020**, *35*, doi:10.1264/jsme2.ME20101.
15. Lovato, G.; Augusto, I.M.G.; Ferraz Júnior, A.D.N.; Albanez, R.; Ratusznei, S.M.; Etchebehere, C.; Zaiat, M.; Rodrigues, J.A.D. Reactor Start-up Strategy as Key for High and Stable Hydrogen Production from Cheese Whey Thermophilic Dark Fermentation. *Int J Hydrogen Energy* **2021**, *46*, 27364–27379, doi:https://doi.org/10.1016/j.ijhydene.2021.06.010.
16. Sivaramakrishnan, R.; Shanmugam, S.; Sekar, M.; Mathimani, T.; Incharoensakdi, A.; Kim, S.-H.; Parthiban, A.; Edwin Geo, V.; Brindhadevi, K.; Pugazhendhi, A. Insights on Biological Hydrogen Production Routes and Potential Microorganisms for High Hydrogen Yield. *Fuel* **2021**, *291*, 120136, doi:https://doi.org/10.1016/j.fuel.2021.120136.
17. Kanai, T.; Imanaka, H.; Nakajima, A.; Uwamori, K.; Omori, Y.; Fukui, T.; Atomi, H.; Imanaka, T. Continuous Hydrogen Production by the Hyperthermophilic Archaeon, *Thermococcus kodakaraensis* KOD1. *J Biotechnol* **2005**, *116*, 271–282, doi:https://doi.org/10.1016/j.jbiotec.2004.11.002.
18. Robb, F.T.; Techtmann, S.M. Life on the Fringe: Microbial Adaptation to Growth on Carbon Monoxide. *F1000Res* **2018**, *7*, doi:10.12688/f1000research.16059.1.

19. Techtmann, S.; Colman, A.; Murphy, M.; Schackwitz, W.; Goodwin, L.; Robb, F. Regulation of Multiple Carbon Monoxide Consumption Pathways in Anaerobic Bacteria. *Frontiers in Microbiology* 2011, *2*.
20. Jeoung, J.-H.; Fesseler, J.; Goetzl, S.; Dobbek, H. Carbon Monoxide. Toxic Gas and Fuel for Anaerobes and Aerobes: Carbon Monoxide Dehydrogenases. In *The Metal-Driven Biogeochemistry of Gaseous Compounds in the Environment*; Kroneck, P.M.H., Torres, M.E.S., Eds.; Springer Netherlands: Dordrecht, 2014; pp. 37–69 ISBN 978-94-017-9269-1.
21. Hallenbeck, P.C.; Benemann, J.R. Biological Hydrogen Production; Fundamentals and Limiting Processes. *Int J Hydrogen Energy* **2002**, *27*, 1185–1193, doi:https://doi.org/10.1016/S0360-3199(02)00131-3.
22. Hay, J.X.W.; Wu, T.Y.; Juan, J.C.; Md. Jahim, J. Biohydrogen Production through Photo Fermentation or Dark Fermentation Using Waste as a Substrate: Overview, Economics, and Future Prospects of Hydrogen Usage. *Biofuels, Bioproducts and Biorefining* **2013**, *7*, 334–352, doi:https://doi.org/10.1002/bbb.1403.
23. Das, D.; Veziroglu, T. Advances in Biological Hydrogen Production Processes. *Int J Hydrogen Energy* **2008**, *33*, 6046–6057, doi:10.1016/j.ijhydene.2008.07.098.
24. Chen, S.-D.; Lee, K.-S.; Lo, Y.-C.; Chen, W.-M.; Wu, J.-F.; Lin, C.-Y.; Chang, J.-S. Batch and Continuous Biohydrogen Production from Starch Hydrolysate by *Clostridium* Species. *Int J Hydrogen Energy* **2008**, *33*, 1803–1812, doi:https://doi.org/10.1016/j.ijhydene.2008.01.028.
25. Fabiano, B.; Perego, P. Thermodynamic Study and Optimization of Hydrogen Production by *Enterobacter aerogenes*. *Int J Hydrogen Energy* **2002**, *27*, 149–156, doi:https://doi.org/10.1016/S0360-3199(01)00102-1.
26. De Maayer, P.; Brumm, P.J.; Mead, D.A.; Cowan, D.A. Comparative Analysis of the *Geobacillus* Hemicellulose Utilization Locus Reveals a Highly Variable Target for Improved Hemicellulolysis. *BMC Genomics* **2014**, *15*, 836, doi:10.1186/1471-2164-15-836.
27. Junghare, M.; Subudhi, S.; Lal, B. Improvement of Hydrogen Production under Decreased Partial Pressure by Newly Isolated Alkaline Tolerant Anaerobe, *Clostridium butyricum* TM-9A: Optimization of Process Parameters. *Int J Hydrogen Energy* **2012**, *37*, 3160–3168, doi:https://doi.org/10.1016/j.ijhydene.2011.11.043.
28. Martins, M.; Pereira, I.A.C.; Pita, M.; De Lacey, A.L. Biological Production of Hydrogen BT - Enzymes for Solving Humankind's Problems: Natural and Artificial Systems in Health,

Agriculture, Environment and Energy. In; Moura, J.J.G., Moura, I., Maia, L.B., Eds.; Springer International Publishing: Cham, 2021; pp. 247–273 ISBN 978-3-030-58315-6.

29. Wang, J.; Yin, Y. *Clostridium* Species for Fermentative Hydrogen Production: An Overview. *Int J Hydrogen Energy* **2021**, *46*, 34599–34625, doi:https://doi.org/10.1016/j.ijhydene.2021.08.052.
30. Ferreira Maluf Braga, A.; Zaiat, M. Fundamentals of Biofuel Production Using Anaerobic Digestion: Metabolic Pathways and Factors Affecting the Process BT - Renewable Energy Technologies for Energy Efficient Sustainable Development. In; Sinharoy, A., Lens, P.N.L., Eds.; Springer International Publishing: Cham, 2022; pp. 3–21 ISBN 978-3-030-87633-3.
31. Sivaramakrishnan, R.; Shanmugam, S.; Sekar, M.; Mathimani, T.; Incharoensakdi, A.; Kim, S.-H.; Parthiban, A.; Edwin Geo, V.; Brindhadevi, K.; Pugazhendhi, A. Insights on Biological Hydrogen Production Routes and Potential Microorganisms for High Hydrogen Yield. *Fuel* **2021**, *291*, 120136, doi:https://doi.org/10.1016/j.fuel.2021.120136.
32. Tapia-Venegas, E.; Cabrol, L.; Brandhoff, B.; Hamelin, J.; Trably, E.; Steyer, J.P.; Ruiz-Filippi, G. Adaptation of Acidogenic Sludge to Increasing Glycerol Concentrations for Biohydrogen Production. *Appl Microbiol Biotechnol* **2015**, *99*, 8295–8308, doi:10.1007/s00253-015-6832-6.
33. Cai, G.; Jin, B.; Saint, C.; Monis, P. Genetic Manipulation of Butyrate Formation Pathways in *Clostridium butyricum*. *J Biotechnol* **2011**, *155*, 269–274, doi:https://doi.org/10.1016/j.jbiotec.2011.07.004.
34. Hallenbeck, P.C.; Abo-Hashesh, M.; Ghosh, D. Strategies for Improving Biological Hydrogen Production. *Bioresour Technol* **2012**, *110*, 1–9, doi:https://doi.org/10.1016/j.biortech.2012.01.103.
35. Alfano, M.; Cavazza, C. The Biologically Mediated Water–Gas Shift Reaction: Structure, Function and Biosynthesis of Monofunctional [NiFe]-Carbon Monoxide Dehydrogenases. *Sustain Energy Fuels* **2018**, *2*, 1653–1670, doi:10.1039/C8SE00085A.
36. Fukuyama, Y.; Inoue, M.; Omae, K.; Yoshida, T.; Sako, Y. Chapter Three - Anaerobic and Hydrogenogenic Carbon Monoxide-Oxidizing Prokaryotes: Versatile Microbial Conversion of a Toxic Gas into an Available Energy. In; Gadd, G.M., Sariaslani, S.B.T.-A. in A.M., Eds.; Academic Press, 2020; Vol. 110, pp. 99–148 ISBN 0065-2164.
37. Diender, M.; Stams, A.J.M.; Sousa, D.Z. Pathways and Bioenergetics of Anaerobic Carbon Monoxide Fermentation. *Front Microbiol* **2015**, *6*.

38. Sinharoy, A.; Baskaran, D.; Pakshirajan, K. Sustainable Biohydrogen Production by Dark Fermentation Using Carbon Monoxide as the Sole Carbon and Energy Source. *Int J Hydrogen Energy* **2019**, *44*, 13114–13125, doi:https://doi.org/10.1016/j.ijhydene.2019.03.130.
39. Detman, A.; Laubitz, D.; Chojnacka, A.; Kiela, P.R.; Salamon, A.; Barberán, A.; Chen, Y.; Yang, F.; Błaszczyk, M.K.; Sikora, A. Dynamics of Dark Fermentation Microbial Communities in the Light of Lactate and Butyrate Production. *Microbiome* **2021**, *9*, 158, doi:10.1186/s40168-021-01105-x.
40. Dzulkarnain, E.L.N.; Audu, J.O.; Wan Dagang, W.R.Z.; Abdul-Wahab, M.F. Microbiomes of Biohydrogen Production from Dark Fermentation of Industrial Wastes: Current Trends, Advanced Tools and Future Outlook. *Bioresour Bioprocess* **2022**, *9*, 16, doi:10.1186/s40643-022-00504-8.
41. Song, J.; An, D.; Ren, N.; Zhang, Y.; Chen, Y. Effects of pH and ORP on Microbial Ecology and Kinetics for Hydrogen Production in Continuously Dark Fermentation. *Bioresour Technol* **2011**, *102*, 10875–10880, doi:https://doi.org/10.1016/j.biortech.2011.09.024.
42. Swiatkiewicz, J.; Slezak, R.; Krzystek, L.; Ledakowicz, S. Production of Volatile Fatty Acids in a Semi-Continuous Dark Fermentation of Kitchen Waste: Impact of Organic Loading Rate and Hydraulic Retention Time. *Energies (Basel)* **2021**, *14*, doi:10.3390/en14112993.
43. Saleem, A.; Umar, H.; Shah, T.A.; Tabassum, R. Fermentation of Simple and Complex Substrates to Biohydrogen Using Pure *Bacillus cereus* RTUA and RTUB Strains. *Environ Technol Innov* **2020**, *18*, 100704, doi:https://doi.org/10.1016/j.eti.2020.100704.
44. Ulhiza, T.A.; Mohamad Puad, N.I.; Azmi, A.S. Optimization of Culture Conditions for Biohydrogen Production from Sago Wastewater by *Enterobacter aerogenes* Using Response Surface Methodology. *Int J Hydrogen Energy* **2018**, *43*, 22148–22158, doi:https://doi.org/10.1016/j.ijhydene.2018.10.057.
45. Bisaillon, A.; Turcot, J.; Hallenbeck, P.C. The Effect of Nutrient Limitation on Hydrogen Production by Batch Cultures of *Escherichia coli*. *Int J Hydrogen Energy* **2006**, *31*, 1504–1508, doi:https://doi.org/10.1016/j.ijhydene.2006.06.016.
46. Zhang, L.; Chung, J.; Ren, N.; Sun, R. Effects of the Ecological Factors on Hydrogen Production and [Fe–Fe]-Hydrogenase Activity in *Ethanoligenens harbinense* YUAN-3. *Int J Hydrogen Energy* **2015**, *40*, 6792–6797, doi:https://doi.org/10.1016/j.ijhydene.2015.02.015.
47. Alvarado-Cuevas, Z.D.; López-Hidalgo, A.M.; Ordoñez, L.G.; Oceguera-Contreras, E.; Ornelas-Salas, J.T.; De León-Rodríguez, A. Biohydrogen Production Using Psychrophilic

Bacteria Isolated from Antarctica. *Int J Hydrogen Energy* **2015**, *40*, 7586–7592, doi:https://doi.org/10.1016/j.ijhydene.2014.10.063.

48. Estevam, A.; Arantes, M.K.; Andrigheto, C.; Fiorini, A.; da Silva, E.A.; Alves, H.J. Production of Biohydrogen from Brewery Wastewater Using *Klebsiella pneumoniae* Isolated from the Environment. *Int J Hydrogen Energy* **2018**, *43*, 4276–4283, doi:https://doi.org/10.1016/j.ijhydene.2018.01.052.
49. Buitrón, G.; Muñoz-Páez, K.M.; Quijano, G.; Carrillo-Reyes, J.; Albarrán-Contreras, B.A. Biohydrogen Production from Winery Effluents: Control of the Homoacetogenesis through the Headspace Gas Recirculation. *Journal of Chemical Technology & Biotechnology* **2020**, *95*, 544–552, doi:https://doi.org/10.1002/jctb.6263.
50. Seid, N.; Ochsenreither, K.; Neumann, A. Caproate Production from Enset Fiber in One-Pot Two-Step Fermentation Using Anaerobic Fungi (*Neocallimastix cameroonii* Strain G341) and Clostridium Kluyveri DSM 555. *Microb Cell Fact* **2023**.
51. Alves, J.I.; van Gelder, A.H.; Alves, M.M.; Sousa, D.Z.; Plugge, C.M. *Moorella stamsii* Sp. Nov., a New Anaerobic Thermophilic Hydrogenogenic Carboxydotroph Isolated from Digester Sludge. *Int J Syst Evol Microbiol* **2013**, *63*, 4072–4076, doi:10.1099/ijs.0.050369-0.
52. Mohr, T.; Aliyu, H.; Biebinger, L.; Gödert, R.; Hornberger, A.; Cowan, D.; De Maayer, P.; Neumann, A. Effects of Different Operating Parameters on Hydrogen Production by *Parageobacillus thermoglucosidasius* DSM 6285. *AMB Express* **2019**, *9*, 207, doi:10.1186/s13568-019-0931-1.
53. Slepova, T. V; Sokolova, T.G.; Lysenko, A.M.; Tourova, T.P.; Kolganova, T. V; Kamzolkina, O. V; Karpov, G.A.; Bonch-Osmolovskaya, E.A. *Carboxydocella sporoproducens* sp. Nov., a Novel Anaerobic CO-Utilizing/H_2-Producing Thermophilic Bacterium from a Kamchatka Hot Spring. *Int J Syst Evol Microbiol* **2006**, *56*, 797–800, doi:https://doi.org/10.1099/ijs.0.63961-0.
54. Balk, M.; Heilig, H.G.H.J.; van Eekert, M.H.A.; Stams, A.J.M.; Rijpstra, I.C.; Sinninghe-Damsté, J.S.; de Vos, W.M.; Kengen, S.W.M. Isolation and Characterization of a New CO-Utilizing Strain, *Thermoanaerobacter thermohydrosulfuricus* subsp. *carboxydovorans*, Isolated from a Geothermal Spring in Turkey. *Extremophiles* **2009**, *13*, 885–894, doi:10.1007/s00792-009-0276-9.
55. Parshina, S.N.; Sipma, J.; Nakashimada, Y.; Henstra, A.M.; Smidt, H.; Lysenko, A.M.; Lens, P.N.L.; Lettinga, G.; Stams, A.J.M. *Desulfotomaculum carboxydivorans* Sp. Nov., a Novel

Sulfate-Reducing Bacterium Capable of Growth at 100% CO. *Int J Syst Evol Microbiol* **2005**, *55*, 2159–2165, doi:https://doi.org/10.1099/ijs.0.63780-0.

56. Kochetkova, T. V; Rusanov, I.I.; Pimenov, N. V; Kolganova, T. V; Lebedinsky, A. V; Bonch-Osmolovskaya, E.A.; Sokolova, T.G. Anaerobic Transformation of Carbon Monoxide by Microbial Communities of Kamchatka Hot Springs. *Extremophiles* **2011**, *15*, 319–325, doi:10.1007/s00792-011-0362-7.
57. Nazina, T.N.; Tourova, T.P.; Poltaraus, A.B.; Novikova, E. V; Grigoryan, A.A.; Ivanova, A.E.; Lysenko, A.M.; Petrunyaka, V. V; Osipov, G.A.; Belyaev, S.S.; et al. Taxonomic Study of Aerobic Thermophilic Bacilli: Descriptions of *Geobacillus subterraneus* Gen. Nov., Sp. Nov. and *Geobacillus uzenensis* Sp. Nov. from Petroleum Reservoirs and Transfer of *Bacillus stearothermophilus*, *Bacillus thermocatenulatus, Bacillus thermoleovorans, Bacillus kaustophilus, Bacillus thermodenitrificans* to Geobacillus as the New Combinations *G. Stearothermophilus*, G. Th. *Int J Syst Evol Microbiol* **2001**, *51*, 433–446, doi:10.1099/00207713-51-2-433.
58. Brumm, P.; Land, M.L.; Hauser, L.J.; Jeffries, C.D.; Chang, Y.-J.; Mead, D.A. Complete Genome Sequence of *Geobacillus* Strain Y4.1MC1, a Novel CO-Utilizing *Geobacillus thermoglucosidasius* Strain Isolated from Bath Hot Spring in Yellowstone National Park. *Bioenergy Res* **2015**, *8*, 1039–1045, doi:10.1007/s12155-015-9585-2.
59. Mohr, T.; Aliyu, H.; Küchlin, R.; Polliack, S.; Zwick, M.; Neumann, A.; Cowan, D.; De Maayer, P. CO - Dependent Hydrogen Production by the Facultative Anaerobe *Parageobacillus thermoglucosidasius*. *Microb Cell Fact* **2018**, 1–12, doi:10.1186/s12934-018-0954-3.
60. Aliyu, H.; Mohr, T.; Cowan, D.; De Maayer, P.; Neumann, A. Time-Course Transcriptome of *Parageobacillus thermoglucosidasius* DSM 6285 Grown in the Presence of Carbon Monoxide and Air. *Int J Mol Sci.* **2020**, 1–17, doi:10.3390/ijms21113870.
61. Mohr, T.; Aliyu, H.; Küchlin, R.; Zwick, M.; Cowan, D.; Neumann, A.; De Maayer, P. Comparative Genomic Analysis of *Parageobacillus thermoglucosidasius* Strains with Distinct Hydrogenogenic Capacities. **2018**, 1–10.
62. Aliyu, H.; Kastner, R.; De Maayer, P.; Neumann, A. Carbon Monoxide Induced Metabolic Shift in the Carboxydotrophic *Parageobacillus thermoglucosidasius* DSM 6285. *Microorganisms* 2021, *9*.
63. Shen, N.; Dai, K.; Xia, X.-Y.; Zeng, R.J.; Zhang, F. Conversion of Syngas (CO and H2) to Biochemicals by Mixed Culture Fermentation in Mesophilic and Thermophilic Hollow-Fiber

Membrane Biofilm Reactors. *J Clean Prod* **2018**, *202*, 536–542, doi:https://doi.org/10.1016/j.jclepro.2018.08.162.

64. Kim, M.-S.; Fitriana, H.N.; Kim, T.W.; Kang, S.G.; Jeon, S.G.; Chung, S.H.; Park, G.W.; Na, J.-G. Enhancement of the Hydrogen Productivity in Microbial Water Gas Shift Reaction by *Thermococcus onnurineus* NA1 Using a Pressurized Bioreactor. *Int J Hydrogen Energy* **2017**, *42*, 27593–27599, doi:https://doi.org/10.1016/j.ijhydene.2017.07.024.
65. Lee, K.-S.; Tseng, T.-S.; Liu, Y.-W.; Hsiao, Y.-D. Enhancing the Performance of Dark Fermentative Hydrogen Production Using a Reduced Pressure Fermentation Strategy. *Int J Hydrogen Energy* **2012**, *37*, 15556–15562, doi:https://doi.org/10.1016/j.ijhydene.2012.04.039.
66. Chen, Y.; Yin, Y.; Wang, J. Recent Advance in Inhibition of Dark Fermentative Hydrogen Production. *Int J Hydrogen Energy* **2021**, *46*, 5053–5073, doi:https://doi.org/10.1016/j.ijhydene.2020.11.096.
67. Stein, U.H.; Abbasi-Hosseini, M.; Kain, J.; Fuchs, W.; Bochmann, G. Influence of Gas-Release Strategies on the Production of Biohydrogen and Biobutanol in ABE Fermentation. *Biofuels* **2022**, *13*, 9–15, doi:10.1080/17597269.2019.1619246.
68. Yerushalmi, L.; Volesky, B.; Szczesny, T. Effect of Increased Hydrogen Partial Pressure on the Acetone-Butanol Fermentation by *Clostridium acetobutylicum*. *Appl Microbiol Biotechnol* **1985**, *22*, 103–107, doi:10.1007/BF00250028.
69. Neubeck, A.; Sjöberg, S.; Price, A.; Callac, N.; Schnürer, A. Effect of Nickel Levels on Hydrogen Partial Pressure and Methane Production in Methanogens. *PLoS One* **2016**, *11*, e0168357.
70. Lee, K.-S.; Tseng, T.-S.; Liu, Y.-W.; Hsiao, Y.-D. Enhancing the Performance of Dark Fermentative Hydrogen Production Using a Reduced Pressure Fermentation Strategy. *Int J Hydrogen Energy* **2012**, *37*, 15556–15562, doi:https://doi.org/10.1016/j.ijhydene.2012.04.039.
71. Zagrodnik, R.; Duber, A.; Seifert, K. Dark-Fermentative Hydrogen Production from Synthetic Lignocellulose Hydrolysate by a Mixed Bacterial Culture: The Relationship between Hydraulic Retention Time and PH Conditions. *Bioresour Technol* **2022**, *358*, 127309, doi:https://doi.org/10.1016/j.biortech.2022.127309.
72. Skidmore, B.E.; Baker, R.A.; Banjade, D.R.; Bray, J.M.; Tree, D.R.; Lewis, R.S. Syngas Fermentation to Biofuels: Effects of Hydrogen Partial Pressure on Hydrogenase Efficiency. *Biomass Bioenergy* **2013**, *55*, 156–162, doi:https://doi.org/10.1016/j.biombioe.2013.01.034.

73. Sim, Y.-B.; Jung, J.-H.; Park, J.-H.; Bakonyi, P.; Kim, S.-H. Effect of Shear Velocity on Dark Fermentation for Biohydrogen Production Using Dynamic Membrane. *Bioresour Technol* **2020**, *308*, 123265, doi:https://doi.org/10.1016/j.biortech.2020.123265.

74. Sinharoy, A.; Pakshirajan, K.; Lens, P.N.L. Syngas Fermentation for Bioenergy Production: Advances in Bioreactor Systems BT - Renewable Energy Technologies for Energy Efficient Sustainable Development. In; Sinharoy, A., Lens, P.N.L., Eds.; Springer International Publishing: Cham, 2022; pp. 325–358 ISBN 978-3-030-87633-3.

75. Chezeau, B.; Fontaine, J.P.; Vial, Ch. Analysis of Liquid-to-Gas Mass Transfer, Mixing and Hydrogen Production in Dark Fermentation Process. *Chemical Engineering Journal* **2019**, *372*, 715–727, doi:https://doi.org/10.1016/j.cej.2019.04.191.

76. Buitrón, G.; Muñoz-Páez, K.M.; Quijano, G.; Carrillo-Reyes, J.; Albarrán-Contreras, B.A. Biohydrogen Production from Winery Effluents: Control of the Homoacetogenesis through the Headspace Gas Recirculation. *Journal of Chemical Technology & Biotechnology* **2020**, *95*, 544–552, doi:https://doi.org/10.1002/jctb.6263.

77. Shen, N.; Dai, K.; Xia, X.-Y.; Zeng, R.J.; Zhang, F. Conversion of Syngas (CO and H_2) to Biochemicals by Mixed Culture Fermentation in Mesophilic and Thermophilic Hollow-Fiber Membrane Biofilm Reactors. *J Clean Prod* **2018**, *202*, 536–542, doi:https://doi.org/10.1016/j.jclepro.2018.08.162.

78. Zhao, Y.; Haddad, M.; Cimpoia, R.; Liu, Z.; Guiot, S.R. Performance of a *Carboxydothermus hydrogenoformans*-Immobilizing Membrane Reactor for Syngas Upgrading into Hydrogen. *Int J Hydrogen Energy* **2013**, *38*, 2167–2175, doi:https://doi.org/10.1016/j.ijhydene.2012.11.038.

79. Haddad, M.; Cimpoia, R.; Guiot, S.R. Performance of *Carboxydothermus hydrogenoformans* in a Gas-Lift Reactor for Syngas Upgrading into Hydrogen. *Int J Hydrogen Energy* **2014**, *39*, 2543–2548, doi:https://doi.org/10.1016/j.ijhydene.2013.12.022.

80. Romão, B.B.; Silva, F.T.M.; Costa, H.C. de B.; do Carmo, T.S.; Cardoso, S.L.; Ferreira, J. de S.; Batista, F.R.X.; Cardoso, V.L. Alternative Techniques to Improve Hydrogen Production by Dark Fermentation. *3 Biotech* **2019**, *9*, 18, doi:10.1007/s13205-018-1538-y.

81. Sinharoy, A.; Pakshirajan, K. A Novel Application of Biologically Synthesized Nanoparticles for Enhanced Biohydrogen Production and Carbon Monoxide Bioconversion. *Renew Energy* **2020**, *147*, 864–873, doi:https://doi.org/10.1016/j.renene.2019.09.027.

82. Singhvi, M.; Maharjan, A.; Thapa, A.; Jun, H.-B.; Soo Kim, B. Nanoparticle-Associated Single Step Hydrogen Fermentation for the Conversion of Starch Potato Waste Biomass by

Thermophilic *Parageobacillus thermoglucosidasius*. *Bioresour Technol* **2021**, *337*, 125490, doi:https://doi.org/10.1016/j.biortech.2021.125490.

83. Martínez-Mendoza, L.J.; García-Depraect, O.; Muñoz, R. Unlocking the High-Rate Continuous Performance of Fermentative Hydrogen Bioproduction from Fruit and Vegetable Residues by Modulating Hydraulic Retention Time. *Bioresour Technol* **2023**, *373*, 128716, doi:https://doi.org/10.1016/j.biortech.2023.128716.
84. Wang, J.; Wan, W. Kinetic Models for Fermentative Hydrogen Production: A Review. *Int J Hydrogen Energy* **2009**, *34*, 3313–3323, doi:https://doi.org/10.1016/j.ijhydene.2009.02.031.
85. Moussa, R.N.; Moussa, N.; Dionisi, D. Hydrogen Production from Biomass and Organic Waste Using Dark Fermentation: An Analysis of Literature Data on the Effect of Operating Parameters on Process Performance. *Processes* **2022**, *10*, doi:10.3390/pr10010156.
86. Clion, V.; Dumas, C.; Collin, S.; Ernst, B. Key Factors for Biohydrogen Production by Dark Fermentation. *Can J Chem Eng* **2015**, *93*, 309–316, doi:https://doi.org/10.1002/cjce.22083.
87. Saraphirom, P.; Reungsang, A. Biological Hydrogen Production from Sweet Sorghum Syrup by Mixed Cultures Using an Anaerobic Sequencing Batch Reactor (ASBR). *Int J Hydrogen Energy* **2011**, *36*, 8765–8773, doi:https://doi.org/10.1016/j.ijhydene.2010.08.058.
88. Greening, C.; Biswas, A.; Carere, C.R.; Jackson, C.J.; Taylor, M.C.; Stott, M.B.; Cook, G.M.; Morales, S.E. Genomic and Metagenomic Surveys of Hydrogenase Distribution Indicate H_2 Is a Widely Utilised Energy Source for Microbial Growth and Survival. *ISME J* **2016**, *10*, 761–777, doi:10.1038/ismej.2015.153.
89. Inoue, T.; Takao, K.; Fukuyama, Y.; Yoshida, T.; Sako, Y. Over-Expression of Carbon Monoxide Dehydrogenase-I with an Accessory Protein Co-Expression: A Key Enzyme for Carbon Dioxide Reduction. *Biosci Biotechnol Biochem* **2014**, *78*, 582–587, doi:10.1080/09168451.2014.890027.
90. Aliyu, H.; De Maayer, P.; Neumann, A. Not All That Glitters Is Gold: The Paradox of CO-Dependent Hydrogenogenesis in *Parageobacillus thermoglucosidasius*. *Front Microbiol* **2021**, *12*.
91. Mohr, T.; Aliyu, H.; Küchlin, R.; Zwick, M.; Cowan, D.; Neumann, A.; de Maayer, P. Comparative Genomic Analysis of *Parageobacillus thermoglucosidasius* Strains with Distinct Hydrogenogenic Capacities. *BMC Genomics* **2018**, *19*, 880, doi:10.1186/s12864-018-5302-9.
92. Grahame, D.A.; Stadtman, T.C. Carbon Monoxide Dehydrogenase from Methanosarcina Barkeri. Disaggregation, Purification, and Physicochemical Properties of the Enzyme. *Journal*

of Biological Chemistry **1987**, *262*, 3706–3712, doi:https://doi.org/10.1016/S0021-9258(18)61412-7.

93. Burton, R.; Can, M.; Esckilsen, D.; Wiley, S.; Ragsdale, S.W. Production and Properties of Enzymes That Activate and Produce Carbon Monoxide. *Methods Enzymol* **2018**, *613*, 297–324, doi:10.1016/bs.mie.2018.10.005.
94. Dong, Y.; Zhang, Y.; Liu, D.; Chen, Z. Strain and Process Engineering toward Continuous Industrial Fermentation. *Front Chem Sci Eng* 2023, *17*, 1336–1353.
95. St-Pierre Lemieux, G.; Groleau, D.; Proulx, P. Introduction on Foam and Its Impact in Bioreactors. *Canadian Journal of Biotechnology* **2019**, *3*, 143–157, doi:10.24870/cjb.2019-000131.
96. Tiso, T.; Demling, P.; Karmainski, T.; Oraby, A.; Eiken, J.; Liu, L.; Bongartz, P.; Wessling, M.; Desmond, P.; Schmitz, S.; et al. Foam Control in Biotechnological Processes—Challenges and Opportunities. *Discover Chemical Engineering* **2024**, *4*, doi:10.1007/s43938-023-00039-0.
97. Lim, J.H.; Seo, S.W.; Kim, S.Y.; Jung, G.Y. Refactoring Redox Cofactor Regeneration for High-Yield Biocatalysis of Glucose to Butyric Acid in *Escherichia coli*. *Bioresour Technol* **2013**, *135*, 568–573, doi:10.1016/j.biortech.2012.09.091.
98. Reitzer, L. Catabolism of Amino Acids and Related Compounds. *EcoSal Plus* **2005**, *1*, doi:10.1128/ecosalplus.3.4.7.
99. Xavier, J.C.; Preiner, M.; Martin, W.F. Something Special about CO-Dependent CO_2 Fixation. *FEBS J* **2018**, *285*, 4181–4195, doi:https://doi.org/10.1111/febs.14664.
100. Thauer, R.K.; Fuchs, G.; Käuefer, B.; Schnttker, U. Carbon-Monoxide Oxidation in Cell-Free Extracts of *Clostridium pasteurianum*. *Eur J Biochem* **1974**, *45*, 343–349, doi:https://doi.org/10.1111/j.1432-1033.1974.tb03559.x.
101. Fuchs Georg; Schnitker, U.; Thauer, R.K. Carbon Monoxide Oxidation by Growing Cultures of *Clostridium pasteurianum*. *Eur J Biochem* **1974**, *49*, 111–115, doi:https://doi.org/10.1111/j.1432-1033.1974.tb03816.x.
102. Staples, C.R.; Heo, J.; Spangler, N.J.; Kerby, R.L.; Roberts, G.P.; Ludden, P.W. *Rhodospirillum rubrum* CO-Dehydrogenase. Part 1. Spectroscopic Studies of CODH Variant C531A Indicate the Presence of a Binuclear [FeNi] Cluster. *J Am Chem Soc* **1999**, *121*, 11034–11044, doi:10.1021/ja990396i.

103. Heo, J.; Staples, C.R.; Ludden, P.W. Redox-Dependent CO2 Reduction Activity of CO Dehydrogenase from *Rhodospirillum rubrum*. *Biochemistry* **2001**, *40*, 7604–7611, doi:10.1021/bi002554k.
104. Heo, J.; Halbleib, C.M.; Ludden, P.W. Redox-Dependent Activation of CO Dehydrogenase from *Rhodospirillum rubrum*. *Proceedings of the National Academy of Sciences* **2001**, *98*, 7690–7693, doi:10.1073/pnas.141230698.
105. IRENA *Global Energy Transformation: A Roadmap to 2050* ; 2018;
106. Elbeshbishy, E.; Dhar, B.R.; Nakhla, G.; Lee, H.-S. A Critical Review on Inhibition of Dark Biohydrogen Fermentation. *Renewable and Sustainable Energy Reviews* **2017**, *79*, 656–668, doi:https://doi.org/10.1016/j.rser.2017.05.075.
107. Abdalla, A.M.; Hossain, S.; Nisfindy, O.B.; Azad, A.T.; Dawood, M.; Azad, A.K. Hydrogen Production, Storage, Transportation and Key Challenges with Applications: A Review. *Energy Convers Manag* **2018**, *165*, 602–627, doi:https://doi.org/10.1016/j.enconman.2018.03.088.
108. Hosseini, S.E.; Wahid, M.A. Hydrogen Production from Renewable and Sustainable Energy Resources: Promising Green Energy Carrier for Clean Development. *Renewable and Sustainable Energy Reviews* **2016**, *57*, 850–866, doi:https://doi.org/10.1016/j.rser.2015.12.112.
109. van Niel, E.W.J. Biological Processes for Hydrogen Production. In *Anaerobes in Biotechnology*; Hatti-Kaul, R., Mamo, G., Mattiasson, B., Eds.; Springer International Publishing: Cham, 2016; pp. 155–193 ISBN 978-3-319-45651-5.
110. Fukuyama, Y.; Inoue, M.; Omae, K.; Yoshida, T.; Sako, Y. Chapter Three - Anaerobic and Hydrogenogenic Carbon Monoxide-Oxidizing Prokaryotes: Versatile Microbial Conversion of a Toxic Gas into an Available Energy. In; Gadd, G.M., Sariaslani, S.B.T.-A. in A.M., Eds.; Academic Press, 2020; Vol. 110, pp. 99–148 ISBN 0065-2164.
111. Haddad, M.; Cimpoia, R.; Guiot, S.R. Performance of *Carboxydothermus hydrogenoformans* in a Gas-Lift Reactor for Syngas Upgrading into Hydrogen. *Int J Hydrogen Energy* **2014**, *39*, 2543–2548, doi:https://doi.org/10.1016/j.ijhydene.2013.12.022.
112. Lee, S.H.; Kim, M.-S.; Kang, S.G.; Lee, H.S. Biohydrogen Production of Obligate Anaerobic Archaeon *Thermococcus onnurineus* NA1 under Oxic Conditions via Overexpression of FrhAGB-Encoding Hydrogenase Genes. *Biotechnol Biofuels* **2019**, *12*, 24, doi:10.1186/s13068-019-1365-3.

113. Schoelmerich, M.C.; Müller, V. Energy Conservation by a Hydrogenase-Dependent Chemiosmotic Mechanism in an Ancient Metabolic Pathway. *Proceedings of the National Academy of Sciences* **2019**, *116*, 6329–6334, doi:10.1073/pnas.1818580116.
114. Adachi, Y.; Inoue, M.; Yoshida, T.; Sako, Y. Genetic Engineering of Carbon Monoxide-Dependent Hydrogen-Producing Machinery in *Parageobacillus thermoglucosidasius*. *Microbes Environ* **2020**, *35*, doi:10.1264/jsme2.ME20101.
115. Merrouch, M.; Hadj-Saïd, J.; Domnik, L.; Dobbek, H.; Léger, C.; Dementin, S.; Fourmond, V. O_2 Inhibition of Ni-Containing CO Dehydrogenase Is Partly Reversible. *Chemistry – A European Journal* **2015**, *21*, 18934–18938, doi:https://doi.org/10.1002/chem.201502835.
116. Lu, Y.; Koo, J. O_2 Sensitivity and H_2 Production Activity of Hydrogenases—A Review. *Biotechnol Bioeng* **2019**, *116*, 3124–3135, doi:https://doi.org/10.1002/bit.27136.
117. Yoshinari, I.; Shunsuke, O.; Taiki, H.; Yusuke, O.; Adachi, K.Y.; Ayumi, T.; Masao, I.; Ryoma, K.; Takashi, Y.; Yoshihiko, S. Isolation, Genomic Sequence and Physiological Characterization of *Parageobacillus* sp. G301, an Isolate Capable of Both Hydrogenogenic and Aerobic Carbon Monoxide Oxidation. *Appl Environ Microbiol* **2023**, *89*, e00185-23, doi:10.1128/aem.00185-23.
118. Chiche, D.; Diverchy, C.; Lucquin, A.-C.; Porcheron, F.; Defoort, F. Synthesis Gas Purification. *Oil Gas Sci. Technol. – Rev. IFP Energies nouvelles* **2013**, *68*, 707–723.
119. Ramachandriya, K.; Kundiyana, D.; Sharma, A.; Kumar, A.; Atiyeh, H.; Huhnke, R.; Wilkins, M. Critical Factors Affecting the Integration of Biomass Gasification and Syngas Fermentation Technology. *AIMS Bioeng* **2016**, *3*, 188–210, doi:10.3934/bioeng.2016.2.188.
120. Wickham, H.; Averick M; Bryan J; Chang W; McGowan LD; François R; Grolemund G; Hayes A; Henry L; Hester J; et al. Welcome to the Tidyverse. *J Open Source Softw* **2019**, *4*, 1686.
121. R Core Team R: A Language and Environment for Statistical Computing 2023.
122. Neumann, A.; Dörsam, S.; Oswald, F.; Ochsenreither, K. Microbial Production of Value-Added Chemicals from Pyrolysis Oil and Syngas. In *Sustainable Production of Bulk Chemicals: Integration of Bio-Chemo- Resources and Processes*; Xian, M., Ed.; Springer Netherlands: Dordrecht, 2015; pp. 69–105 ISBN 978-94-017-7475-8.
123. Cripps, R.E.; Eley, K.; Leak, D.J.; Rudd, B.; Taylor, M.; Todd, M.; Boakes, S.; Martin, S.; Atkinson, T. Metabolic Engineering of *Geobacillus thermoglucosidasius* for High Yield Ethanol Production. *Metab Eng* **2009**, *11*, 398–408, doi:10.1016/j.ymben.2009.08.005.

124. Tang, Y.J.; Sapra, R.; Joyner, D.; Hazen, T.C.; Myers, S.; Reichmuth, D.; Blanch, H.; Keasling, J.D. Analysis of Metabolic Pathways and Fluxes in a Newly Discovered Thermophilic and Ethanol-Tolerant *Geobacillus* Strain. *Biotechnol Bioeng* **2009**, *102*, 1377–1386, doi:https://doi.org/10.1002/bit.22181.

125. Najar, I.N.; Thakur, N. A Systematic Review of the Genera *Geobacillus* and *Parageobacillus*: Their Evolution, Current Taxonomic Status and Major Applications. *Microbiology (N Y)* **2020**, *166*, 800–816, doi:10.1099/mic.0.000945.

126. Liu, J.; Han, X.; Tao, F.; Xu, P. Reprogramming a High Robust *Geobacillus thermoglucosidasius*; for Efficient Synthesis of Polymer-Grade Lactic Acid under Extremely High Temperature (60°C). *bioRxiv* **2023**, 2023.04.14.536835, doi:10.1101/2023.04.14.536835.

127. Unden, G. Transcriptional Regulation and Energetics of Alternative Respiratory Pathways in Facultatively Anaerobic Bacteria. *Biochimica et Biophysica Acta (BBA) - Bioenergetics* **1998**, *1365*, 220–224, doi:https://doi.org/10.1016/S0005-2728(98)00071-1.

128. Pin-Ching, M.; Jie, H.; Sharon, S.; Vekalet, T.; Gary, V. Energy Generation from the CO Oxidation-Hydrogen Production Pathway in *Rubrivivax gelatinosus*. *Appl Environ Microbiol* **2005**, *71*, 2870–2874, doi:10.1128/AEM.71.6.2870-2874.2005.

129. Pisa, K.Y.; Huber, H.; Thomm, M.; Müller, V. A Sodium Ion-Dependent A1AO ATP Synthase from the Hyperthermophilic Archaeon *Pyrococcus furiosus*. *FEBS J* **2007**, *274*, 3928–3938, doi:https://doi.org/10.1111/j.1742-4658.2007.05925.x.

130. Vignais, P.M.; Billoud, B. Occurrence, Classification, and Biological Function of Hydrogenases: An Overview. *Chem Rev* **2007**, *107*, 4206–4272, doi:10.1021/cr050196r.

131. Welte, C.; Krätzer, C.; Deppenmeier, U. Involvement of Ech Hydrogenase in Energy Conservation of *Methanosarcina mazei*. *FEBS J* **2010**, *277*, 3396–3403, doi:https://doi.org/10.1111/j.1742-4658.2010.07744.x.

132. Fernandez, V.M.; Hatchikian, E.C.; Cammack, R. Properties and Reactivation of Two Different Deactivated Forms of *Desulfovibrio gigas* Hydrogenase. *Biochimica et Biophysica Acta (BBA) - Protein Structure and Molecular Enzymology* **1985**, *832*, 69–79, doi:https://doi.org/10.1016/0167-4838(85)90175-X.

133. Kim, S.M.; Lee, J.; Kang, S.H.; Heo, Y.; Yoon, H.-J.; Hahn, J.-S.; Lee, H.H.; Kim, Y.H. O_2-Tolerant CO Dehydrogenase via Tunnel Redesign for the Removal of CO from Industrial Fuel Gas. *Nat Catal* **2022**, *5*, 807–817, doi:10.1038/s41929-022-00834-y.

134. Harrison, D.E.F.; Loveless, J.E. Transient Responses of Facultatively Anaerobic Bacteria Growing in Chemostat Culture to a Change from Anaerobic to Aerobic Conditions. *J Gen Microbiol* **1971**, *68*, 45–52, doi:10.1099/00221287-68-1-45.
135. Partridge, J.D.; Scott, C.; Tang, Y.; Poole, R.K.; Green, J. *Escherichia coli* Transcriptome Dynamics during the Transition from Anaerobic to Aerobic Conditions*. *Journal of Biological Chemistry* **2006**, *281*, 27806–27815, doi:https://doi.org/10.1074/jbc.M603450200.
136. Campbell, K.; Herrera-Dominguez, L.; Correia-Melo, C.; Zelezniak, A.; Ralser, M. Biochemical Principles Enabling Metabolic Cooperativity and Phenotypic Heterogeneity at the Single Cell Level. *Curr Opin Syst Biol* **2018**, *8*, 97–108, doi:https://doi.org/10.1016/j.coisb.2017.12.001.
137. Liang, J.; Roberts, A.; van Kranenburg, R.; Bolhuis, A.; Leak, D.J. Relaxed Control of Sugar Utilization in *Parageobacillus thermoglucosidasius* DSM 2542. *Microbiol Res* **2022**, *256*, 126957, doi:https://doi.org/10.1016/j.micres.2021.126957.
138. Metcalfe, G.D.; Sargent, F.; Hippler, M. Hydrogen Production in the Presence of Oxygen by *Escherichia coli* K-12. *Microbiology (N Y)* **2022**, *168*, 001167, doi:10.1099/mic.0.001167.
139. Yunrong, C.; Roberto, K.; Richard, L. A Widely Conserved Gene Cluster Required for Lactate Utilization in *Bacillus subtilis* and Its Involvement in Biofilm Formation. *J Bacteriol* **2009**, *191*, 2423–2430, doi:10.1128/jb.01464-08.
140. Wolfe, A. The Acetate Switch. *Microbiology and Molecular Biology Reviews* **2005**, *69*, 12–50, doi:10.1128/mmbr.69.1.12-50.2005.
141. Achakulwisut, P.; Erickson, P.; Guivarch, C.; Schaeffer, R.; Brutschin, E.; Pye, S. Global Fossil Fuel Reduction Pathways under Different Climate Mitigation Strategies and Ambitions. *Nat Commun* **2023**, *14*, doi:10.1038/s41467-023-41105-z.
142. Mol, M.; Ardila, M.S.; Mol, B.A.; Aliyu, H.; Neumann, A.; de Maayer, P. The Effects of Synthesis Gas Feedstocks and Oxygen Perturbation on Hydrogen Production by *Parageobacillus thermoglucosidasius*. *Microb Cell Fact* **2024**, *23*, 125, doi:10.1186/s12934-024-02391-4.
143. Ardila, M.S.; Aliyu, H.; de Maayer, P.; Neumann, A. Effect of Different Partial Pressures on H2 Production with *Parageobacillus thermoglucosidasius* DSM 6285. *Fermentation* **2024**, *10*, doi:10.3390/fermentation10110592.

144. Chezeau, B.; Fontaine, J.P.; Vial, Ch. Analysis of Liquid-to-Gas Mass Transfer, Mixing and Hydrogen Production in Dark Fermentation Process. *Chemical Engineering Journal* **2019**, *372*, 715–727, doi:https://doi.org/10.1016/j.cej.2019.04.191.

145. Liu, K.; Phillips, J.R.; Sun, X.; Mohammad, S.; Huhnke, R.L.; Atiyeh, H.K. Investigation and Modeling of Gas-Liquid Mass Transfer in a Sparged and Non-Sparged Continuous Stirred Tank Reactor with Potential Application in Syngas Fermentation. *Fermentation* **2019**, *5*, doi:10.3390/fermentation5030075.

146. Harahap, B.M.; Ahring, B.K. Acetate Production from Syngas Produced from Lignocellulosic Biomass Materials along with Gaseous Fermentation of the Syngas: A Review. *Microorganisms* 2023, *11*.

147. Arantes, A.L.; Moreira, J.P.C.; Diender, M.; Parshina, S.N.; Stams, A.J.M.; Alves, M.M.; Alves, J.I.; Sousa, D.Z. Enrichment of Anaerobic Syngas-Converting Communities and Isolation of a Novel Carboxydotrophic *Acetobacterium wieringae* Strain JM. *Front Microbiol* **2020**, *11*, doi:10.3389/fmicb.2020.00058.

148. Redl, S.; Diender, M.; Jensen, T.Ø.; Sousa, D.Z.; Nielsen, A.T. Exploiting the Potential of Gas Fermentation. *Ind Crops Prod* **2017**, *106*, 21–30, doi:10.1016/j.indcrop.2016.11.015.

149. Ardila, M.S.; Aliyu, H.; de Maayer, P.; Neumann, A. Batch and Semi-Continuous Fermentation with *Parageobacillus thermoglucosidasius* DSM 6285 for H2 Production. *Biotechnology for Biofuels and Bioproducts* **2025**, *18*, 3, doi:10.1186/s13068-024-02597-z.

150. Rodríguez, A.; Hernández-Herreros, N.; García, J.L.; Auxiliadora Prieto, M. Enhancement of Biohydrogen Production Rate in *Rhodospirillum rubrum* by a Dynamic CO-Feeding Strategy Using Dark Fermentation. *Biotechnol Biofuels* **2021**, *14*, doi:10.1186/s13068-021-02017-6.

151. Hernández-Herreros, N.; Rodríguez, A.; Galán, B.; Auxiliadora Prieto, M. Boosting Hydrogen Production in *Rhodospirillum rubrum* by Syngas-Driven Photoheterotrophic Adaptive Evolution. *Bioresour Technol* **2024**, *406*, doi:10.1016/j.biortech.2024.130972.

152. Do, Y.S.; Smeenk, J.; Broer, K.M.; Kisting, C.J.; Brown, R.; Heindel, T.J.; Bobik, T.A.; DiSpirito, A.A. Growth of *Rhodospirillum rubrum* on Synthesis Gas: Conversion of CO to H2 and Poly-β-Hydroxyalkanoate. *Biotechnol Bioeng* **2007**, *97*, 279–286, doi:10.1002/bit.21226.

153. Perret, L.; Boukis, N.; Sauer, J. Synthesis Gas Fermentation at High Cell Density: How pH and Hydrogen Partial Pressure Affect Productivity and Product Ratio in Continuous Fermentation. *Bioresour Technol* **2024**, *391*, doi:10.1016/j.biortech.2023.129894.

154. Esquivel-Elizondo, S.; Delgado, A.G.; Rittmann, B.E.; Krajmalnik-Brown, R. The Effects of CO_2 and H_2 on CO Metabolism by Pure and Mixed Microbial Cultures. *Biotechnol Biofuels* **2017**, *10*, 220, doi:10.1186/s13068-017-0910-1.

155. Pinhal, S.; Ropers, D.; Geiselmann, J.; De Jong, H.; Metcalf, W.W. Acetate Metabolism and the Inhibition of Bacterial Growth by Acetate. *J Bacteriol* **2019**, *201*, 147–166.

156. Younesi, H.; Najafpour, G.; Ku Ismail, K.S.; Mohamed, A.R.; Kamaruddin, A.H. Biohydrogen Production in a Continuous Stirred Tank Bioreactor from Synthesis Gas by Anaerobic Photosynthetic Bacterium: *Rhodopirillum rubrum*. *Bioresour Technol* **2008**, *99*, 2612–2619, doi:10.1016/j.biortech.2007.04.059.

157. Najafpour, G.; Younesi, H.; Mohamed, A.R. Effect of Organic Substrate on Hydrogen Production from Synthesis Gas Using *Rhodospirillum rubrum,* in Batch Culture. *Biochem Eng J* **2004**, *21*, 123–130, doi:10.1016/j.bej.2004.06.001.

158. Agyekum, E.B.; Nutakor, C.; Agwa, A.M.; Kamel, S. A Critical Review of Renewable Hydrogen Production Methods: Factors Affecting Their Scale-Up and Its Role in Future Energy Generation. *Membranes* 2022, *12*.

159. Zainal, B.S.; Ker, P.J.; Mohamed, H.; Ong, H.C.; Fattah, I.M.R.; Rahman, S.M.A.; Nghiem, L.D.; Mahlia, T.M.I. Recent Advancement and Assessment of Green Hydrogen Production Technologies. *Renewable and Sustainable Energy Reviews* 2024, *189*.

160. Tashie-Lewis, B.C.; Nnabuife, S.G. Hydrogen Production, Distribution, Storage and Power Conversion in a Hydrogen Economy - A Technology Review. *Chemical Engineering Journal Advances* 2021, *8*.

161. Paredes-Barrada, M.; Kopsiaftis, P.; Claassens, N.J.; van Kranenburg, R. *Parageobacillus thermoglucosidasius* as an Emerging Thermophilic Cell Factory. *Metab Eng* **2024**, *83*, 39–51, doi:https://doi.org/10.1016/j.ymben.2024.03.001.

162. Kantzow, C.; Weuster-Botz, D. Effects of Hydrogen Partial Pressure on Autotrophic Growth and Product Formation of *Acetobacterium woodii*. *Bioprocess Biosyst Eng* **2016**, *39*, 1325–1330, doi:10.1007/s00449-016-1600-2.

163. Van Niel, E.W.J.; Claassen, P.A.M.; Stams, A.J.M. Substrate and Product Inhibition of Hydrogen Production by the Extreme Thermophile, *Caldicellulosiruptor saccharolyticus*. *Biotechnol Bioeng* **2003**, *81*, 255–262, doi:10.1002/bit.10463.

164. Díaz, D.B.; Neumann, A.; Aliyu, H. Thermophilic Water Gas Shift Reaction at High Carbon Monoxide and Hydrogen Partial Pressures in *Parageobacillus thermoglucosidasius* KP1013. *Fermentation* **2022**, *8*, doi:10.3390/fermentation8110596.

165. Esquivel-Elizondo, S.; Chairez, I.; Salgado, E.; Aranda, J.S.; Baquerizo, G.; Garcia-Peña, E.I. Controlled Continuous Bio-Hydrogen Production Using Different Biogas Release Strategies. *Appl Biochem Biotechnol* **2014**, *173*, 1737–1751, doi:10.1007/s12010-014-0961-8.

166. Zhang, K.; Ren, N.-Q.; Cao, G.-L.; Wang, A.-J. Biohydrogen Production Behavior of Moderately Thermophile *Thermoanaerobacterium thermosaccharolyticum* W16 under Different Gas-Phase Conditions. *Int J Hydrogen Energy* **2011**, *36*, 14041–14048, doi:https://doi.org/10.1016/j.ijhydene.2011.04.056.

167. Mandal, B.; Nath, K.; Das, D. Improvement of Biohydrogen Production Under Decreased Partial Pressure of H_2 by *Enterobacter cloacae*. *Biotechnol Lett* **2006**, *28*, 831–835, doi:10.1007/s10529-006-9008-8.

168. Kosourov, S.N.; Batyrova, K.A.; Petushkova, E.P.; Tsygankov, A.A.; Ghirardi, M.L.; Seibert, M. Maximizing the Hydrogen Photoproduction Yields in *Chlamydomonas reinhardtii* Cultures: The Effect of the H_2 Partial Pressure. *Int J Hydrogen Energy* **2012**, *37*, 8850–8858, doi:10.1016/j.ijhydene.2012.01.082.

169. Laurent, B.; Serge, H.; Julien, M.; Christopher, H.; Philippe, T. Effects of Hydrogen Partial Pressure on Fermentative Biohydrogen Production by a Chemotropic *Clostridium* Bacterium in a New Horizontal Rotating Cylinder Reactor. *Energy Procedia* **2012**, *29*, 34–41, doi:https://doi.org/10.1016/j.egypro.2012.09.006.

170. Stein, U.H.; Abbasi-Hosseini, M.; Kain, J.; Fuchs, W.; Bochmann, G. Influence of Gas-Release Strategies on the Production of Biohydrogen and Biobutanol in ABE Fermentation. *Biofuels* **2019**, *13*, 9–15, doi:10.1080/17597269.2019.1619246.

171. Hurst, K.M.; Lewis, R.S. Carbon Monoxide Partial Pressure Effects on the Metabolic Process of Syngas Fermentation. *Biochem Eng J* **2010**, *48*, 159–165, doi:https://doi.org/10.1016/j.bej.2009.09.004.

172. Jung, G.Y.; Kim, J.R.; Park, J.-Y.; Park, S. Hydrogen Production by a New Chemoheterotrophic Bacterium *Citrobacter* sp. Y19. *Int J Hydrogen Energy* **2002**, *27*, 601–610, doi:https://doi.org/10.1016/S0360-3199(01)00176-8.

173. Clark, D.P. The Fermentation Pathways of *Escherichia coli* . *FEMS Microbiol Lett* **1989**, *63*, 223–234, doi:10.1111/j.1574-6968.1989.tb03398.x.

174. Zhao, Y.; Cimpoia, R.; Liu, Z.; Guiot, S.R. Kinetics of CO Conversion into H_2 by *Carboxydothermus hydrogenoformans*. *Appl Microbiol Biotechnol* **2011**, *91*, 1677–1684, doi:10.1007/s00253-011-3509-7.

175. Sivalingam, V.; Haugen, T.; Wentzel, A.; Dinamarca, C. Effect of Elevated Hydrogen Partial Pressure on Mixed Culture Homoacetogenesis. *Chemical Engineering Science: X* **2021**, *12*, 100118, doi:https://doi.org/10.1016/j.cesx.2021.100118.

List of Figures

List of Tables

Appendix

Supplementary material 1

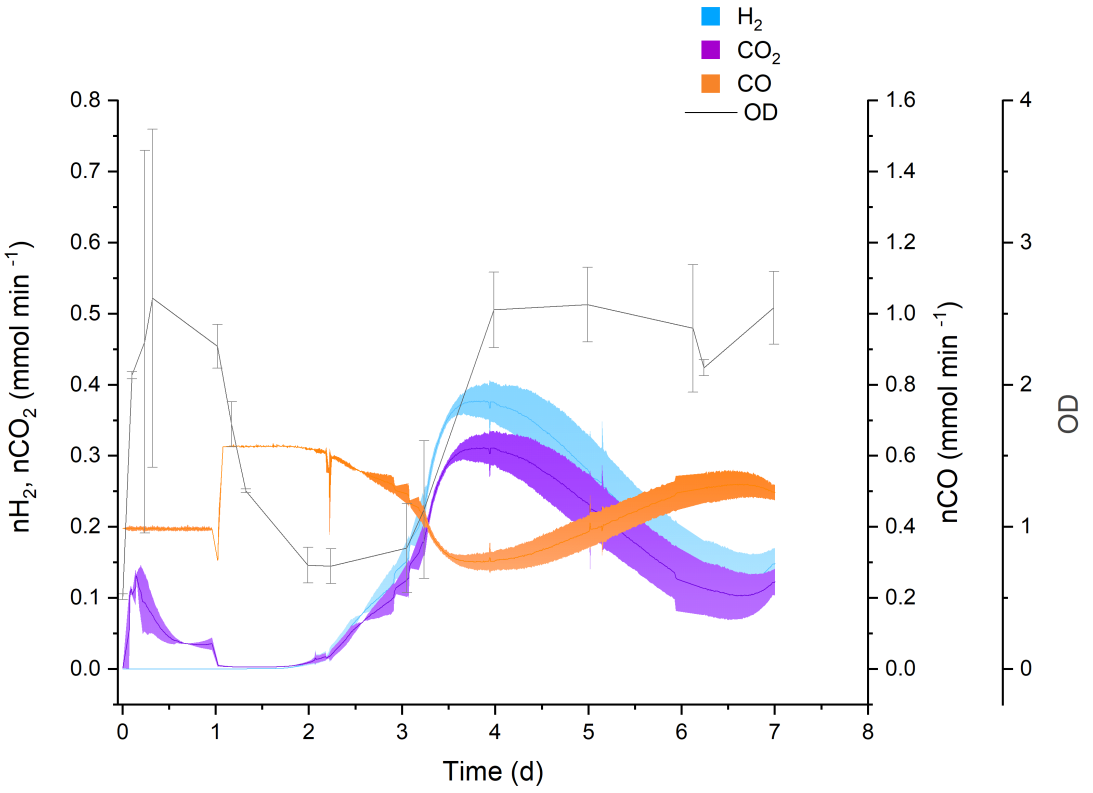

Supplementary figure 1. Batch fermentation in mLB medium. *P. thermoglucosidasius* DSM 6285 was cultivated at 55°C, 500 rpm, pH 6.8, during 7d. The H_2 and CO_2 production rate (mmol min^{-1}), together with the CO consumption rate (mmol min^{-1}), are the average of two bioreactors, with the standard deviation indicated by the colored regions.

Electron selectivity

The electron fluxes were calculated based on the conversion factors and the amount of each compound, following Equation 1.

$$e^{-}mmol_X = \dot{n}_X * eeq_X \quad (1)$$

Where $\dot{n}_X$ is the daily uptake rate of the substrates or the daily production rate of the products and eeq_X is the electron equivalents for each compound.

The selectivity of the process towards the products was calculated with Equation 2.

$$e^{-}mol\ Selectivity\ [\%] = \frac{\sum e^{-}mmol_{Products}}{\sum e^{-}mmol_{Substrates}} * 100\% \quad (2)$$

The sum of the daily $e^{-}mol$ from carbon monoxide (CO) and glucose was the $\sum e^{-}mmol_{Substrates}$, while the sum of the daily $e^{-}mol$ from acetate, formate, lactate and propionate was presented as $\sum e^{-}mmol_{Products}$. However, this was decided only when consumption of the metabolites was not observed, when consumed, they were accounted as substrates in the balance.

Table S1. Conversion factors

Compound	Molecular Weight (g/mol)	mol e^{-}/mol
CO	28.0	2
CO_2	44.0	0
Hydrogen	2.0	2
Glucose	180.1	24
Formate	46.1	2
Acetate	60.0	8
Lactate	90.0	12
Propionate	74.0	14

Supplementary material 2

The online version of the manuscript contains supplementary material available at:
https://doi.org/10.1186/s12934- 024- 02391-4

Table S1. Significant differences observed between different initial gas headspace compositions.

Table S2. Significant differences observed between CO/H2 yields.

Table S3. Significant differences observed between pre-hydrogenogenic phase O2 addition conditions.

Table S4. Significant differences observed between hydrogenogenic phase O2 addition conditions.

Table S5. Significant differences in H2 levels observed between sampling points. Table S6. Significant differences observed between variable O2 additions during peak hydrogenogenic period.

Supplementary material 3

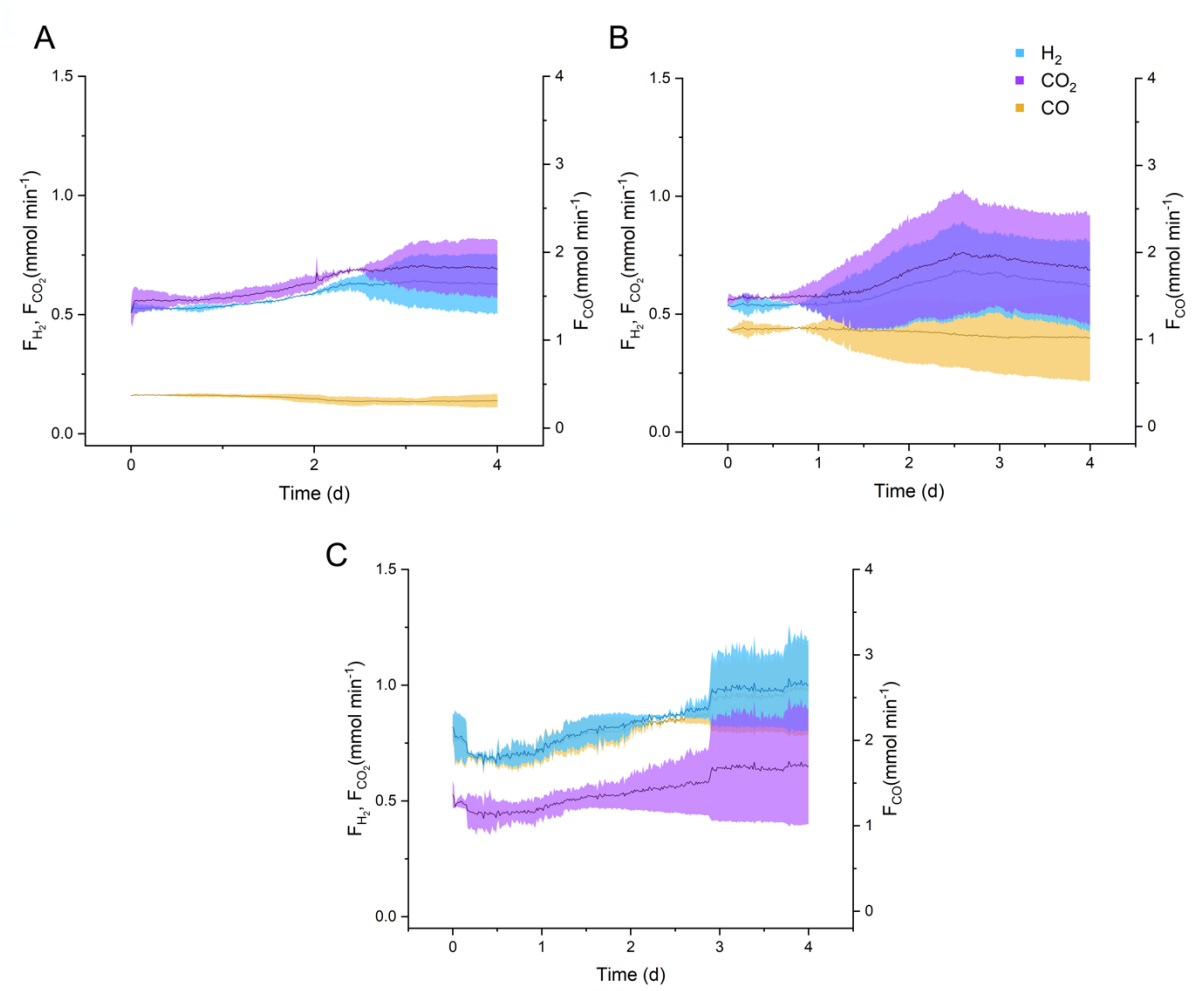

Supplementary figure 1. Syngas fermentation with increasing CO. A) 10 % CO, B) 30 % CO and C) 50% CO. The CO, H_2 and CO_2 out-flow rate (mmol min^{-1}), are the average of two bioreactors, with the standard deviation indicated by the colored regions.

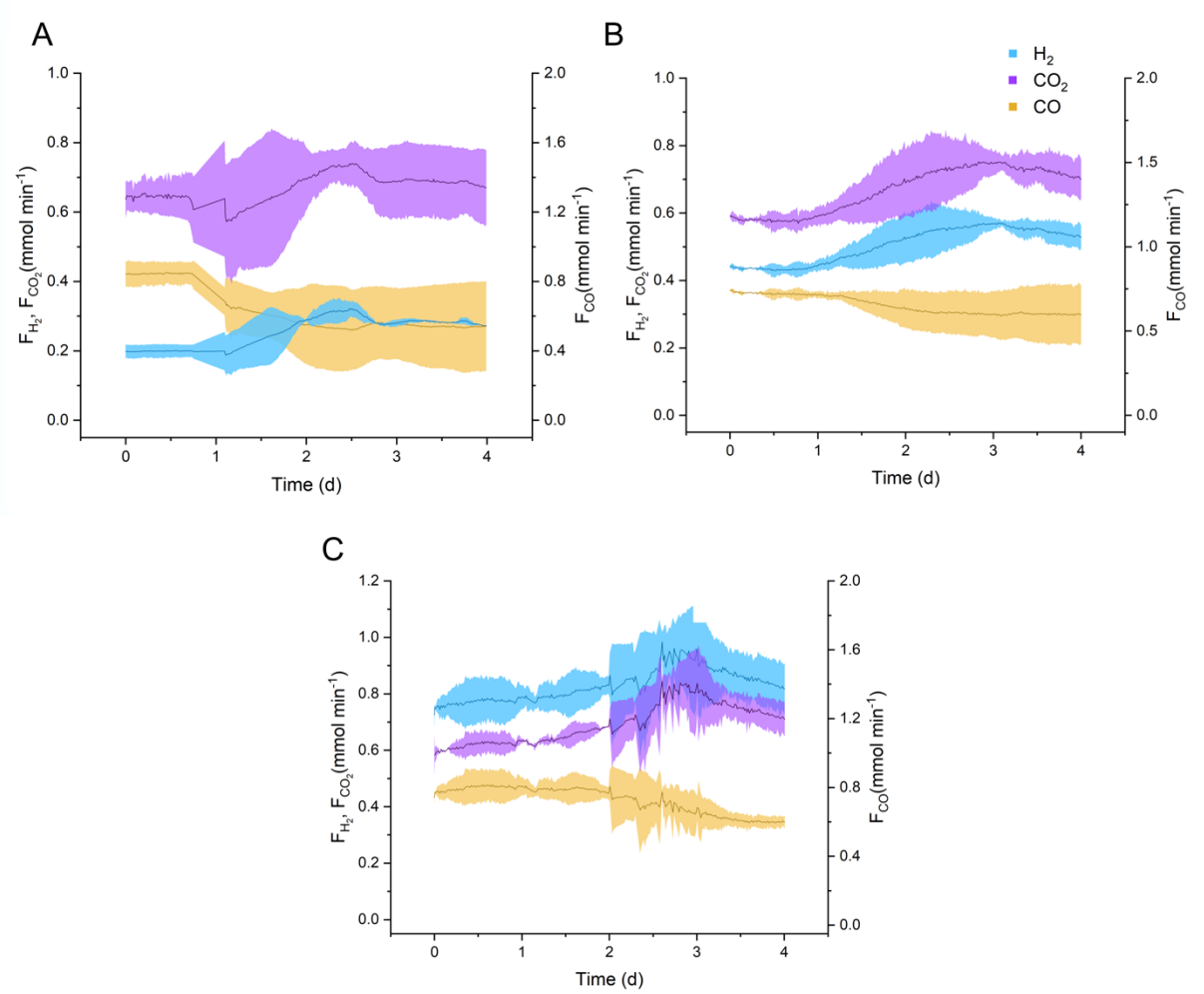

Supplementary figure 2. Syngas fermentation with increasing H_2. A) 5 % H_2, B) 12 % H_2 and C) 20 % H_2. The CO, H_2 and CO_2 out-flow rate (mmol min^{-1}), are the average of two bioreactors, with the standard deviation indicated by the colored regions.

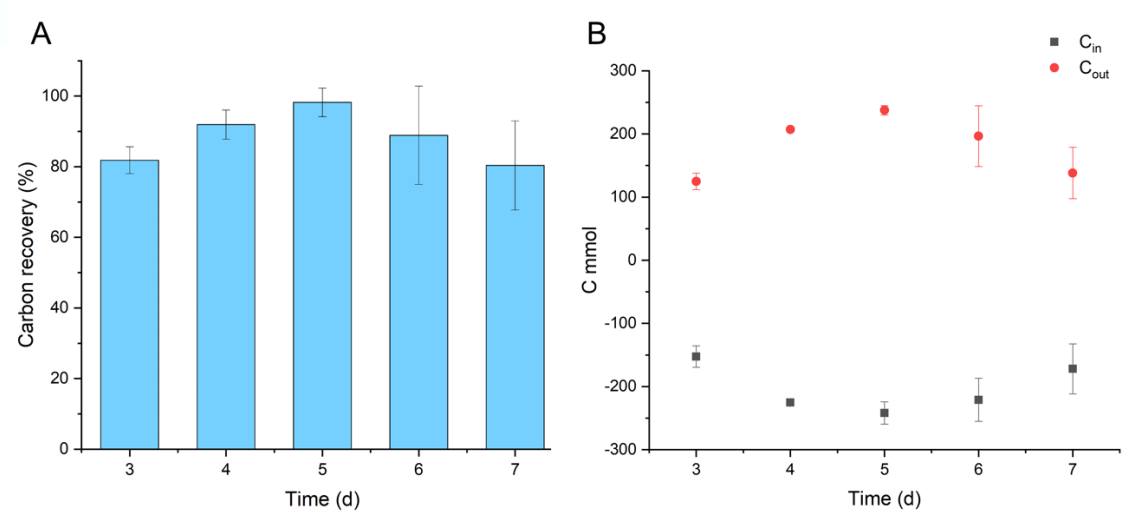

Supplementary figure 3. A) Carbon recovery for the acetate batch fermentation. B) Carbon selectivity (C mmol), C_{in} indicates the carbon in (CO, acetate), while C_{out} indicates carbon out (biomass, formate, lactate, butyrate, propionate, valerate, iso-butyrate, iso-valerate). The data shown represent the average of two reactors, with error bars indicating the standard deviation.

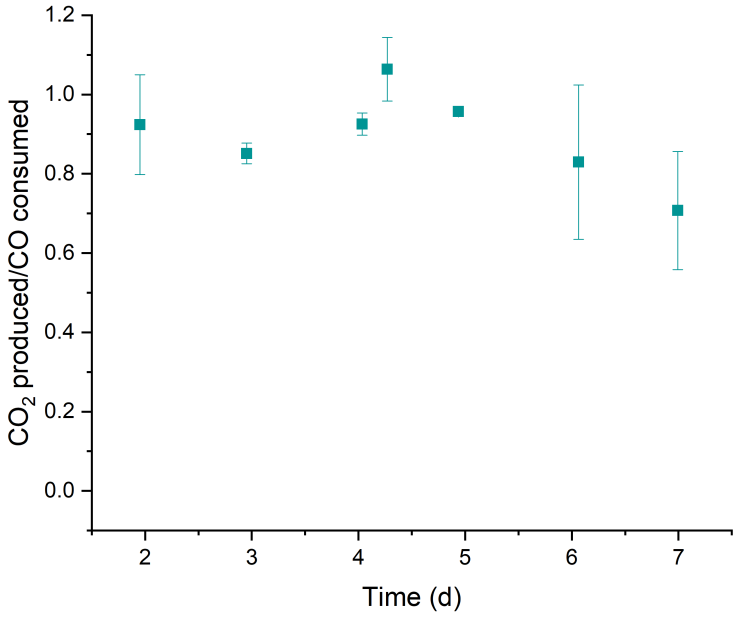

Supplementary figure 4. Quotient in terms of CO_2 produced and CO consumed during the batch fermentation with acetate as additional carbon source. The data shown represent the average of two reactors, with error bars indicating the standard deviation.

Electron selectivity

The electron fluxes were determined using conversion factors and the quantities of each compound, as described in Equation 1.

$$e^{-}mmol_X = \dot{n}_X * eeq_X \quad (1)$$

Here, $\dot{n}_X$ represents the daily uptake rate of the substrates or the daily production rate of the products, while eeq_X is the electron equivalents for each compound.
The process selectivity towards the products was calculated with Equation 2.

$$e^{-}mol\ Selectivity\ [\%] = \frac{\sum e^{-}mmol_{Products}}{\sum e^{-}mmol_{Substrates}} * 100\% \quad (2)$$

The total daily $e^{-}mol$ was derived from the sum of electron moles contributed by carbon monoxide (CO) and glucose (Syngas fermentations) or acetate ($\sum e^{-}mmol_{Substrates}$). Similarly, the electron flow associated with the products ($\sum e^{-}mmol_{Products}$) was calculated from the sum of the daily $e^{-}mol$ from acetate, formate, lactate, and propionate. However, this calculation was only applied when these metabolites were not consumed; if they were consumed, they were instead considered substrates in the balance.

Carbon selectivity

The carbon fluxes were determined using conversion factors and the quantities of each compound, as described in Equation 3.

$$C\ mmol_X = \dot{n}_X * eeq_X \quad (3)$$

The carbon selectivity towards the products was calculated with Equation 4.

$$C\ mol\ Selectivity\ [\%] = \frac{\sum C\ mmol_{Products}}{\sum C\ mmol_{Substrates}} * 100\% \quad (4)$$

The total daily $C\ mol$ was derived from the sum of electron moles contributed by carbon monoxide (CO) and acetate ($\sum C\ mmol_{Substrates}$). Similarly, the carbon associated with the products ($\sum C\ mmol_{Products}$) was calculated with the sum of the daily $C\ mol$ from biomass, formate, lactate, butyrate, propionate, valerate, iso-butyrate, and iso-valerate.

Conversion factors

The electron balance was performed using the conversion factors in Table S1. This is based on the oxidation state of each element of the compounds. For example for acetate (CH_3COO^-), each element has an oxidation number, for carbon is +4, hydrogen is +1, and oxygen contributes to -2 electrons. Due to the molecular formula of acetate $C_2H_4O_2$, each element´s oxidation number is multiplied by the number of atoms, for carbon, this would be 2 x 4, for hydrogen is 4 x 1 and for oxygen 2 x (-2). Everything sums (8+4+(-4)) to 8 electrons.
Now, for the carbon mol calculations, this is the number of carbon atoms in each compound that is used as the conversion factor.

Table S1. Conversion factors

Compound	Molecular Weight (g/mol)	mol e^-/mol	mol C/mol
CO	28.0	2	1
CO_2	44.0	0	1
Biomass	24.6	-	1
Hydrogen	2.0	2	0
Glucose	180.1	24	6
Formate	46.1	2	1
Acetate	60.0	8	2
Lactate	90.0	12	3
Propionate	74.0	14	3

Supplementary material 4

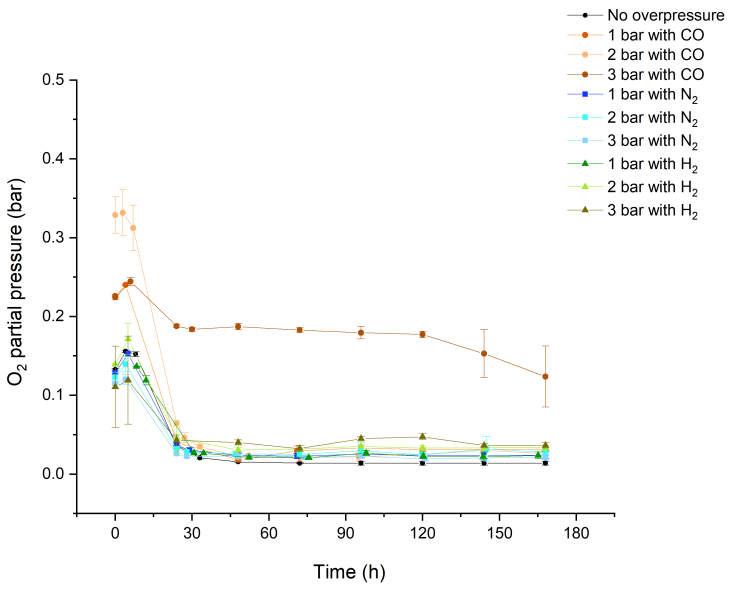

Figure S1. Oxygen partial pressure for all fermentations.

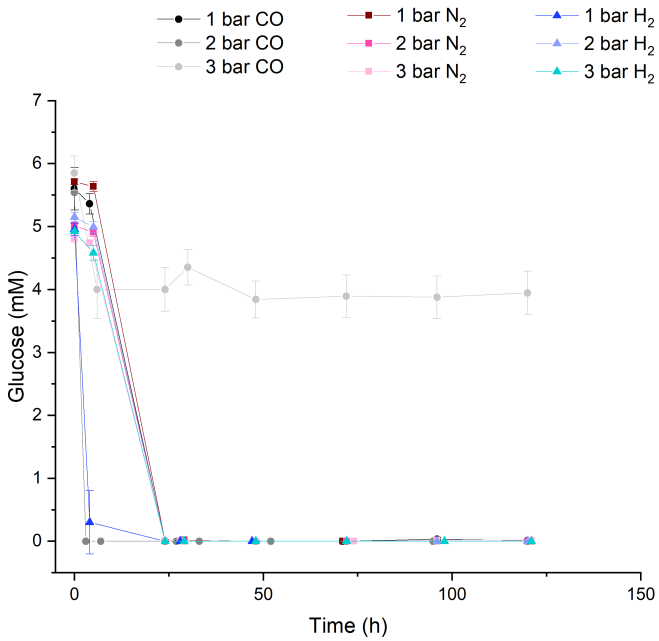

Figure S2. Glucose consumption over all fermentations.

Electron selectivity

Following Equation 1, the electron fluxes were calculated considering the conversion factors and the amount of each compound.

$$e^{-}mmol_X = \dot{n}_X * eeq_X \quad (1)$$

Where $\dot{n}_X$ is the daily uptake rate of the substrates or the daily production rate of the products and eeq_X is the electron equivalents for each compound.

The Equation 2 was used to calculate the selectivity of the process towards the products.

$$e^{-}mol\ Selectivity\ [\%] = \frac{\sum e^{-}mmol_{Products}}{\sum e^{-}mmol_{Substrates}} * 100\% \quad (2)$$

The sum of the daily $e^{-}mol$ from carbon monoxide (CO) and glucose was the $\sum e^{-}mmol_{Substrates}$, while the sum of the daily $e^{-}mol$ from acetate, formate, lactate and propionate was presented as $\sum e^{-}mmol_{Products}$. However, this was decided only when consumption of the metabolites was not observed, when consumed, they were accounted as substrates in the balance.

Table S1. Conversion factors

Compound	Molecular Weight (g/mol)	mol e^{-}/mol
CO	28.0	2
CO_2	44.0	0
Hydrogen	2.0	2
Glucose	180.1	24
Formate	46.1	2
Acetate	60.0	8
Lactate	90.0	12
Butyrate	88	20
Propionate	74.0	7
Valerate	102	15
Iso-butyrate	88	20
Iso-valerate	102	15